GEOLOGY AND HYDROCARBON POTENTIAL OF THE BARNETT SHALE (MISSISSIPPIAN) IN THE NORTHERN DELAWARE BASIN, WEST TEXAS AND SOUTHEASTERN NEW MEXICO

By

TRAVIS J. KINLEY

Bachelor of Science, 2004
University of Wyoming
Laramie, Wyoming

Submitted to the Graduate Faculty of
The College of Science and Engineering
Texas Christian University
In partial fulfillment of the requirements for the degree of

MASTER OF SCIENCE

December, 2006

ACKNOWLEDGEMENTS

I gratefully acknowledge the help and support of all individuals and organizations whose financial, intellectual, and motivational support has helped me to complete this project. I began this project as a relatively inexperienced, but passionate student of geology. Through the course of the past two years I have had the chance to learn from many experienced and knowledgeable people that have facilitated in the development of my future career as a petroleum geologist.

First, I would like to thank Mark Pospisil and XTO Energy, whose sole financial support for this project have made it possible to acquire the data that was needed to carry out such a task. I am very grateful for your interest in and generosity toward the development of my career.

I would also like to gratefully acknowledge Lance Cook at XTO Energy who was the inspiration for this project, and provided me with a tremendous amount of guidance and support throughout the course of this endeavor. In addition, I would like to thank Casey Patterson and Steve Weiner at XTO who have helped me with many technical aspects and provided much needed motivational support. Also, I would like to express my thanks to Dan Jarvie at Humble Geochemical Services for his generosity in providing the geochemical data used in the project, and David Prose for his initial help in starting this project.

Most importantly, a big thanks, and debt of gratitude is owed to Dr. John Breyer at TCU whose dedication and guidance have been a tremendous help to me. Your motivational support and patience have been invaluable.

Finally, I would like to thank my wonderful wife, Crissy, who has been a tremendous support throughout my college career.

TABLE OF CONTENTS

LIST OF FIGURES

LIST OF TABLES

Introduction

The Barnett Shale (Mississippian) is source, seal and reservoir for a world-class, natural-gas accumulation in the Fort Worth basin (Montgomery *et al.* 2005). The goal of this study was to evaluate the hydrocarbon potential of the Barnett Shale in the Delaware basin. To do this, I examined the stratigraphy and structure of the Barnett Shale and its organic matter content, burial history and thermal maturity. I have identified specific areas within the Delaware basin for gas producers to focus their future exploration and production efforts.

Cross sections, isopach maps and structure maps based on well-log correlations show the relationship of the Barnett Shale to the underlying "Mississippian lime" and Woodford Formation, and to the overlying Pennsylvanian strata. Specific subunits within the Barnett have been identified and mapped, and I have related my findings to the paleogeography of the study area during the Mississippian.

Well-log analysis, geochemical data sets and thin-section analysis were used to determine the organic matter content of the Barnett and the thermal history of the unit. From these data sets I have constructed burial history curves, thermal maturation curves and plots of total organic carbon along with maps showing the geothermal gradient and variation in thermal maturity of the Barnett Shale in the Delaware basin. I have also constructed a shale gas activity map of the basin that highlights the recent drilling and production testing activity by various operators in the area (Plate I, in pocket).

Geographic and Geologic Setting

The Permian basin region is in the southern mid-continent portion of the North American craton (Hills and Galley 1988). It extends from the Matador uplift on the north

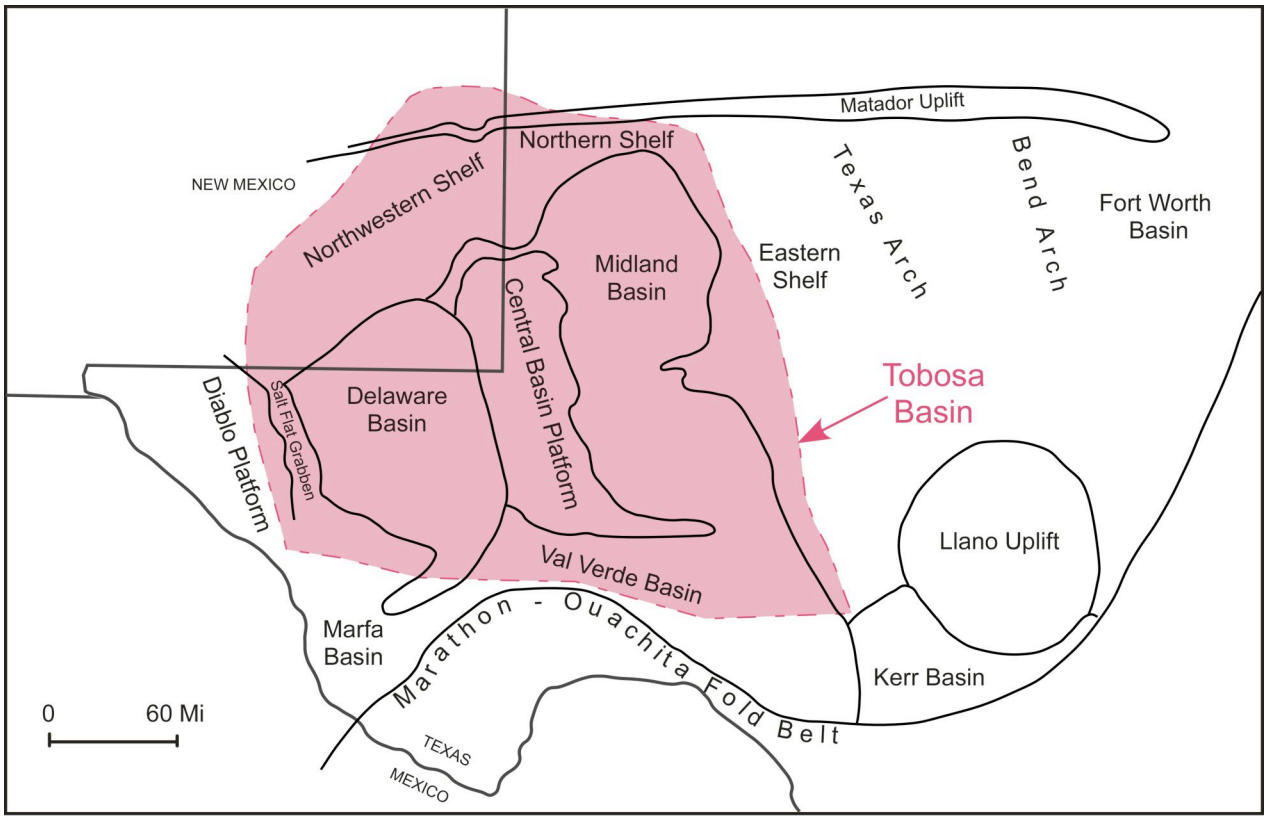

Figure 1. Major geologic features of the Permian basin region. Former extent of the ancestral Tobosa basin shown in pink. Modified from Frenzel *et al.* (1988).

to the Marathon-Ouachita fold belt on the south and from the Bend arch on the east to the Diablo platform on the west (Fig. 1). The Permian basin proper is divided into the deeper Delaware basin to the west and the shallower Midland basin to the east by the Central Basin uplift. Mississippian strata found today in the Delaware basin of west Texas and southeastern New Mexico accumulated in a larger, Early Paleozoic structural depression known as the Tobosa basin (Adams 1965). The Tobosa basin subsided throughout the Early and middle Paleozoic, and received approximately 7,000 feet (2,333 meters) of Cambrian through Mississippian sediment.

The Delaware basin began to evolve as a separate entity in the Late Paleozoic with the uplift of the Central Basin platform and the northward advancement of the Marathon-Ouachita fold belt. This tectonism also led to the development of the Val Verde, Kerr and Marfa basins. Subsidence and sedimentation continued in the Delaware basin throughout the remainder of the Paleozoic, with approximately 20,000 feet (6,666 meters) of Lower Pennsylvanian through Permian sediment accumulating in the basin. During this time the basin underwent a complex tectonic evolution in several stages (Vertrees *et al.* 1959; Adams 1965; Hills 1984; Hills and Galley 1988).

During the Late Precambrian and Early Cambrian the Permian basin region consisted of eroded, low-lying hills (Flawn 1956). Early and Middle Cambrian strata are absent suggesting that the area was above sea level at this time (Hills and Galley 1988). In the Late Cambrian and Early Ordovician, the sea transgressed northward and northwestward across the region (Adams 1965; Hills and Galley 1988). The Lower Ordovician Ellenburger Group was deposited in a broad, shallow sea that flooded the region. A thick sequence of Lower Ordovician carbonates accumulated on a shallow shelf in the area that is now the Delaware basin. The Tobosa basin remained primarily a site of

carbonate deposition from the Middle Ordovician through the Middle Devonian (Hills 1984, 1985; Hills and Galley 1988).

In the Late Devonian, a profound change in sedimentation took place all along the southern margin of the North American craton (Hills and Galley 1988). Deposition of carbonate sediments slowed and stopped, and black shales were deposited unconformably on underlying limestones and dolomites. In the Delaware basin, these black shales are represented by the Late Devonian-Early Mississippian Woodford Formation (Hills and Galley 1988). Carbonate deposition returned to the Tobosa basin in the Middle Mississippian with the deposition of the "Mississippian lime" above the Woodford Formation. Upper Mississippian strata consist of dark grey and brown organic-rich shales of the Barnett, which reached a maximum thickness of approximately 2,000 feet (666 meters) along the axis of the Tobosa basin. By the Late Mississippian, approximately 7,000 feet (2,333 meters) of Paleozoic sediments had accumulated in the Tobosa basin (Adams 1965).

The Tobosa basin was fragmented in the Early Pennsylvanian by the uplift of the Central Basin platform and the subsidence of the Delaware and Midland basins (Cys and Gibson 1988). The Delaware basin filled with clastic sediments by the end of the Early Middle Pennsylvanian. In the Middle and Late Pennsylvanian tectonic activity increased and, as the basin subsided, carbonate banks grew along the basin margin (Hills 1984). Clastic sediments were trapped behind the carbonate banks and a starved basin developed.

Tectonic activity peaked again in the Early Permian (Hills 1985). Approximately 20,000 feet (6,666 meters) of basinal clastics accumulated in the rapidly subsiding Delaware basin during the Permian: 14,000 feet (4,666 meters) in the Wolfcampian,

3,000 feet (1,000 meters) in the Leonardian and 3,000 feet (1,000 meters) in the Guadalupian (Cys and Gibson 1988). During the Ochoan, at the close of the Permian, the region was a site of evaporite deposition, with approximately 4,500 feet (1,371 meters) of evaporite sediments accumulating in the area of the Delaware basin. By Late Permian time the Delaware Basin had experienced regional down-warping and rotational tilting toward the east (Adams 1965).

Tectonic activity had largely ceased in the area by the Late Permian (Hills 1985), and redbeds accumulated across the region in the Triassic. Little to no Jurassic or Lower Cretaceous strata are present in the Permian basin suggesting that much subaerial erosion had taken place over the region shortly after the deposition of this strata (Hills 1988). Middle Cretaceous seas advanced across the region depositing sandstones and thin shelf limestones. The area was unaffected by Laramide and Later Tertiary tectonism except on the extreme western edge of the region (Hills 1985; Hills and Galley 1988). Tertiary igneous activity occurred along pre-existing Laramide structural trends near the western margin of the Delaware basin, and affected the thermal maturity of source rocks and hydrocarbons within the basin (Barker and Pawlewicz 1987).

The final structural influence on the formation of the Delaware basin was the overprinting of Cenozoic, basin-and-range style, extensional faulting on the older structural features, which followed the pre-existing structural grain of the region in a northwest-to-southeast direction (Shepard and Walper 1982).

Stratigraphy and Structure

The study area lies in the northern portion of the Delaware basin, and covers approximately 500 square miles (1,300 square kilometers) (Fig. 2). It extends from the Salt Flat graben on the shallow western flank of the basin to the Central Basin platform

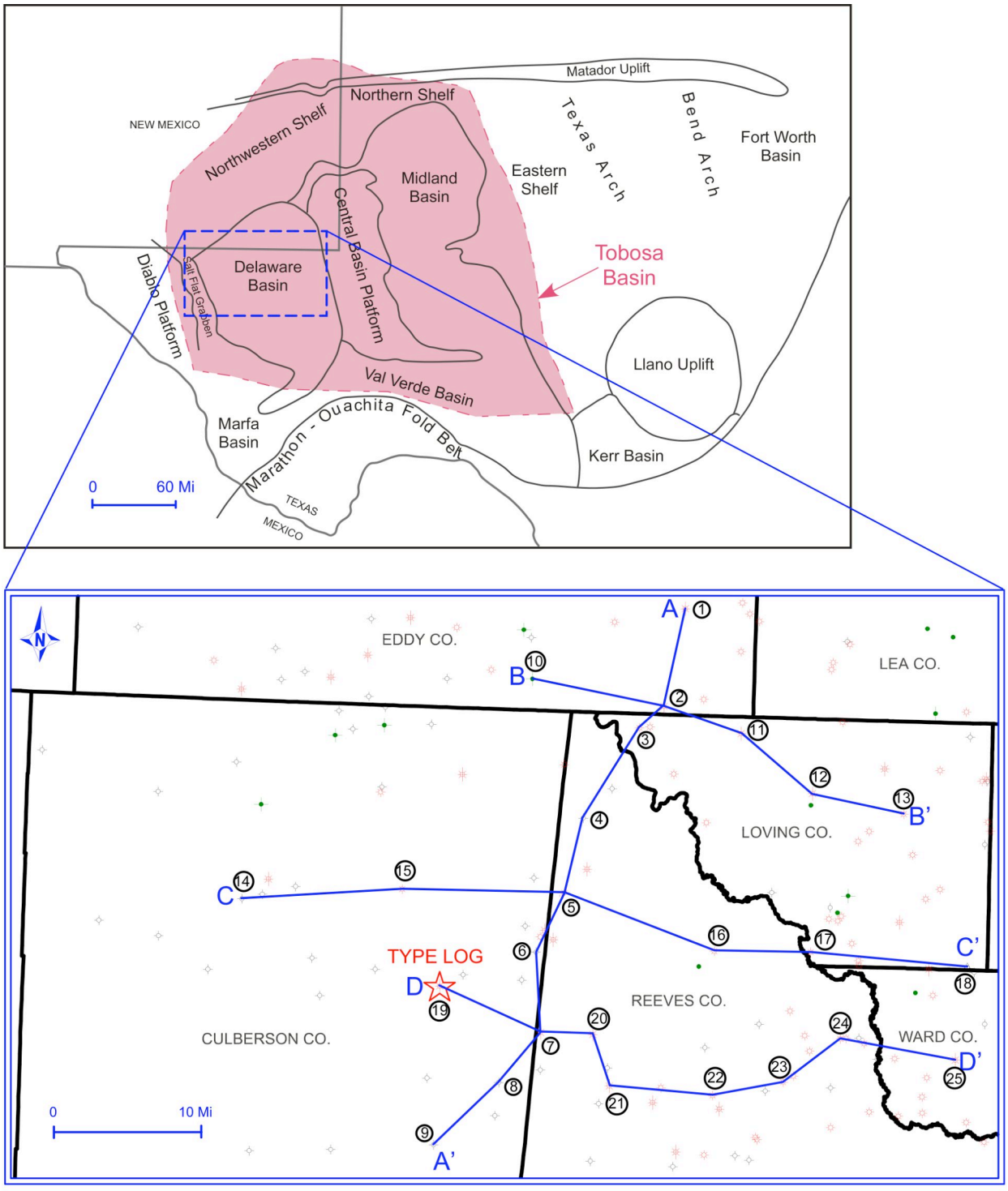

Figure 2. Location of the study area within the Delaware basin. Map also shows the location of the type log and cross sections used in this study. See table 12 for wells used in constructing cross sections.

Table 1. Wells used in constructing cross sections shown in Figure 2. Type log highlighted in yellow.

Location Number	Well Serial Number (APINum)	County	Operator	Well Name	Well Number	Well Desription	WELL TD (ft)
1	30015047490000	EDDY	RICHARDSON & BASS	JF HARRISON FEDERAL	1	Abandoned Gas	16705
2	30015218770000	EDDY	PENROC OIL CORP	ROSS DRAW UNIT	5	Abandoned Gas	16326
3	42301302650000	LOVING	BROWN H L JR	RED BLUFF `12`	3	Gas	17050
4	42389309180000	REEVES	CREDO PETROLEUM CORP	CREDO-OLSON-STATE	1	Dru	15500
5	42389311120000	REEVES	TENNECO OIL CO	TENNECO V P	1	Gas	16500
6	42109314070000	CULBERSON	AMERCN QUASAR PETRO	STATE	1-32	Dry	15900
7	42389309530000	REEVES	R K PETROLEUM CORP	TIERRA-STATE	1	Abandoned Gas	17244
8	42109314250000	CULBERSON	CITIES SERV OIL CO	TRIKEN STATE `A`	1	Dry	12050
9	42109317640000	CULBERSON	TENNECO OIL CO	PLUMMER `2`	1	Dry	13826
10	30015213980000	EDDY	HAMON JAKE L	STATE LG-1175	1	Abandened Oil	14572
11	42301300620000	LOVING	HNG OIL COMPANY	KYLE 10	1	Abandoned Gas	20231
12	42301300420000	LOVING	AMERCN QUASAR PETRO	GRICE DEEP	1	Abandoned Gas	19255
13	42301303280000	LOVING	HUNT OIL CO	BRUNSON GLENN S `17	1	Gas	22500
14	42109313820000	CULBERSON	SHELL OIL CO	SIBLEY	1	Dry	10570
15	42109313590000	CULBERSON	ARCO OIL & GAS CORP	COVINGTON STATE	1	Gas	13500
16	42389312310000	REEVES	R K PETROLEUM CORP	DIXIELAND `10`	1	Gas	19218
17	42301302700000	LOVING	ATAPCO	ARNO GAS UNIT	2	Gas	21700
18	42301303560000	LOVING	CHEVRON	UNIVERSITY `26-19`	WD-1	Service Well	20200
19	42109308240000	CULBERSON	TEXAS PACIFIC OIL CO	M G NEVILL	1	Abandoned Gas	16000
20	42389302690000	REEVES	INEXCO & AMERICAN QU	J COVINGTON	1	Abandoned Gas	18525
21	42389304800000	REEVES	CHAMPLIN PETRO CMPNY	LEWIS-STATE	1	Abandoned Gas	13800
22	42389302490000	REEVES	COYOTE OIL&GAS INC	STATE OF TEXAS `28`	1	Gas	13500
23	42389300810000	REEVES	BURLINGTON RESOURCES	KIRK	1	Gas	16210
24	42389304210000	REEVES	PENNZOIL CO INC	PETREY	1	Gas	19060
25	42475300900000	WARD	HANLEY COMPANY	BASS-WILLIAMS	1	Abandoned Gas	20891

bordering the deeper eastern side. The study area includes parts of Culberson, Reeves, Loving and Ward Counties, Texas, and portions of Eddy and Lea Counties, New Mexico. Logs from approximately 150 wells, which penetrated all or part of the Paleozoic section, were used in this study. Well-logs from the Texas Pacific Oil Company M. G. Nevill #1, near the central portion of the study area, in Culbertson County, Texas, served as the type log for the study.

Subdivisions of the Mississippian

"Mississippian" as used here extends from a pronounced gamma-ray excursion at the top of the underlying Woodford Formation (Devonian-Mississippian) to the lowermost ten-foot-thick sand at the base of the overlying Morrowan (Pennsylvanian) clastics (Fig. 3). Operators in the area refer to the thick limestone at the base of the Mississppian section as the "Mississippian limestone" or "Mississippian lime." The remaining Mississippian section is referred to as the "Barnett Shale." The Mississippian lime is only 40 feet (13 meters) thick on the type log, but is typically much thicker in the deeper portions of the basin.

The Barnett Shale in the northern Delaware basin can be subdivided into an upper clastic unit and a lower limy unit by a pronounced change in resistivity (Fig. 3). The lower limy unit can be further subdivided into five intervals for detailed mapping using well-log markers. Intervals A, C and E are characterized by packages of resistivity markers that can be correlated throughout the study area. The intervening intervals B and D show lower resistivity responses. The top of interval A is the top of the lower Barnett. Interval A is sometimes referred to as the "50 ohmm zone" by workers in the area because it typically exhibits resistivities of 50 to 100 ohm-meters. It is believed to be a significant zone of gas saturation within the Barnett. Overall, the lower Barnett has a

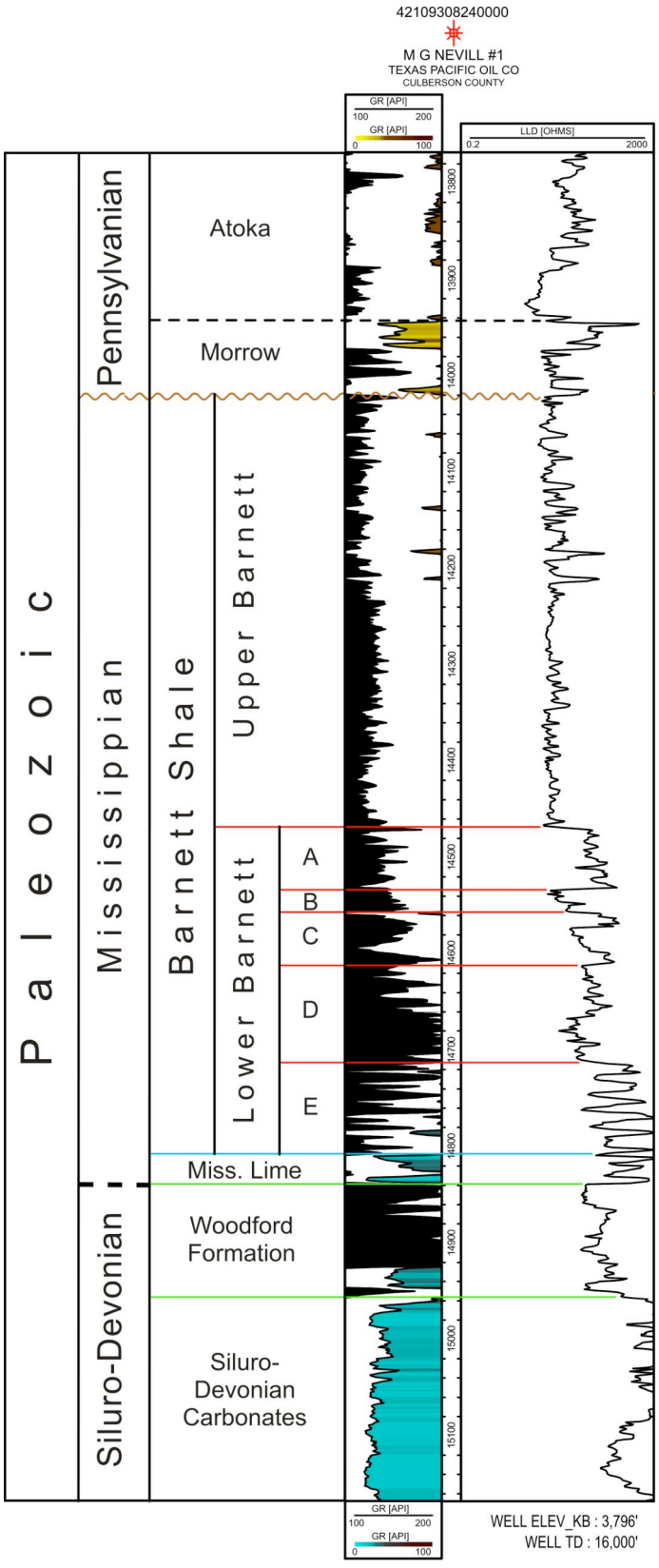

Figure 3. Type log showing stratigraphic subdivisions of Mississippian strata used in this study.

higher total organic carbon (TOC) content than the upper Barnett (see below). Interval D shows a pronounced increase in API gamma-ray count that correlates with an increase in TOC. Interval E, which is marked by a series of resistivity spikes, represents an interfingering, transitional contact with the Mississippian lime. In places the resistivityspikes characteristic of interval E extend down and completely replace the blocky resistivity response characteristic of the Mississippian lime. Furthermore, there is an increase in calcareous material in the cuttings from interval E as it passes downward into the black to dark gray Mississippian lime.

Log responses in the upper Barnett section are highly erratic. Few well-log markers could be correlated from well to well, and none are laterally continuous across the study area. However, the general trend is for API gamma-ray counts to increase from the top to the bottom of the upper Barnett. The upper Barnett is unconformably overlain by Pennsylvanian clastics of Morrowan or Atokan age where the Morrow is not present (Vertrees *et. al.* 1959). The contact between the Mississippian and Pennsylvanian was placed at the base of the lowermost ten-foot-thick sand in the section, as noted previously.

Structure of the Study Area

The Mississippian lime and Barnett Shale accumulated in the ancestral Tobosa basin, which was fragmented into the Delaware and Midland basins by uplift of the Central Basin platform near the end of the Mississippian and beginning of the Pennsylvanian (Hills 1984, 1985; Hills and Galley 1988). Structure-contour maps on the top of the Woodford (base of the Mississippian lime), the top of the lower Barnett and the top of the upper Barnett are nearly identical (compare Figs. 4, 5 and 6), suggesting no

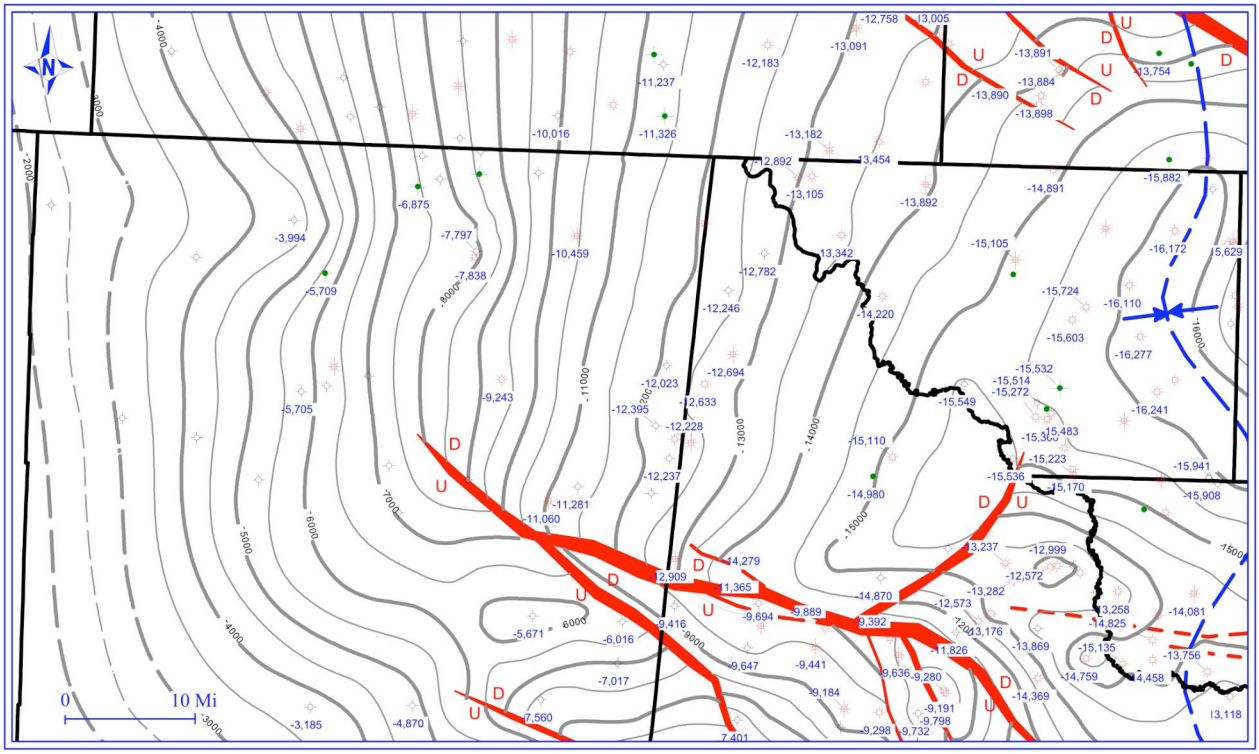

Figure 4. Structure contour map on the top of the Woodford Formation. Elevation (ft) posted for wells where formation top was picked. Contour interval, 500 ft. Faults shown in red. Dashed blue line to east shows location of basin axis.

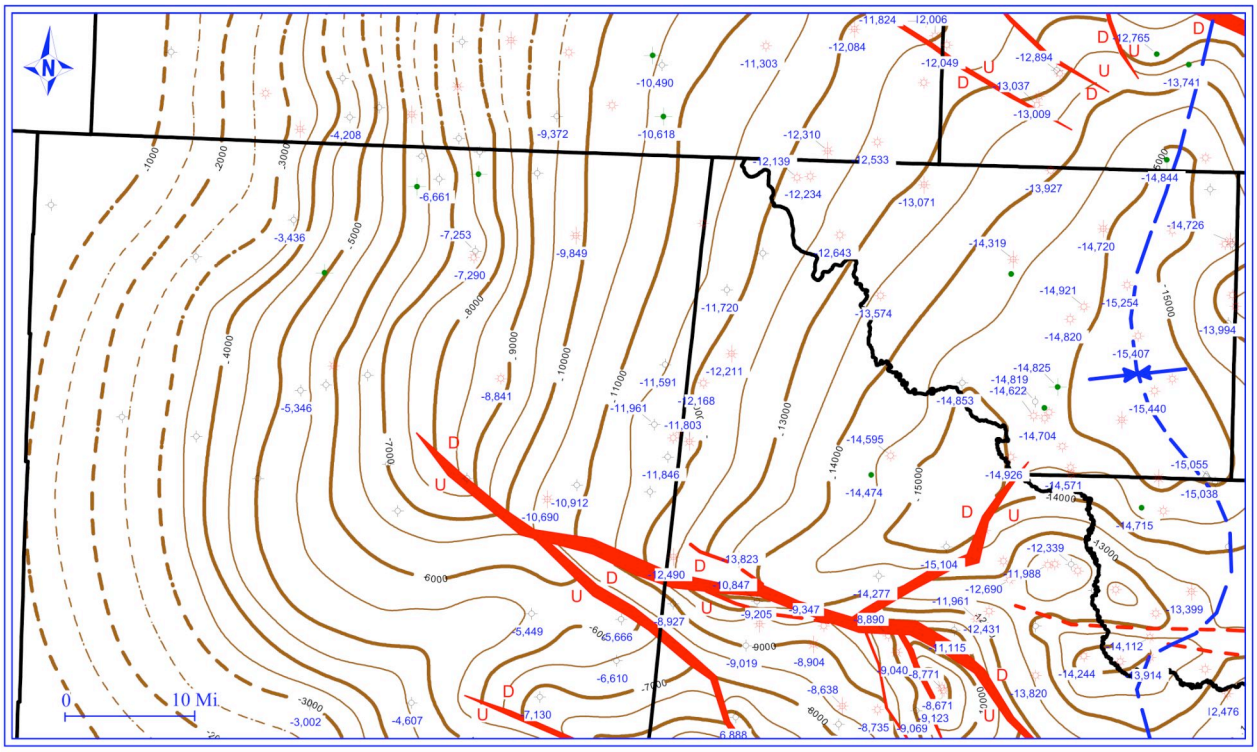

Figure 5. Structure contour map on the top of the lower Barnett. Elevation (ft) posted for wells where formation top was picked. Contour interval, 500 ft. Faults shown in red. Dashed blue line to east shows location of basin axis.

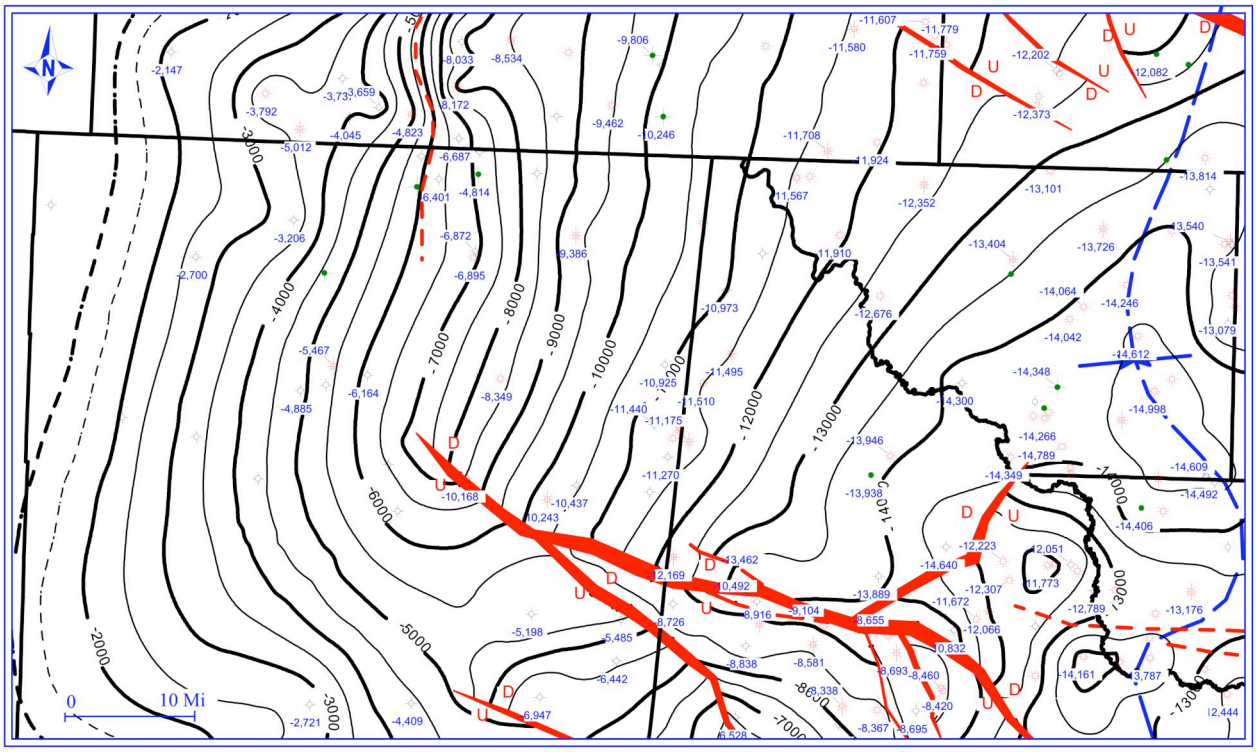

Figure 6. Structure contour map on the top of the upper Barnett. Elevation (ft) posted for wells where formation top was picked. Contour interval, 500 ft. Faults shown in red. Dashed blue line to east shows location of basin axis.

differential movement took place within the Tobosa basin while the Mississippian strata were being deposited.

The Delaware basin is asymmetric with its axis running roughly north-south near the eastern edge of the basin alongside the Central Basin platform. From the west, the strata dip gently eastward toward the axis of the basin. The dip is steepest on the eastern side of the study area in Culberson County, and lessens on the eastern side in Reeves, Loving and Ward Counties. Mississippian strata dip steeply to the west toward the axis of the basin from the Central Basin platform. The measured depth to the top of the Barnett varies from approximately 7,000 feet (2,333 meters) along the western edge of the basin to greater than 18,000 feet (6,000 meters) along the basin axis.

The predominant fault trend in the study area is west-northwest; with some conjugate faulting trending approximately 30 to 60 degrees from the main trend. The fault planes must dip steeply, because the position of the faults does not change much from the top of the Woodford to the top of the upper Barnett (Figs. 4, 5, and 6). Also, the well-logs show no indication of fault-cut in the offset wells, indicating the fault planes are dipping too steeply to cut the boreholes at angles greater than 60 degrees.

Patterns of Sediment Accumulation

Isopach maps and cross sections show the pattern of sediment accumulation in the study area. The major depocenter was located in the northeast portion of the study area, where more than 2,000 feet (666 meters) of Mississippian strata accumulated. In general, the Mississippian section thins along strike from north to south (Fig. 7) and thickens downdip from west to east (Figs. 8, 9, and 10). The base of the Mississippian appears to be conformable with the underlying Woodford Shale. However, a major regional unconformity separates the upper part of the Barnett from the overlying Pennsylvanian

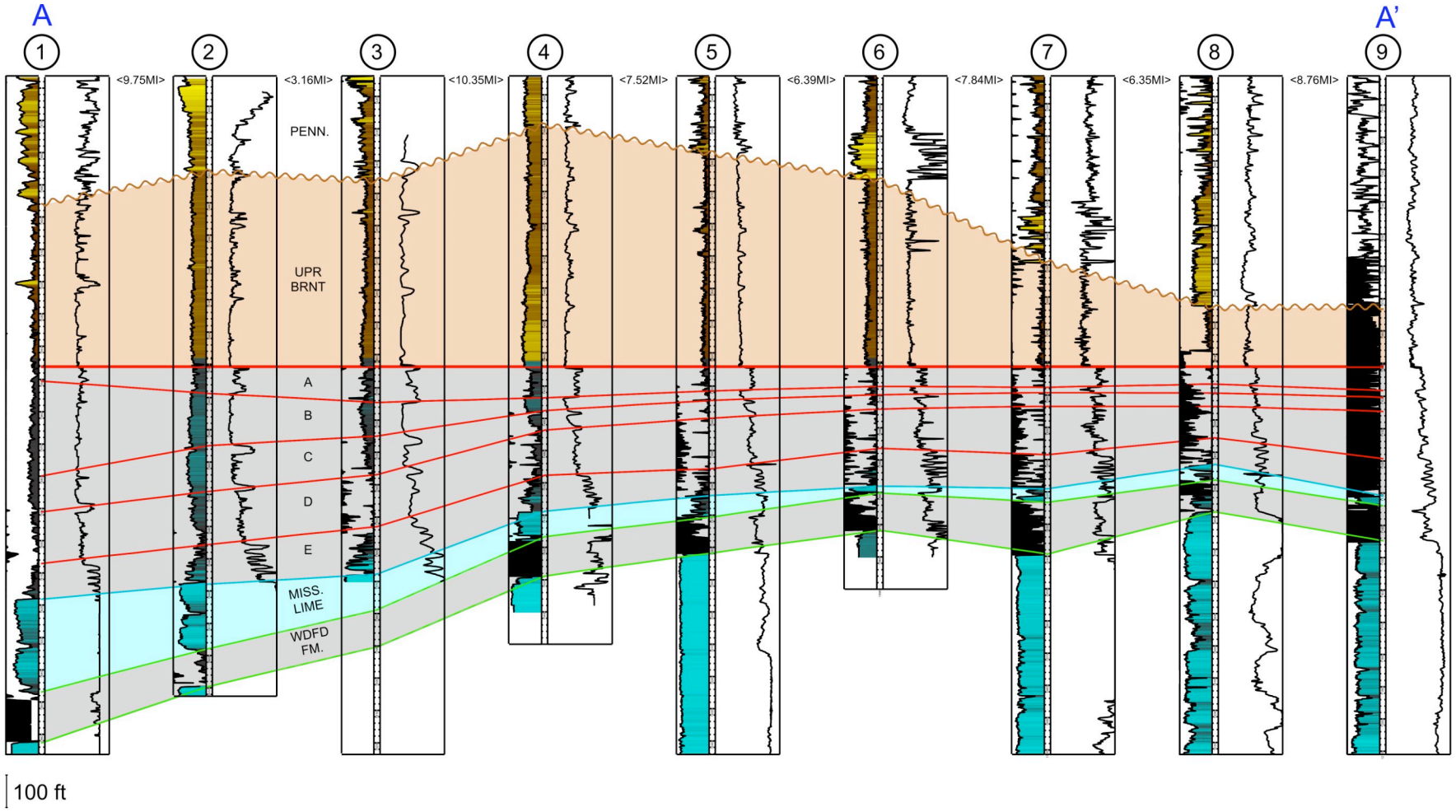

Figure 7. Cross section A-A' showing the variation in thickness along strike from north to south across the study area. Stratigraphic datum is the top of the lower Barnett (interval A). Well logs--left-hand track, gamma ray log; right-hand track, deep resistivity curve. PENN., Pennsylvanian; UPR BRNT, upper Barnett; A, B, C, D and E, intervals in the lower Barnett; MISS. LIME, Mississippian limestone; WDFD FM., Woodford Formation. See Figure 2 for location of cross section.

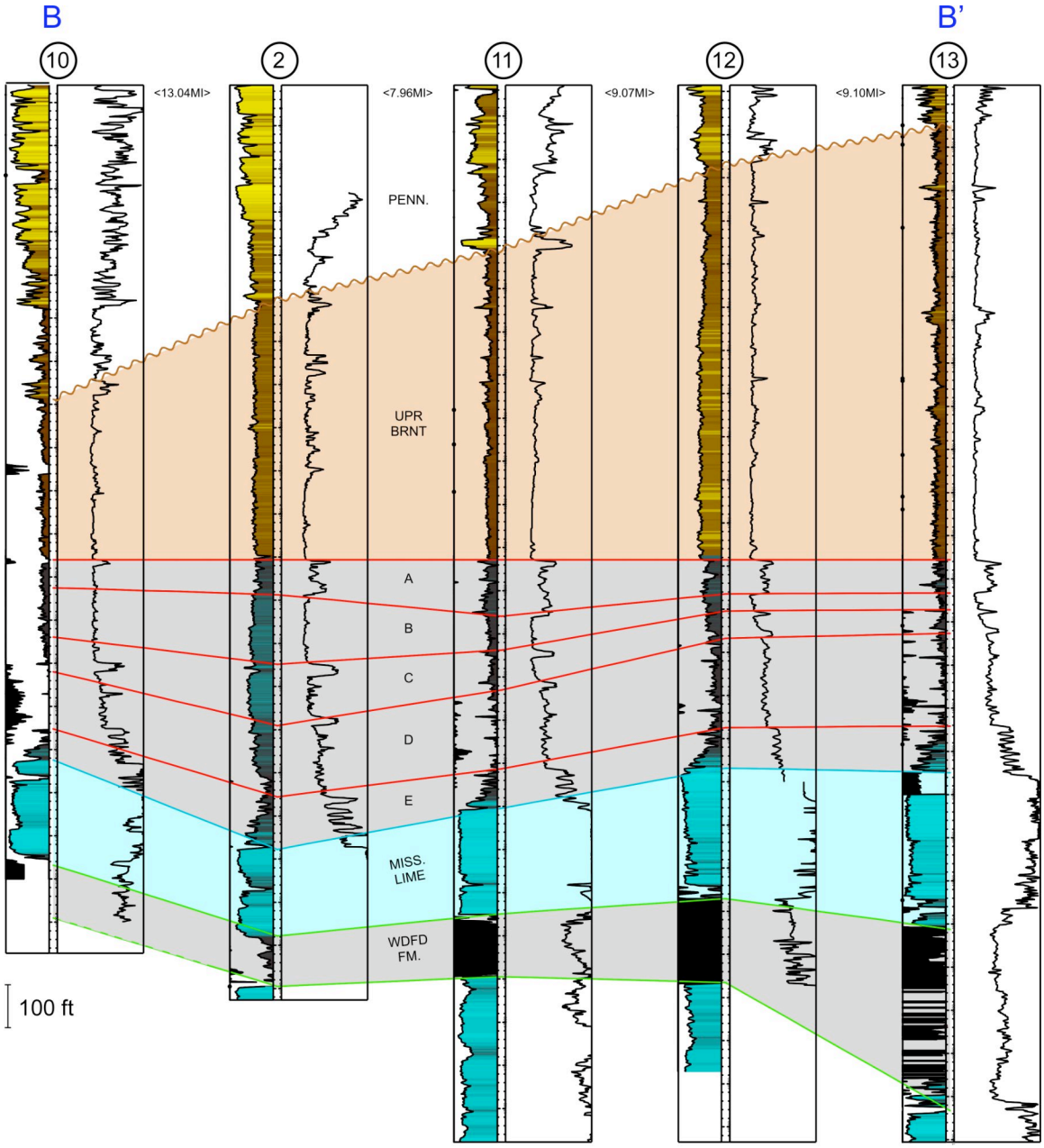

Figure 8. Cross section B-B' showing variation in thickness of stratigraphic units in dip direction from west to east across the northern portion of the study area. See Figure 2 for cross section location.

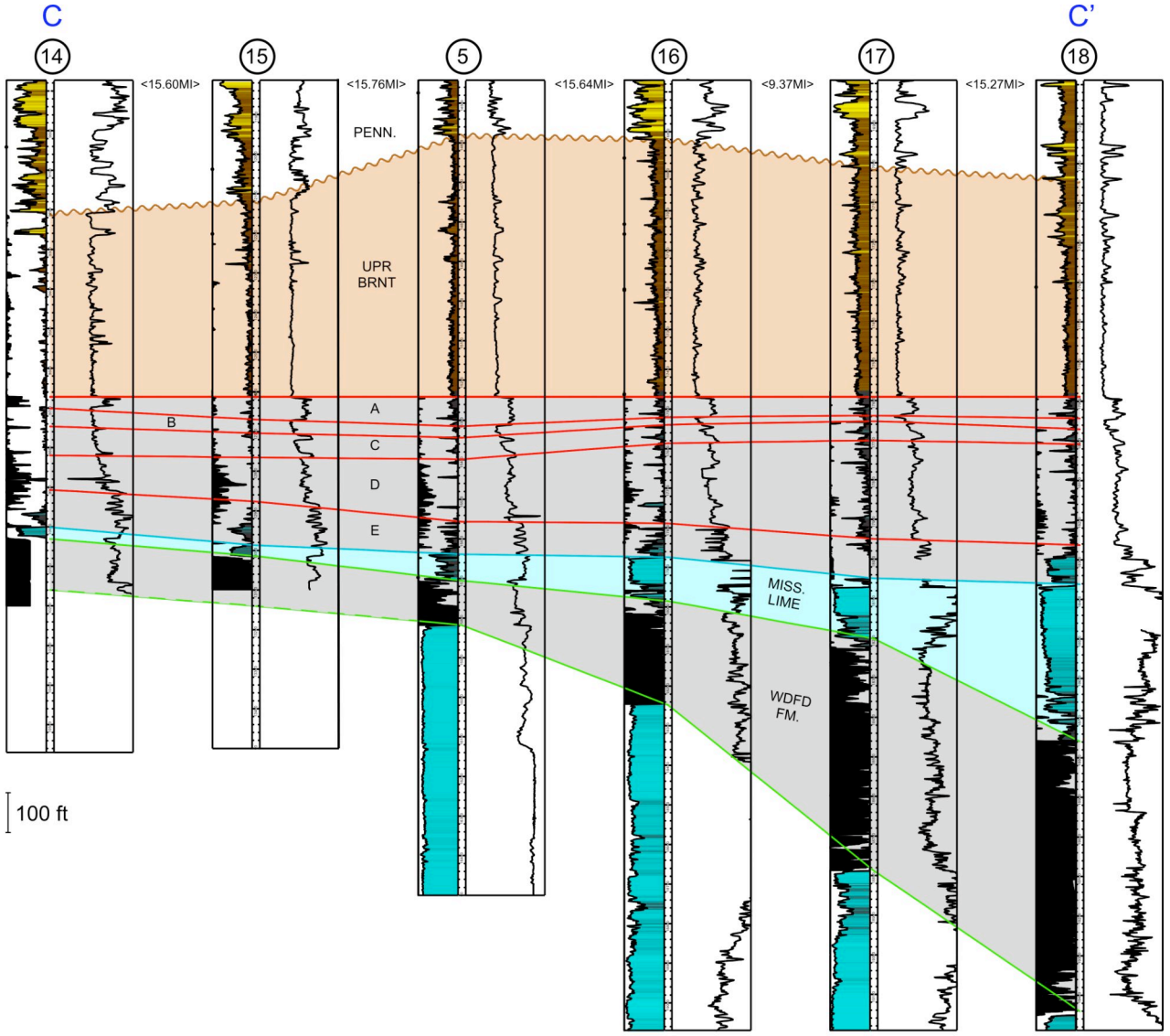

Figure 9. Cross section C-C' showing variation in thickness of stratigraphic units in dip direction from west to east across the central portion of the study area. See Figure 2 for cross section location.

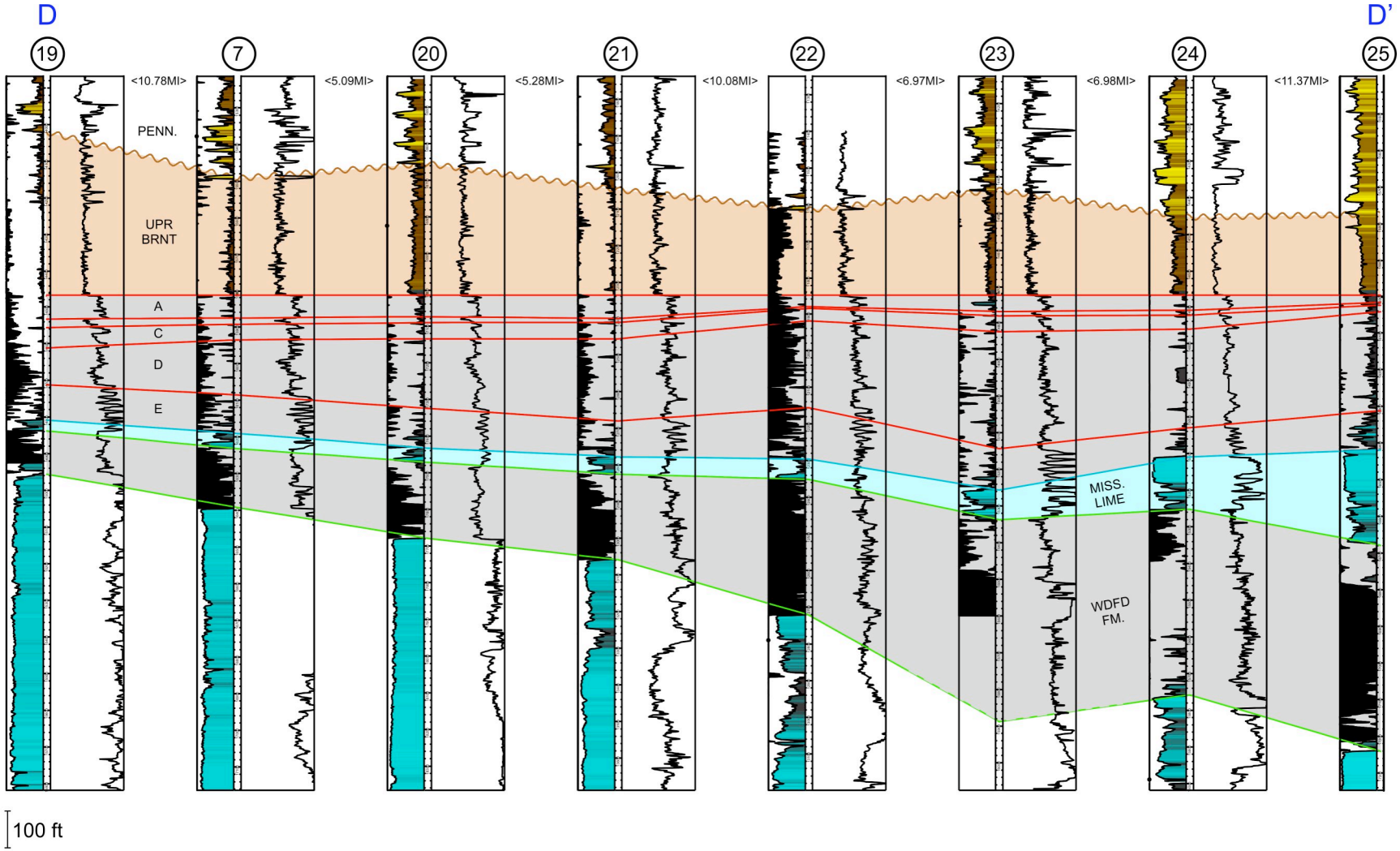

Figure 10. Cross section D-D' showing variation in thickness of stratigraphic units in dip direction from west to east in the southern portion of the study area. See Figure 2 for cross section location.

clastics. The thickness of the upper Barnett seen on the cross sections represents its original depositional thickness as modified by compaction and Late Mississippian/Early Pennsylvanian erosion. Nowhere in the study area does the pre-Pennsylvanian unconformity cut entirely through the upper Barnett. The thickness of the lower Barnett and Mississippian lime seen on the cross sections and isopach maps represents their original depositional thickness modified only by compaction.

The Mississippian section increases in thickness from 400 feet (133 meters) in the southwest portion of the study area to more than 2,000 feet (666 meters) in the northeast corner (Fig. 11). The Mississippian lime and the Barnett Shale both contribute to this increase. The Mississippian lime increases from approximately 6 feet (2 meters) to more than 500 feet (166 meters) (Fig. 12). Most of this increase takes place across a hinge line trending NW-SE through southeastern Eddy County, New Mexico, and western Loving and Ward Counties, Texas. The rapid thickening of the limestone across this hinge line may indicate an area of more rapid subsidence and greater deposition during the Middle Mississippian. The isopach map of the lower Barnett shows an increase in thickness from about 200 feet (66 meters) in southwestern Culberson County to more than 700 feet (233 meters) in southwestern Eddy County (Fig. 13). A striking increase in the thickness of interval D seems to account for the greater thickness of the lower Barnett seen on the eastern side of the study area (Figs. 8, 9 and 10). This interval has a higher gamma-ray count and higher TOC content than the other subunits of the lower Barnett (see below). Isopach maps of the subunits of the lower Barnett can be found in Appendix I. The upper Barnett is the thickest of the Mississippian units in the study area. It reaches a maximum thickness of almost 1,200 feet (400 meters) in northeastern Loving County (Fig. 14). A

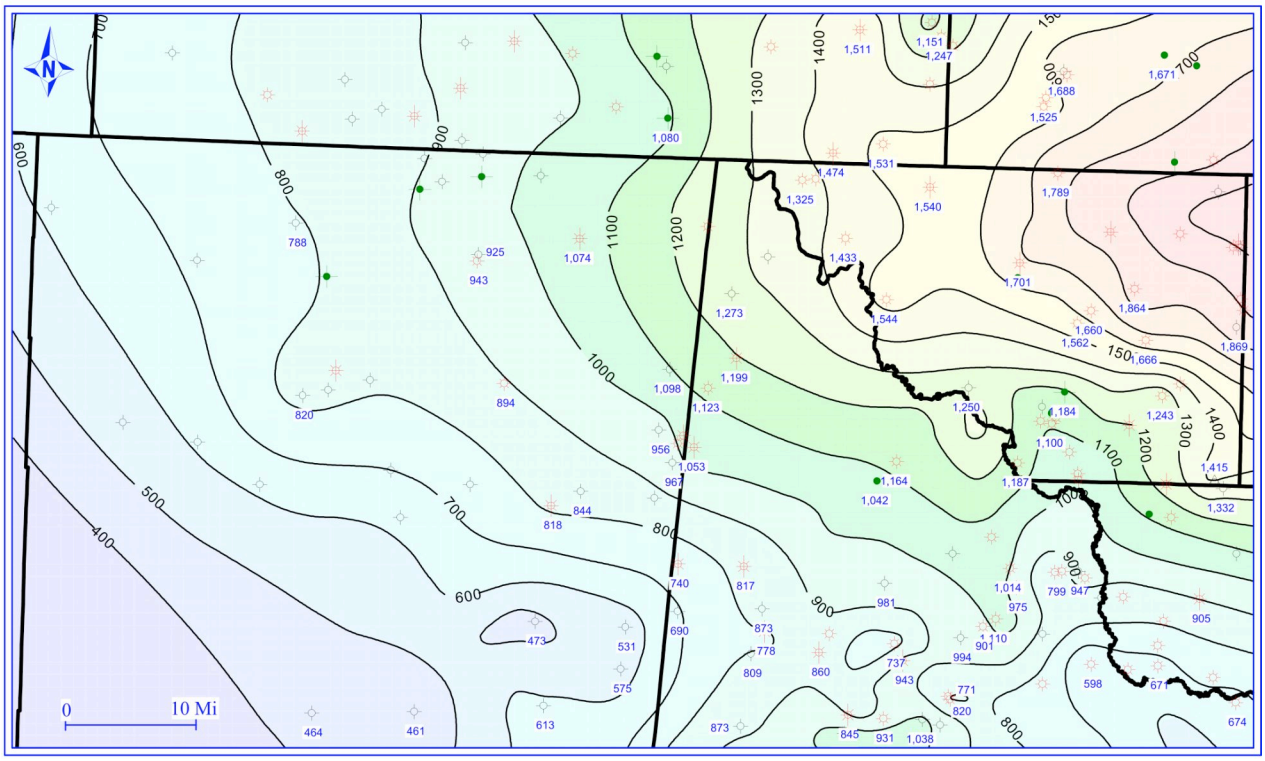

Figure 11. Isopach map for the Mississippian. Values (ft) posted for wells where an isopach thickness was measured. Contour interval, 100 feet.

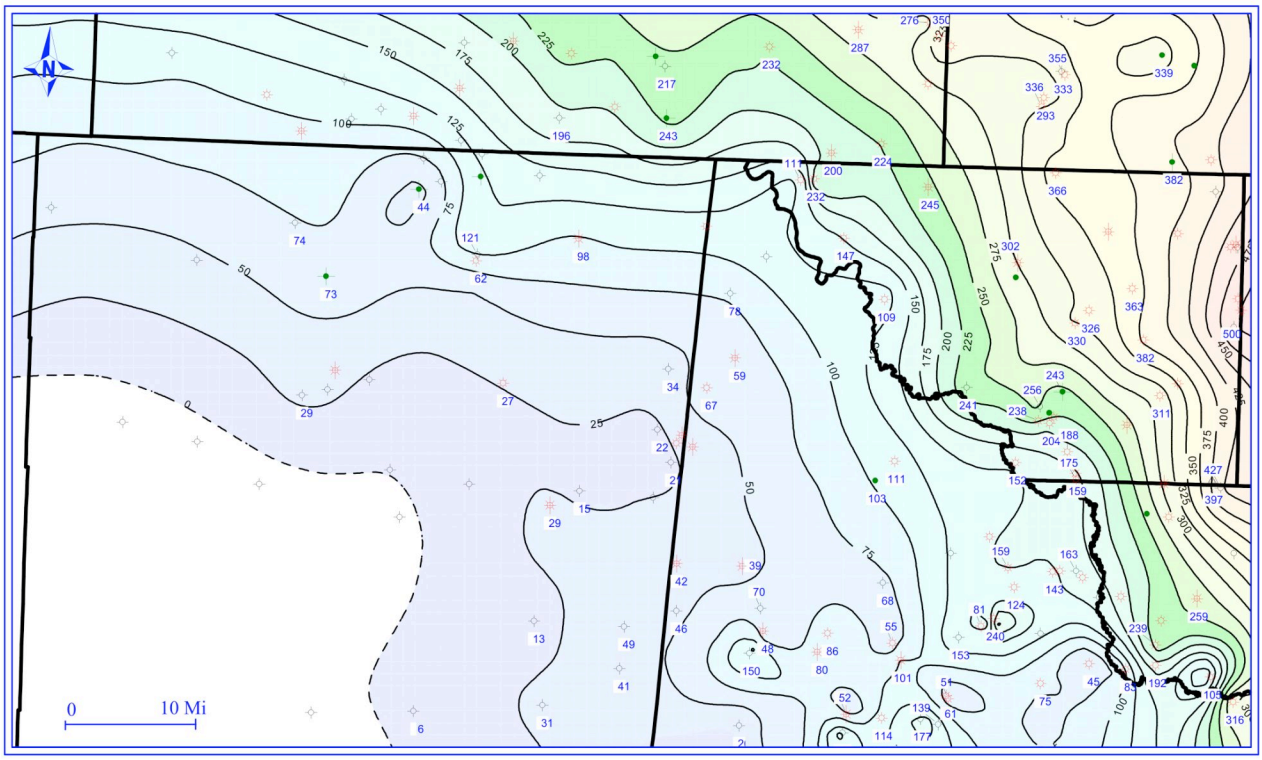

Figure 12. Isopach map of the Mississippian limestone. Values posted for wells where an isopach thickness was measured. Contour interval, 25 feet.

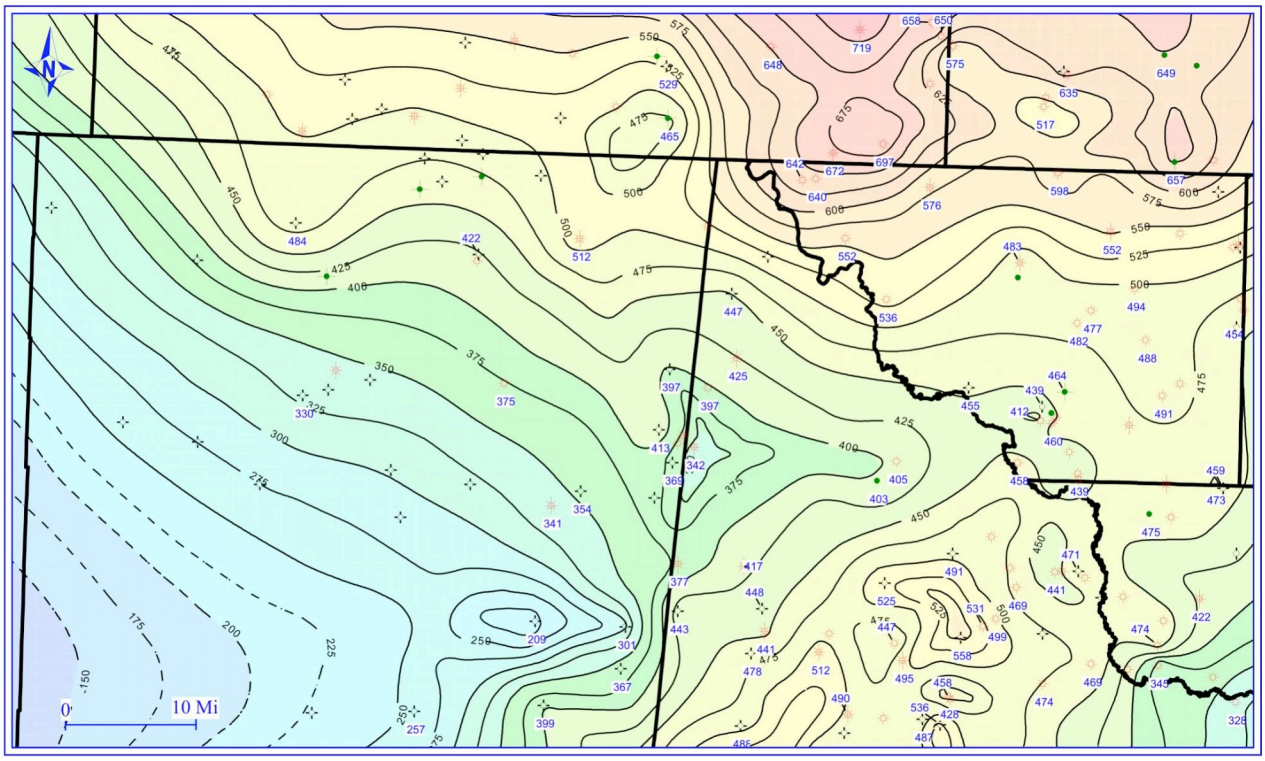

Figure 13. Isopach map of the lower Barnett. Values posted for wells where an isopach thickness was measured. Contour interval, 25 feet.

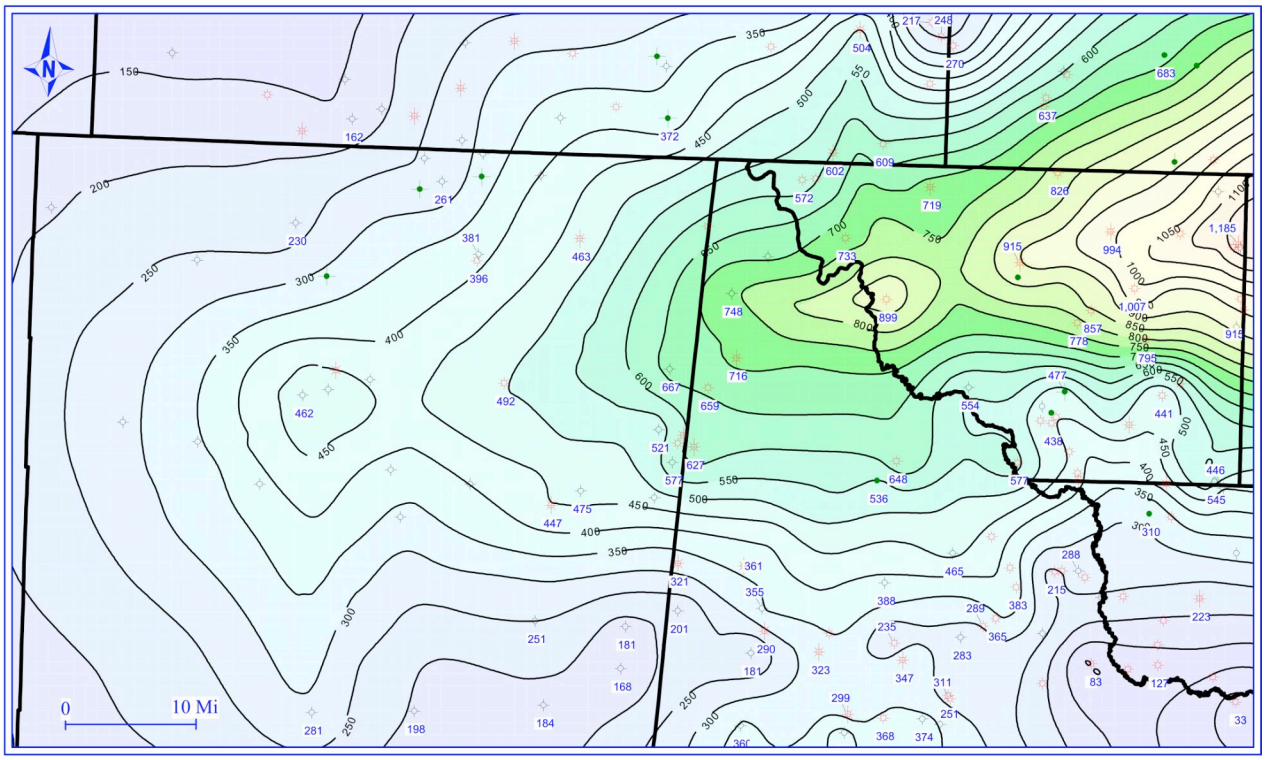

Figure 14. Isopach map of the upper Barnett. Values (ft) posted for wells where an isopach thickness was measured. Contour interval, 50 feet.

pronounced isopach thick opening toward the east trends nearly east-west across northern Loving, Reeves and Culberson counties.

Regional Context

Wright (1979) recognizes two major depositional settings for Mississippian strata in the Permian basin--a limestone shelf to the north and a shale basin to the south (Fig. 15). The shallow-water shelf limestones thin basinward and grade into deeper water limestones and then into the basinal black shales of the Barnett. According to Wright (1979), the shale facies reaches a maximum thickness in northern Reeves and Loving Counties, Texas and southern Eddy and southeastern Lea Counties, New Mexico. The eastern edge of the shale basin was defined by the ancestral Central basin platform. The Diablo uplift and Pedernal massif were positive elements, which shed sediments into the Mississippian seaway.

The general west-to-east thickening of the Mississippian intervals seen on the isopach maps (Figs. 11, 12, 13 and 14) mirrors the isopach changes mapped by Wright (1979). The east-west-trending isopach thicks in the northeast portion of the study area correlate with the Mississippian depocenter of the ancestral Tobosa Basin (Fig. 15). The southwest-to-northeast-trending increases in thickness seen on the isopach maps also reflect an increasing thickness toward the Mississippian depocenter.

Petrology

I had no access to core, but I obtained mud logs and cuttings for five wells from the Texas Bureau of Economic Geology (Fig. 16, Table 2). I analyzed the cuttings in all five wells. The M. G. Nevill #1 and the Ross Draw Unit #5 were chosen for more detailed petrologic analysis because both wells had porosity logs available. Samples from

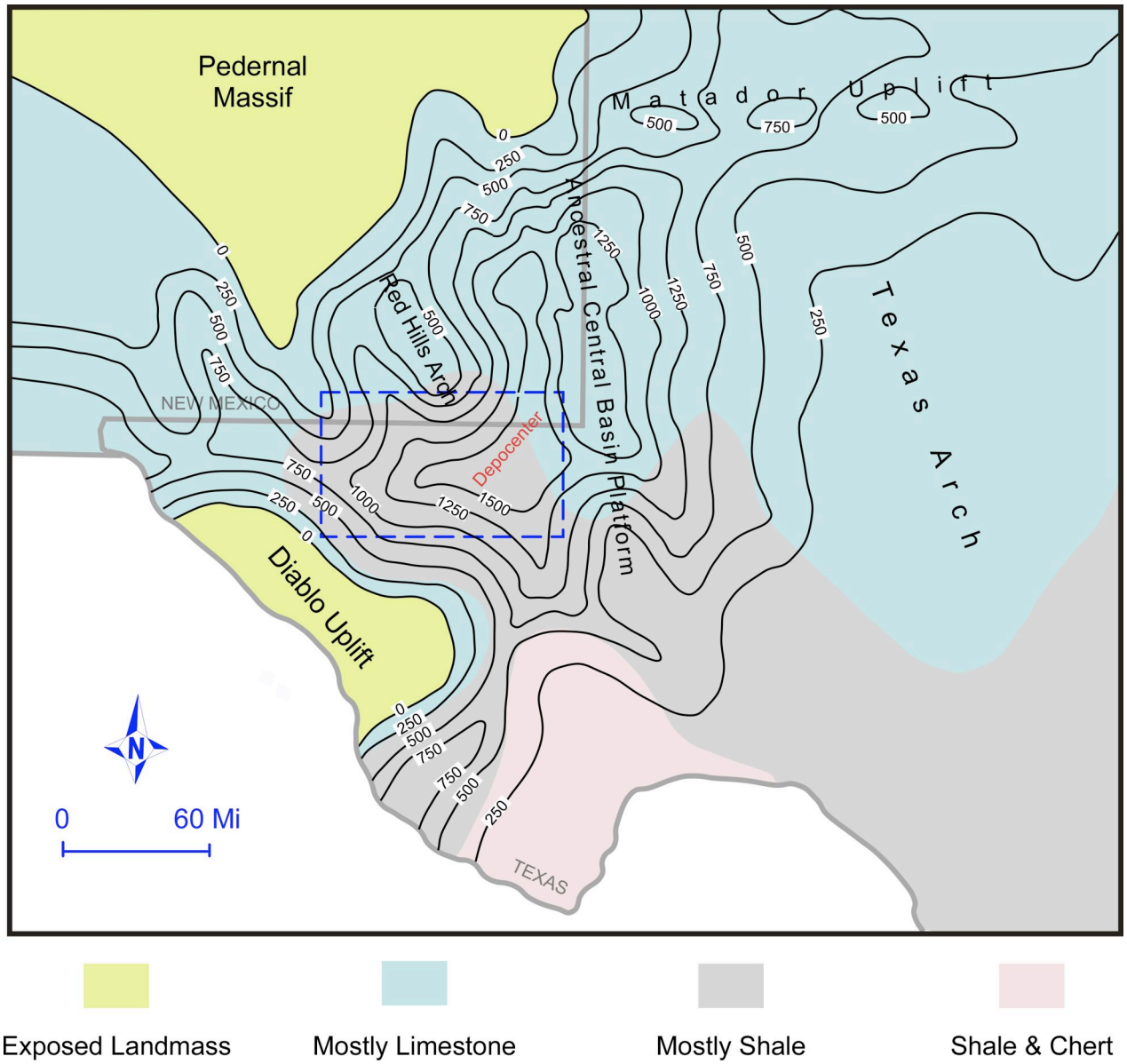

Figure 15. Paleogeographic map showing exposed landmasses and lithofacies distribution patterns in the Permian basin region during the Mississippian. Isopach map shows that the greatest thickness of Mississippian strata accumulated in the eastern portion of the study area (dashed blue box). Contour interval, 250 feet. After Wright (1979).

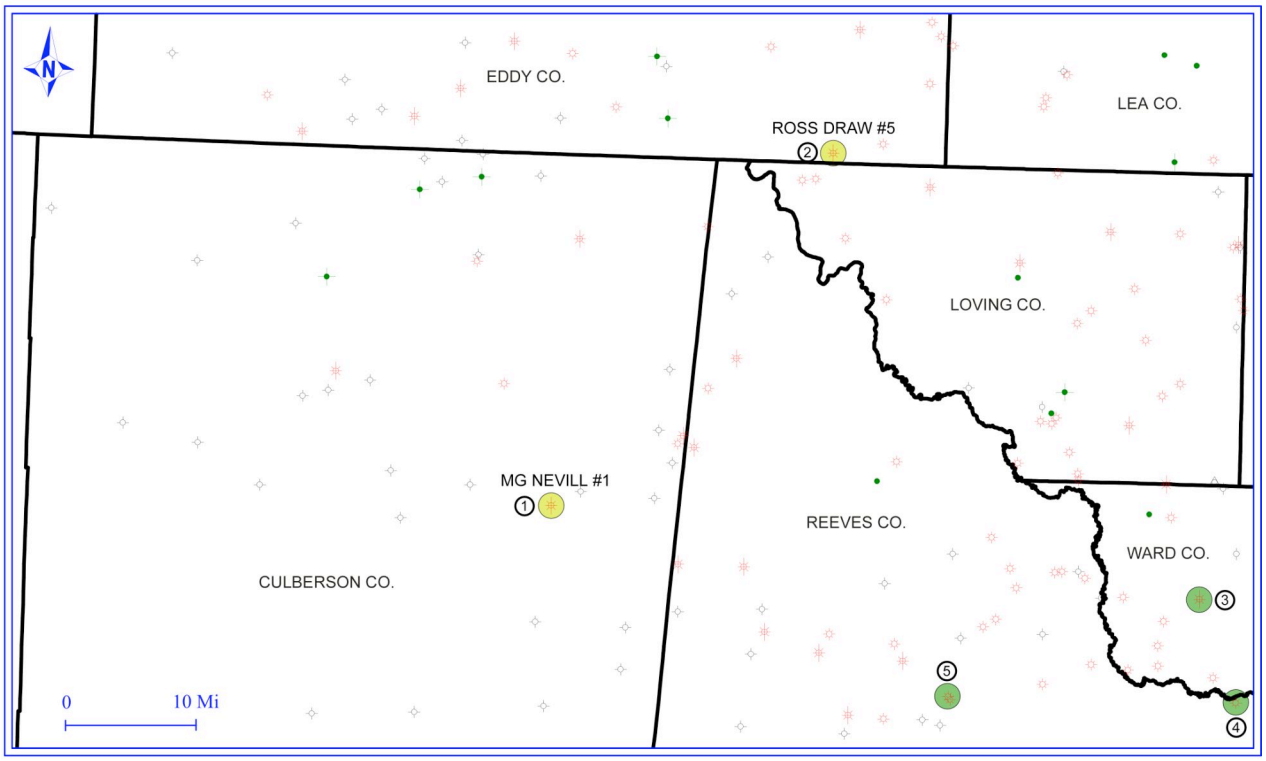

Figure 16. Map showing the location of wells from which cuttings were obtained for visual inspection (wells 1-5) and detailed petrological analysis (wells 1 and 2). See Table 2 for list of wells.

Table 2. Wells from which cuttings were obtained for visual inspection and detailed petrological analysis.

Location Number	Well Serial Number (APINum)	County	Operator	Well Name	Well Number	Well Description	WELL TD (ft)
1	42109308240000	CULBERSON	TEXAS PACIFIC OIL CO	M G NEVILL	1	Abandoned Gas	16000
2	30015218770000	EDDY	PENROC OIL CORP	ROSS DRAW UNIT	5	Abandoned Gas	16326
3	42475300900000	WARD	HANLEY COMPANY	BASS-WILLIAMS	1	Abandoned Gas	20891
4	42389301870000	REEVES	ATLANTIC RICHFLD CO	WORSHAM	1	Gas	19854
5	42389005640000	REEVES	TEXAS O&G CORP	TOYAH UNT-ARTHGRSSON	6	Gas	12750

the upper Barnett and lower Barnett intervals A, C, D and E were selected for thin-section, SEM and x-ray diffraction (XRD) analysis (Figs. 17 and 18).

The transition from the dirty, fine-grained sandstone of the Pennsylvanian strata to the silty, gray shale of the upper Barnett was easily recognizable in the cuttings. The amount of silt decreases downward through the upper Barnett. The color of the cuttings changes from dark gray in the upper Barnett to black in the more organic rich and friable lower Barnett. Both the upper Barnett and the lower Barnett contain scattered amounts of pyrite and calcite. The shale cuttings become increasingly calcareous in the lowermost part of the Barnett and transition into the grey, shaley cuttings of the Mississippian lime. There is a sharp contrast between the Mississippian lime and the black shale of the underlying Woodford Formation. See Appendix II for descriptions of cuttings.

Intervals A, C and D in the lower Barnett have distinctive resistivity and neutron porosity responses. Thin-sections made from the cuttings reveal little in terms of a petrologic explanation for these responses. In the M. G. Nevill #1 the three intervals show little variation in lithology (Appendix III). All are composed of organic-rich shale with varying amounts of detrital silt and some pyrite. Pieces of silty shale show distinct laminations that consist of quartz and calcite. Interval D seems to have more carbonaceous shale than intervals A or C. Similar lithologies are present in the three intervals in the Ross Draw Unit #5 (Appendix III). SEM images of cuttings from the three intervals show little difference among them and also fail to provide an explanation for their unique log character. In both wells the SEM images for cuttings from intervals A, C and D show mainly clays with some scattered dolomite rhombs and pyrite framboids (Appendix IV).

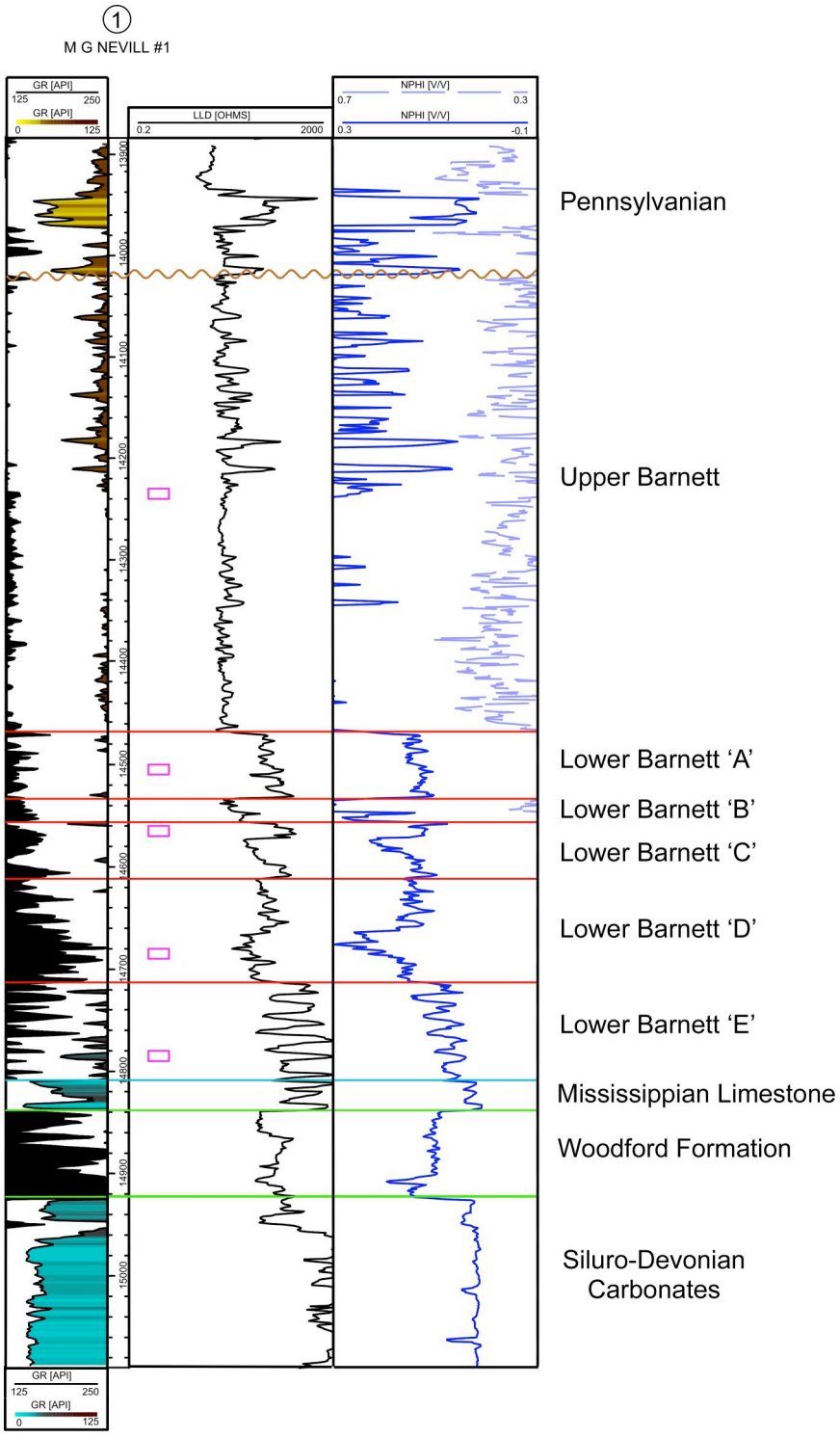

Figure 17. Well-log for the M. G. Nevill #1 showing the intervals sampled for detailed petrologic analysis (pink boxes).

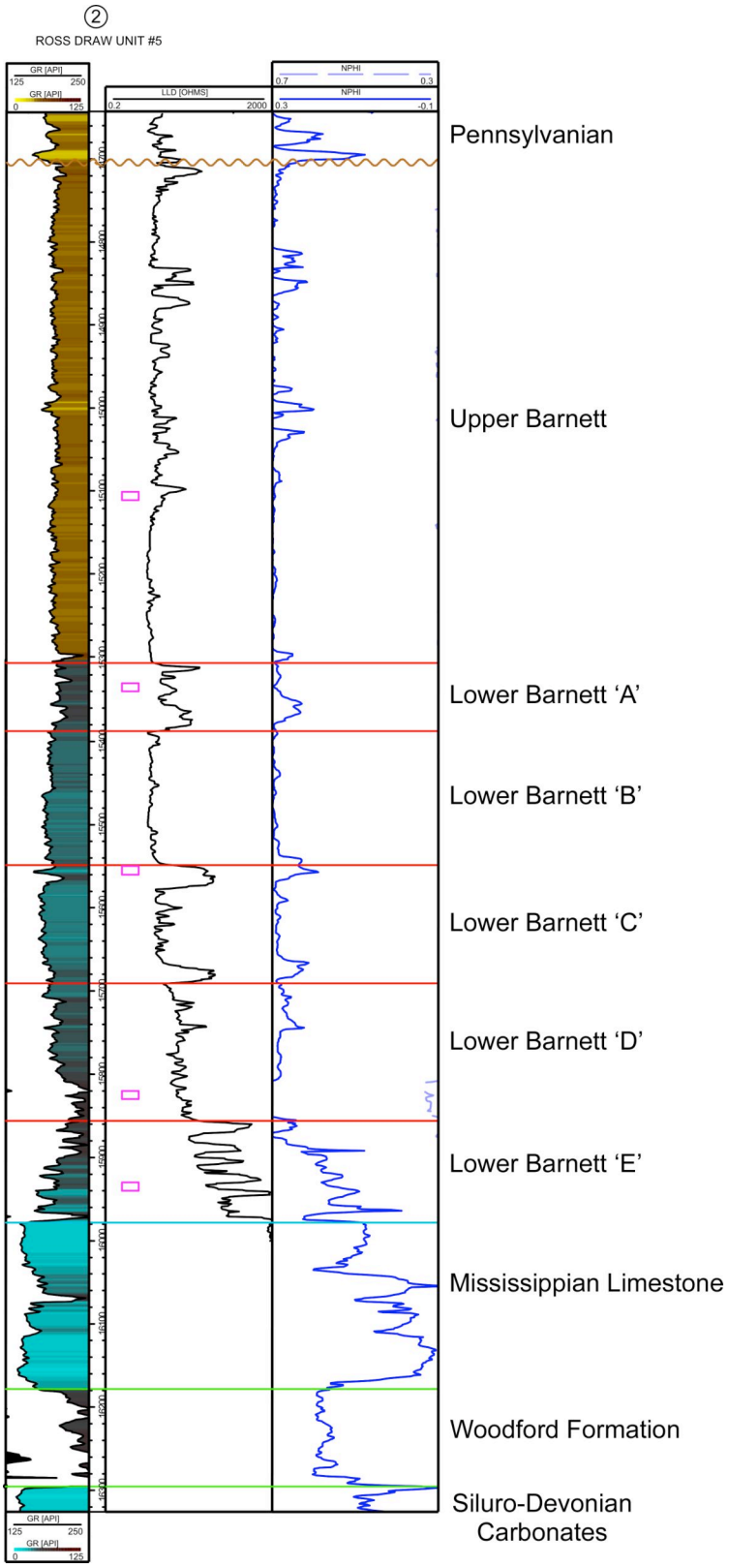

Figure 18. Well-log for the Ross Draw Unit #5 showing the intervals sampled for detailed petrologic analysis (pink boxes).

Cuttings from the upper Barnett and intervals A, C, D and E in the lower Barnett in both the M. G. Nevill #1 and the Ross Draw Unit #5 were analyzed using x-ray diffraction (XRD) techniques. Clays dominate in all the samples (40-60%), followed by quartz (30-50%)—presumably silt—and carbonate material (7-25%) (Tables 3 and 4). The dominant clay types in the two wells are different in all of the intervals tested. Illitic clays dominate in the M. G. Nevill #1 and kaolinitic clays in the Ross Draw Unit #5. Kaolinite is transformed to illite during the course of diagenesis at temperatures of 212-230° F (100-110°C), which lies in the middle of the oil generation window (Burst 1969). The Barnett in the M. G. Nevill #1 is at a shallower depth but has a higher vitrinite reflectance value than the Barnett in the Ross Draw Unit #5 (compare Figs. 5 and 16), suggesting the clays may have been subjected to higher temperatures (see below).

Organic Geochemistry

Samples from ten wells were analyzed to determine the quantity, stratigraphic distribution, type and thermal maturity of organic matter in the Barnett Shale. Samples were taken from the upper Barnett and from intervals A, C, D and E in the lower Barnett in each well. All the samples were analyzed using the Rock-Eval Pyrolysis technique. Samples from five wells were analyzed for this study (Table 5), and data from five additional wells were donated by Dan Jarvie (Humble Geochemical Services) (Figs. 19-22). The organic matter found in the Barnett was primarily Type II marine algal kerogen based on visual inspection during maturity analysis.

The lower Barnett has higher average total organic carbon (TOC) than the upper Barnett (Table 5). Interval D has the highest average TOC of any of the intervals in the lower Barnett. It averages 4.40 weight percent TOC. TOC values from the Barnett Shale in the Fort Worth basin average about 4% (Montgomery *et. al.* 2005). Interval D typically

Table 3. X-ray diffraction data for the M. G. Nevill #1 showing the wt. % of various mineral fractions for each depth interval given below. Upper, upper Barnett; A, C, D and E, intervals in the lower Barnett. See Figure 16 for well location and Figure 17 for intervals sampled.

OMNI LABORATORIES, INC.
X-RAY DIFFRACTION
(WEIGHT %)

Well: MG Nevill No. 1
Area: Culberson County, Texas
Sample Type: Cuttings

File No: G-34596
Date: 01/27/06
Analyst: G. Walker

	Sample	CLAYS				CARBONATES			OTHER MINERALS						TOTALS		
	Depth (ft)	Chlorite	Kaolinite	Illite	Mx I/S*	Calcite	Dol/Ank	Siderite	Quartz	K-spar	Plag.	Pyrite	Zeolite	Barite	Clays	Carb.	Other
Upper	14230-14240	8	5	29	10	1	6	1	35	1	2	2	0	0	52	8	40
A	14510-14520	7	4	37	9	0	4	7	26	2	2	2	0	0	57	11	32
C	14570-14580	5	4	32	8	2	4	2	36	2	3	2	0	0	49	8	43
D	14690-14700	4	3	26	6	3	6	2	41	3	4	2	0	0	39	11	50
E	14780-14790	3	2	19	5	13	9	3	31	4	9	2	0	0	29	25	46
	AVERAGE	5	4	28	8	4	6	3	34	2	4	2	0	0	45	13	42

* Randomly interstratified mixed-layer illite/smectite
¹ May include the Fe-rich variety

Table 4. X-ray diffraction data for the Ross Draw Unnit #5 showing the wt. % of various mineral fractions for each depth interval given below. Upper, upper Barnett; A, C, D and E, intervals in the lower Barnett. See Figure 16 for well location and Figure 18 for intervals sampled.

OMNI LABORATORIES, INC.
X-RAY DIFFRACTION
(WEIGHT %)

Well: Ross Draw Unit No. 5
Area: Eddy County, Texas
Sample Type: Cuttings

File No: G-34596
Date: 01/27/06
Analyst: G. Walker

	Sample	CLAYS				CARBONATES			OTHER MINERALS						TOTALS		
	Depth (ft)	Chlorite	Kaolinite	Illite	Mx I/S*	Calcite	Dol/Ank	Siderite	Quartz	K-spar	Plag.	Pyrite	Zeolite	Barite	Clays	Carb.	Other
Upper	15100-15110	6	22	9	12	4	3	3	35	2	2	2	0	Tr	49	10	41
A	15340-15350	9	24	13	12	2	5	3	28	1	2	1	0	0	58	10	32
C	15560-15570	8	27	12	13	1	2	4	29	1	2	1	0	0	60	7	33
D	15820-15830	8	21	20	13	3	2	3	23	2	3	2	0	0	62	8	30
E	15940-15950	6	21	14	10	8	3	3	29	2	3	1	0	0	51	14	35
	AVERAGE	7	23	14	12	4	3	3	29	2	2	1	0	Tr	56	10	34

* Randomly interstratified mixed-layer illite/smectite
¹ May include the Fe-rich variety

Table 5. Rock-eval pyrolysis and vitrinite reflectance data. UPR, upper Barnett; A, C, D and E, intervals in the lower Barnett; WDFD, Woodford Formation. See Figure 16 for well locations.

Location Number	API Number	Well Name	County	State	Depth (ft.)	Zone	Leco TOC	S1	S2	S3	S1/S2	Tmax (°C)		Cal. %Ro	Meas. %Ro	HI	OI	S2/S3	S1/TOC	PI
1	42109308240000	M G Nevill #1	Culberson	TX	14230	UPR	3.19	0.75	0.41	0.17	1.83	318	*	-1.00		13	5	2	24	0.65
	42109308240000	M G Nevill #1	Culberson	TX	14500	A	2.21	0.31	0.50	0.29	0.62	333	*	-1.00	1.91	23	13	2	14	0.38
	42109308240000	M G Nevill #1	Culberson	TX	14560	C	4.88	1.16	0.81	0.40	1.43	318	*	-1.00		17	8	2	24	0.59
	42109308240000	M G Nevill #1	Culberson	TX	14680	D	4.82	1.26	0.79	0.29	1.59	319	*	-1.00	1.93	16	6	3	26	0.61
	42109308240000	M G Nevill #1	Culberson	TX	14780	E	3.53	1.30	0.75	0.37	1.73	318	*	-1.00		21	10	2	37	0.63
	42109308240000	M G Nevill #1	Culberson	TX	14920	WDFD	3.50	1.35	1.09	0.18	1.24	324	*	-1.00	2.17	31	5	6	39	0.55
2	30015218770000	Ross Draw Unit #5	Eddy	NM	15100	UPR	1.61	0.20	0.58	0.47	0.34	401	*	0.06		36	29	1	12	0.26
	30015218770000	Ross Draw Unit #5	Eddy	NM	15330	A	1.79	0.34	0.49	0.27	0.69	326	*	-1.00	1.88	27	15	2	19	0.41
	30015218770000	Ross Draw Unit #5	Eddy	NM	15550	C	1.74	0.29	0.36	0.33	0.81	382	*	-1.00		21	19	1	17	0.45
	30015218770000	Ross Draw Unit #5	Eddy	NM	15820	D	2.96	0.80	0.55	0.27	1.45	317	*	-1.00	2.19	19	9	2	27	0.59
	30015218770000	Ross Draw Unit #5	Eddy	NM	15930	E	3.01	0.74	0.34	0.18	2.18	316	*	-1.00		11	6	2	25	0.69
3	42475300900000	Bass-Williams #1	Ward	TX	15850	UPR	1.95	0.39	0.49	0.35	0.80	323	*	-1.00		25	18	1	20	0.44
	42475300900000	Bass-Williams #1	Ward	TX	16000	A	3.86	1.26	1.14	0.48	1.11	318	*	-1.00	1.63	30	12	2	33	0.53
	42475300900000	Bass-Williams #1	Ward	TX	16030	C	3.92	0.97	0.93	0.43	1.04	317	*	-1.00		24	11	2	25	0.51
	42475300900000	Bass-Williams #1	Ward	TX	16250	D	5.86	1.33	1.05	0.71	1.27	318	*	-1.00	1.54	18	12	1	23	0.56
	42475300900000	Bass-Williams #1	Ward	TX	16390	E	1.73	0.52	0.54	0.35	0.96	321	*	-1.00		31	20	2	30	0.49
	42475300900000	Bass-Williams #1	Ward	TX	16990	WDFD	6.54	1.40	0.91	0.48	1.54	318	*	-1.00	2.07	14	7	2	21	0.61
4	42389301870000	Worsham #1	Reeves	TX	15040	C	3.66	1.25	0.96	0.26	1.30	466		1.23	1.61	26	7	4	34	0.57
	42389301870000	Worsham #1	Reeves	TX	15270	D	3.88	0.95	0.83	0.24	1.14	316	*	-1.00	1.60	21	6	3	24	0.53
	42389301870000	Worsham #1	Reeves	TX	15340	E	2.02	0.99	0.50	0.19	1.98	312	*	-1.00		25	9	3	49	0.66
	42389301870000	Worsham #1	Reeves	TX	15960	WDFD	5.48	0.85	0.87	0.76	0.98	336	*	-1.00	1.75	16	14	1	16	0.49
5	42389005640000	Toyh Unt-Arthgrsson #6	Reeves	TX	11320	UPR	3.92	1.07	0.77	0.19	1.39	485		1.57		20	5	4	27	0.58
	42389005640000	Toyh Unt-Arthgrsson #6	Reeves	TX	11500	A	3.60	0.74	0.60	0.30	1.23	428	*	0.54	1.39	17	8	2	21	0.55
	42389005640000	Toyh Unt-Arthgrsson #6	Reeves	TX	11540	C	3.75	0.76	0.65	0.21	1.17	437	*	0.71		17	6	3	20	0.54
	42389005640000	Toyh Unt-Arthgrsson #6	Reeves	TX	11770	D	3.32	1.12	0.60	0.19	1.87	386	*	-1.00	1.46	18	6	3	34	0.65
	42389005640000	Toyh Unt-Arthgrsson #6	Reeves	TX	11890	E	3.57	1.07	0.63	0.24	1.70	310	*	-1.00		18	7	3	30	0.63

Note: "-1" indicates not measured or meaningless ratio

* Tmax data not reliable due to poor S2 peak

TOC = weight percent organic carbon in rock
S1, S2 = mg hydrocarbons per gram of rock
S3 = mg carbon dioxide per gram of rock
Tmax = °C

HI = hydrogen index = S2 x 100 / TOC
OI = oxygen index = S3 x 100 / TOC
S1/TOC = normalized oil content = S1 x 100 / TOC
PI = production index = S1 / (S1+S2)
Calculcated%VRo = 0.0180 x Tmax - 7.16 (Jarvie et al., 2001)
Measured %Ro = measured vitrinite reflectance

Notes:
c = Rock-Eval analysis checked and confirmed
lc = Leco TOC analysis checked and confirmed

Pyrogram:
n=normal
ltS2sh = low temperature S2 shoulder
ltS2p = low temperature S2 peak
htS2p = high temperature S2 peak
f = flat S2 peak
na = printer malfunction pyrogram not available

Humble Geochemical Services Division

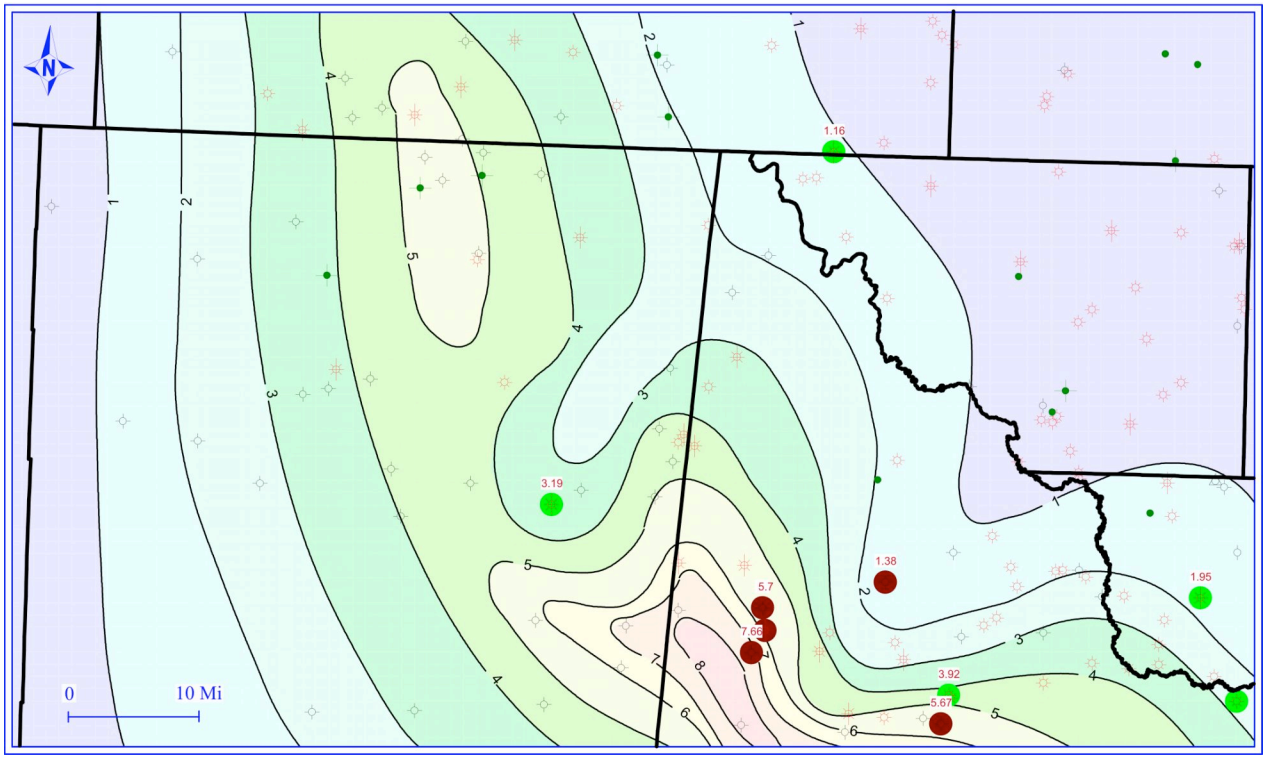

Figure 19. Weight-percent TOC in the upper Barnett. Colored circles show wells with available data. Data from wells shown in red made available by Dan Jarvie, Humble Geochemical Services. Contour Interval, 1 wt. % TOC.

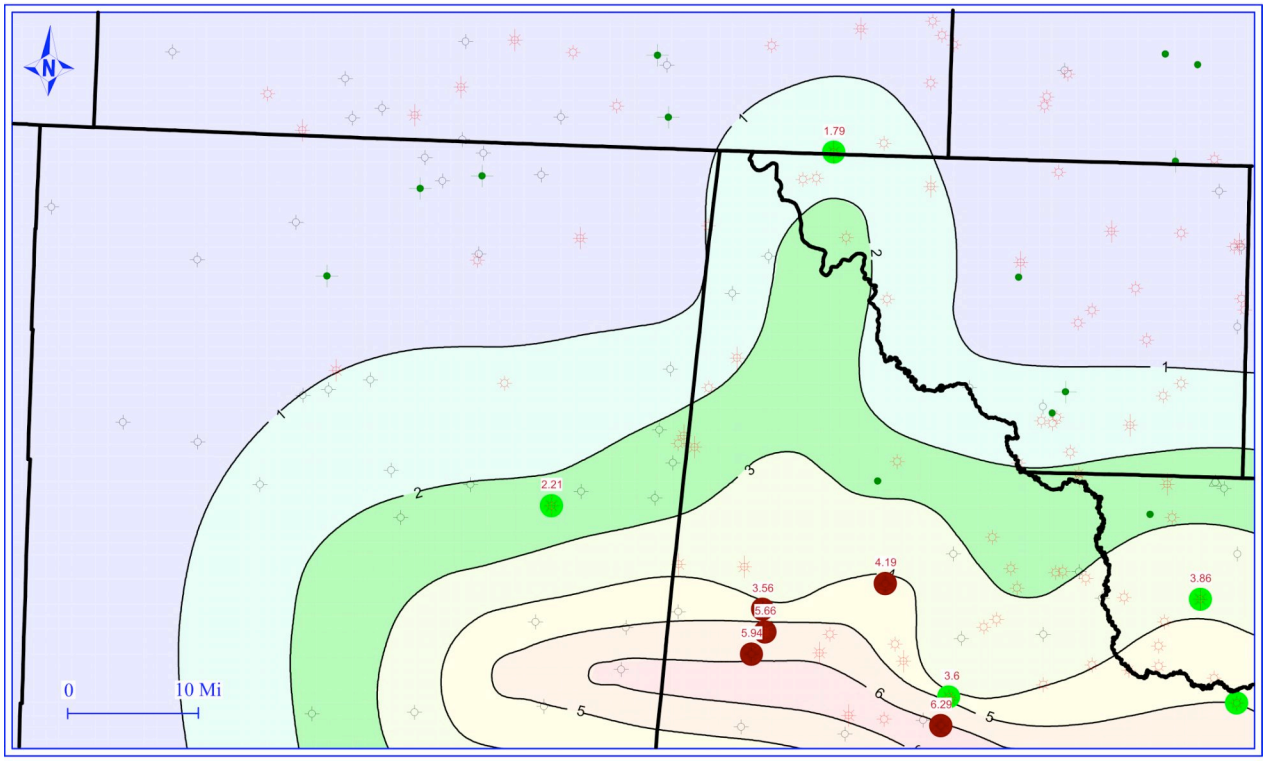

Figure 20. Weight-percent TOC in the lower Barnett interval A. Colored circles show wells with available data. Data from wells shown in red made available by Dan Jarvie, Humble Geochemical Services. Contour Interval, 1 wt. % TOC.

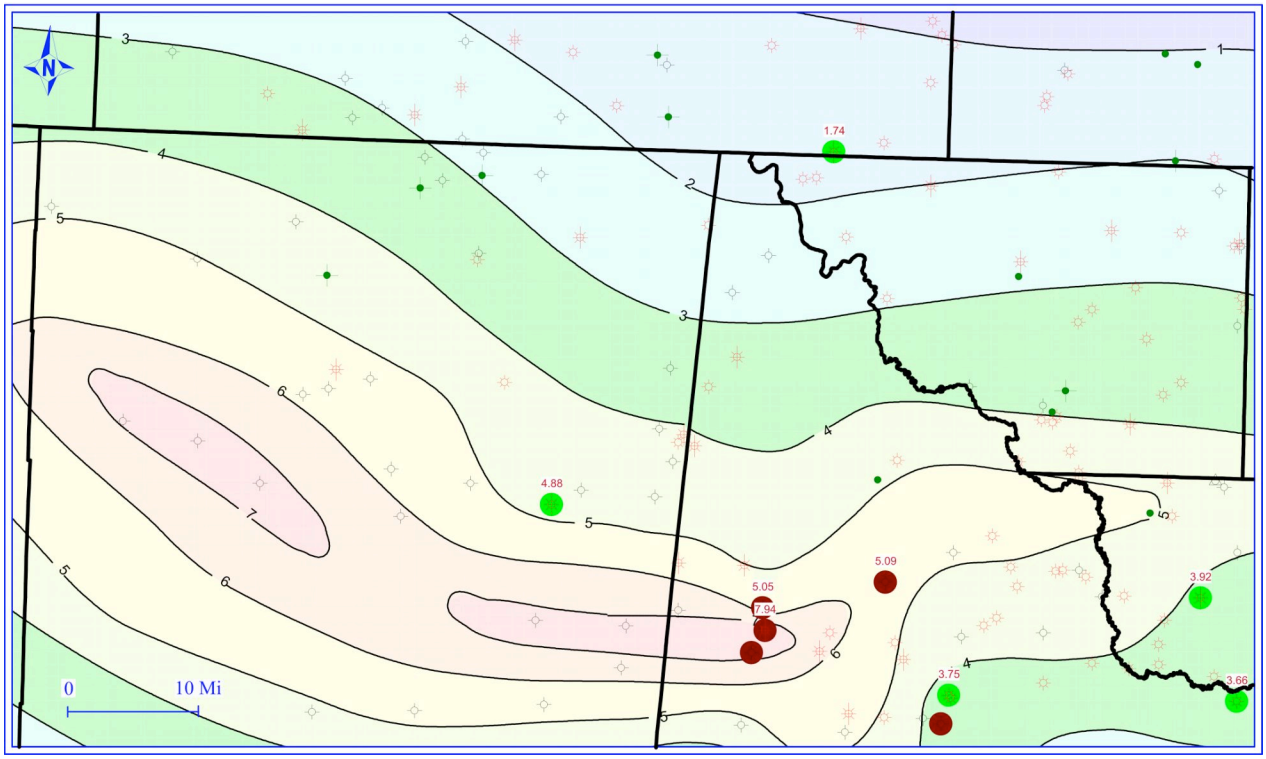

Figure 21. Weight-percent TOC in the lower Barnett interval C. Colored circles show wells with available data. Data from wells shown in red made available by Dan Jarvie, Humble Geochemical Services. Contour Interval, 1 wt. % TOC.

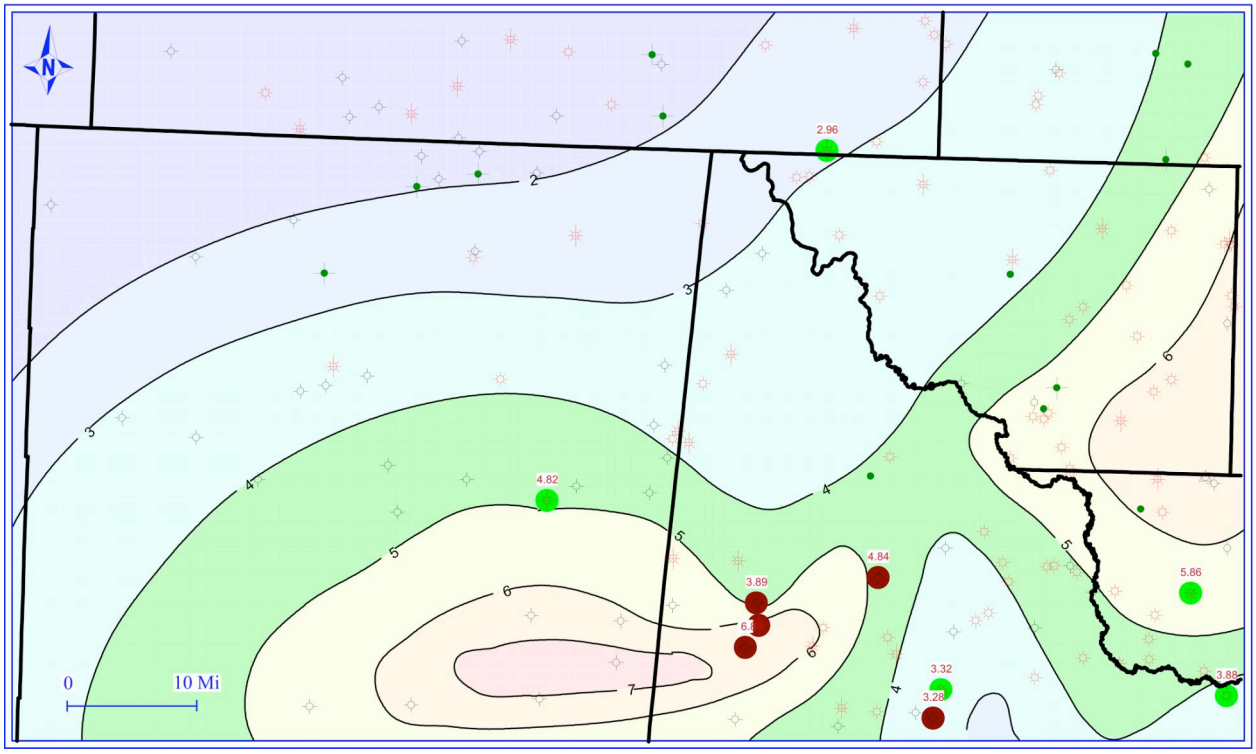

Figure 22. Weight-percent TOC in the lower Barnett interval D. Colored circles show wells with available data. Data from wells shown in red made available by Dan Jarvie, Humble Geochemical Services. Contour Interval, 1 wt. % TOC.

has higher gamma-ray counts than the other intervals in the lower Barnett. Statistically, the correlation between TOC and gamma-ray count was weak, but as a rule of thumb, TOC increases with the gamma-ray count.

TOC values calculated from combined resistivity and porosity log responses following Passey *et al.* (1990) do not match the measured values in the wells in the study area. Perhaps this was due to mixing in the 10-foot sampling interval. The amount of TOC within each interval varied across the study area. Samples from the northernmost well have the lowest TOC values for each of the intervals sampled, while TOC values from wells in the southern part of the study area are typically higher (Figs. 19-22). No correlation was found between the thickness of the stratigraphic intervals and TOC values.

The increase in TOC towards the south may reflect higher production and/or better preservation of organic matter in the southern part of the study area at the time of deposition. The southern portion of the study area was in a more distal location with respect to the Mississippian depocenter than the northern portion (Wright 1979). Starved basin conditions may have developed which would have made conditions favorable for the accumulation and preservation of Type II organic matter. Following this reasoning, TOC values should increase south of the study area in the central and south-central portions of the Delaware basin.

Additional organic geochemical data include the amounts of hydrocarbon released as the samples are heated over time. S1 is the first peak measured as the sample is flame ionized. It is proportional to the free hydrocarbons in the sample liberated at 572°F (300°C) (Hunt 1996). The S2 peak is proportional to the hydrocarbon-generating potential as heating continues to 1022°F (550°C). The S1 values are higher than the S2

values for nearly all of the samples analyzed (Table 5). This indicates that the samples contain free hydrocarbons and are thermally mature. The high S1 values also indicate that some of the hydrocarbons that have been generated have not been expelled from the shale (Hunt 1996). The S2 peaks were unusually low, indicating that the samples might have been contaminated with varying amounts of pyrobitumen, and invalidating Tmax, hydrogen Index (HI) and Production Index (PI) calculations (Ruble 2006, personal communication). As kerogen is converted to methane, pyrobitumen is a common by-product as the reaction goes to completion (Hunt 1996). This offers further evidence that the Mississppian shales in study area are mature and have generated hydrocarbons. See Appendix V for the complete geochemical report.

Gas Content

It is difficult to estimate the gas content of the Barnett Shale in the Delaware basin. Few modern porosity logs are available for wells in the study area, and few wells have both density and neutron porosity logs, making it difficult to relate petrologic and geochemical data to log response and gas content. A handful of wells have total gas curves measured from mud logs, which I plotted with the resistivity and porosity curve(s) if available. The majority of these wells show a positive correlation between high gas shows in the lower Barnett and the high resistivity and high neutron porosity (14-18%) packages that comprise intervals A, C and D (Fig. 23).

Kreis and Costa (2005) studied similar high resistivity zones in the Bakken oil-shale play in the Williston Basin. High resistivities in certain members of the Bakken were attributed primarily to the presence of oil, and secondarily to mineralogy, porosity, tortuosity and salinity of the formation waters. This may help explain the correlation

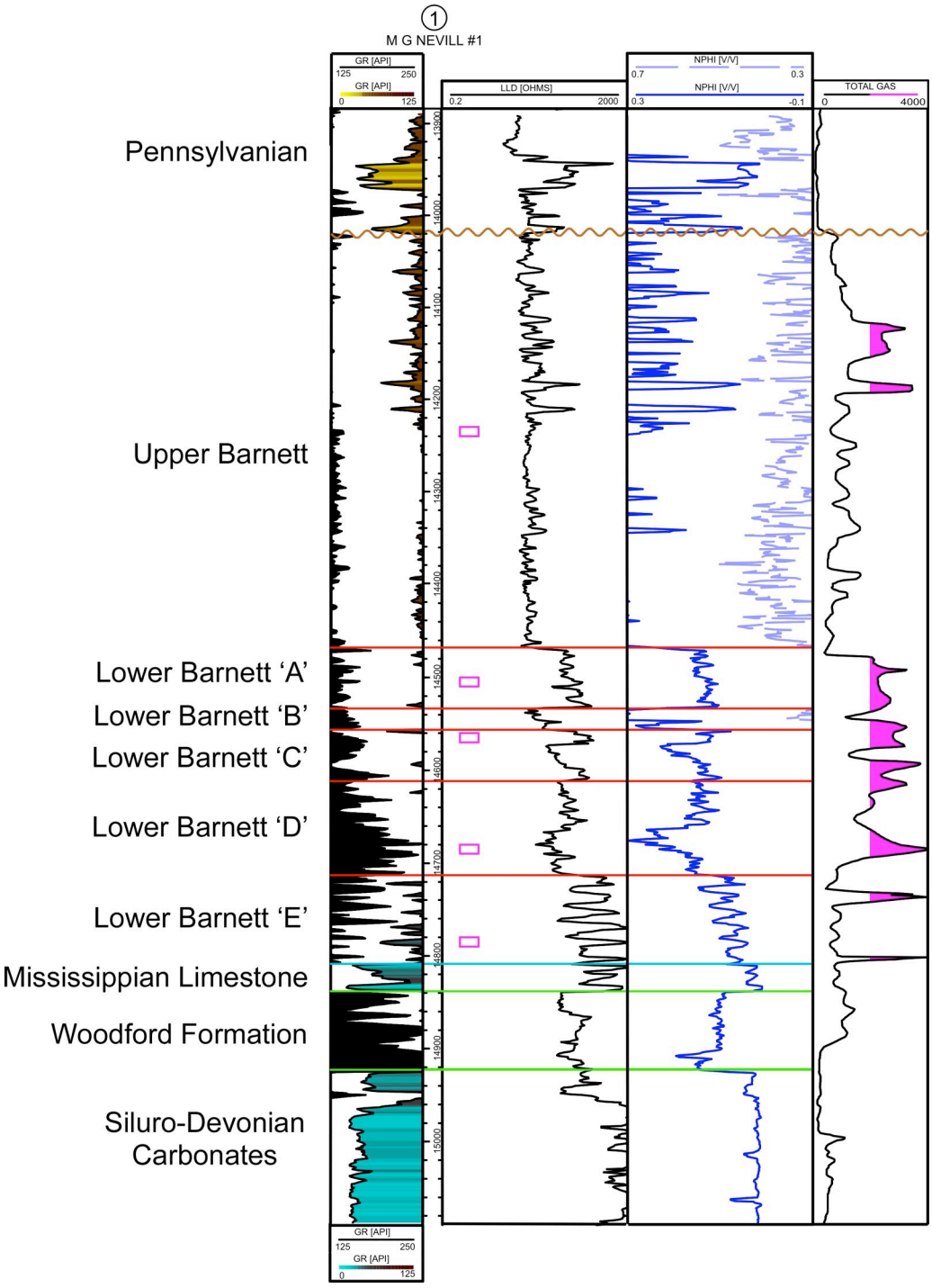

Figure 23. Well-log for the M. G. Nevill #1 showing the total gas curve from the mud log (right) plotted with the neutron porosity curve (NPHI), deep resistivity curve (LLD), and gamma-ray curve (GR). Gas shows greater than 2000 arbitrary units, highlighted in pink.

between gas shows and high resistivity readings found in the lower Barnett. In developing the Bakken play, Kreis and Costa (2005) found it useful to map the net footage of resistivity with values greater than 35 ohmms. Following their practice, I made a net resistivity map that shows some similarity to the maps of TOC in the south-central portion of the study area (compare Fig. 24 with Figs. 19, 20, 21 and 22). I chose a 50 ohmm cutoff and calculated the net footage greater than 50 ohmm from the top of interval A to the top of interval E. I left interval E out of the calculation because the log response there is influenced by the increasingly limy nature of the shale near the contact with the Mississippian lime and not just by the formation fluids. Assuming that the high resistivity readings in the lower Barnett are related to its gas content, and that there is a correlation between the net resistivity and TOC, the gas content can be related to TOC.

Schad (2004) developed a rough relationship between TOC, density, and ultimately the volume of desorbed gas in the Caney Shale (Mississippian) in the Arkoma basin, Oklahoma. Based on the assumption that some portion of the hydrocarbon content in the Barnett is related to TOC, one can estimate the gas in place (GIP) in the lower Barnett in the study area and in other parts of the Delaware basin where the TOC is high. I used this method to estimate the amount of adsorbed GIP in the Barnett Shale in the Delaware basin. Schad (2004) gives the following relationship:

Eqn. 1. Adsorbed shale gas in place (SCF/ton) = (19.866 • TOC (%)) + 10.518

Using a conservative figure of 4% TOC this equation gives a GIP estimate of 11.3 SCF/ton. This can be converted to BCF/square mile using:

Eqn. 2. GIP (BCF/square mile) = 0.002176 • GIP (SCF/ton) • thickness

from Jarvie (2006, personal communication). Using an average thickness of 350 ft for intervals A through D, the equation yields a value of 8.6 BCF/square mile. However, this

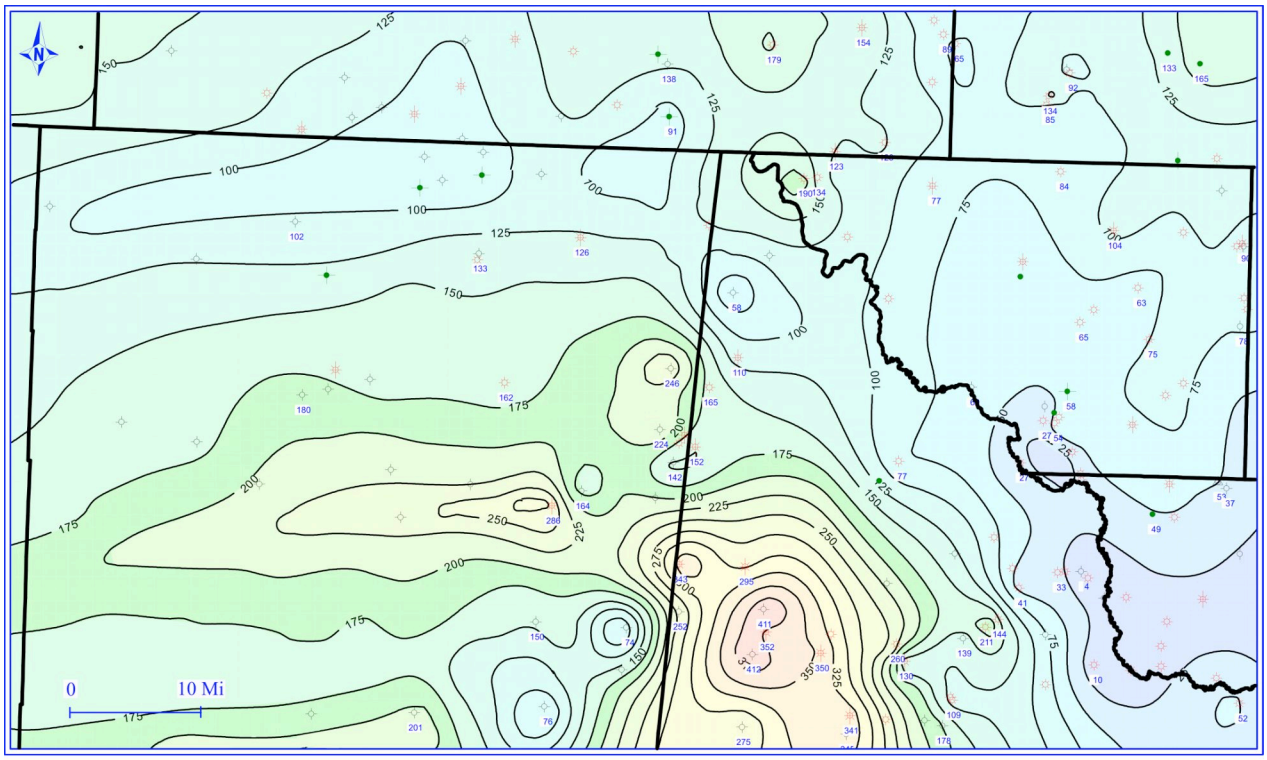

Figure 24. Net resistivity isopach showing the net footage of resistivity greater than 50 ohmms from the top of interval A to the top of interval E in the lower Barnett. Contour interval, 25 feet.

estimate only accounts for the adsorbed gas. To estimate total GIP, both the free gas and the adsorbed gas must be accounted for. Jarvie and Claxton (2002) indicate that free gas accounts for approximately 59% of the total gas in prospective Barnett Shale wells in the Fort Worth basin. Assuming adsorbed gas accounts for 41% of total GIP, a value of 8.6 BCF/square mile for adsorbed gas gives a total GIP of 20.97 BCF/square mile. Applying a 10% recovery factor yields recoverable gas reserves of 2.1 BCF/square mile (2.47 MMCF/acre). This estimate is low compared with total GIP estimates of the Barnett in thermally mature areas in the Fort Worth basin, which are approximately 50-150 BCF/square mile, and have recovery factors ranging from 10% to 15% (Hayden and Pusell 2005). The primary assumptions of my GIP estimates are that the amount of adsorbed gas in place is related to the TOC content by *equation 1* (above), and that the amount of adsorbed gas in place is approximately 41% of the total GIP. Given that *equation 1* was developed in the Arkoma basin, the relationship between TOC and gas in place may not be the same for the Mississippian shale in the Delaware Basin, thus yielding the relatively low total GIP estimate. Also, it is possible that the amount of free gas accounts for greater than 59% of the total GIP. However, this calculation is a useful starting point for estimating total gas volumes for the Barnett in the Delaware basin.

Thermal Maturity

Thermal maturity was measured using vitrinite reflectance of organic matter (%Ro) on 13 samples from 5 wells (Table 5). Nearly all the samples plotted in the dry gas zone of measured maturity (Fig. 25). One well in the southern portion of the study area plotted in the condensate (wet gas) zone. Two wells drilled by Dallas Production immediately south of the study area have produced condensate from the Barnett, implying the shale is not in the gas window in this area. Vitrinite reflectance generally

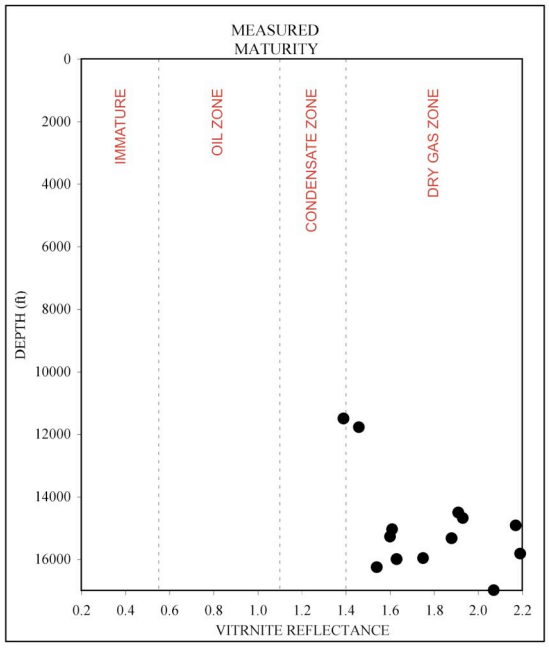

Figure 25. Measured vitrinite reflectance (%Ro) versus depth. See Table 5 for sample locations. Note a general increase in maturity with increasing depth.

increases with depth in the study area (compare Figs. 5 and 26). The deeper, central parts of the basin generally have %Ro values ranging from 1.60 to 2.27. However, the highest vitrinite reflectance values are found to the west, in the shallower part of the basin. These anomalously high %Ro values are likely due to local thermal affects of Tertiary intrusives mapped by Barker and Pawlewicz (1987).

The present-day geothermal gradient was calculated for a number of wells to establish the minimum temperatures to which the rocks have been exposed. Bottom-hole-temperatures (BHT) read from well-logs were corrected for circulation time to provide an estimate of the true BHT. The mean annual surface temperature in the study area is 53°F (12°C) (Hills 1984). The corrected BHT values give an average geothermal gradient of 1.47°F/100 ft (27°C/km) with a correlation coefficient of 90%. The geothermal gradient follows a logarithmic increase to a depth of approximately 8,000 feet (2,666 meters) but increases linearly below that depth (Fig. 27).

The map of the present-day geothermal gradient shows the minimum temperature gradient to which the rocks have been exposed since erosion took place (Fig. 28). The geothermal gradient decreases from west to east toward the basin axis, which indicates that more erosion has taken place there. The area above the Tertiary igneous intrusions has a relatively high geothermal gradient due to the young age of the intrusive bodies, and possibly continued heat flow.

I made a burial history model for the study area using data from the M. G. Nevill #1 and Petromod freeware. Petromod requires a stratigraphic thickness and lithology for each unit in the basin fill (Table 6). Thicknesses and lithologies of the units above the Barnett were taken from Vertrees (1959), Adams (1965), and Frenzel *et al*. (1988). The model assumes a constant heat flow over time, which is related to the thermal

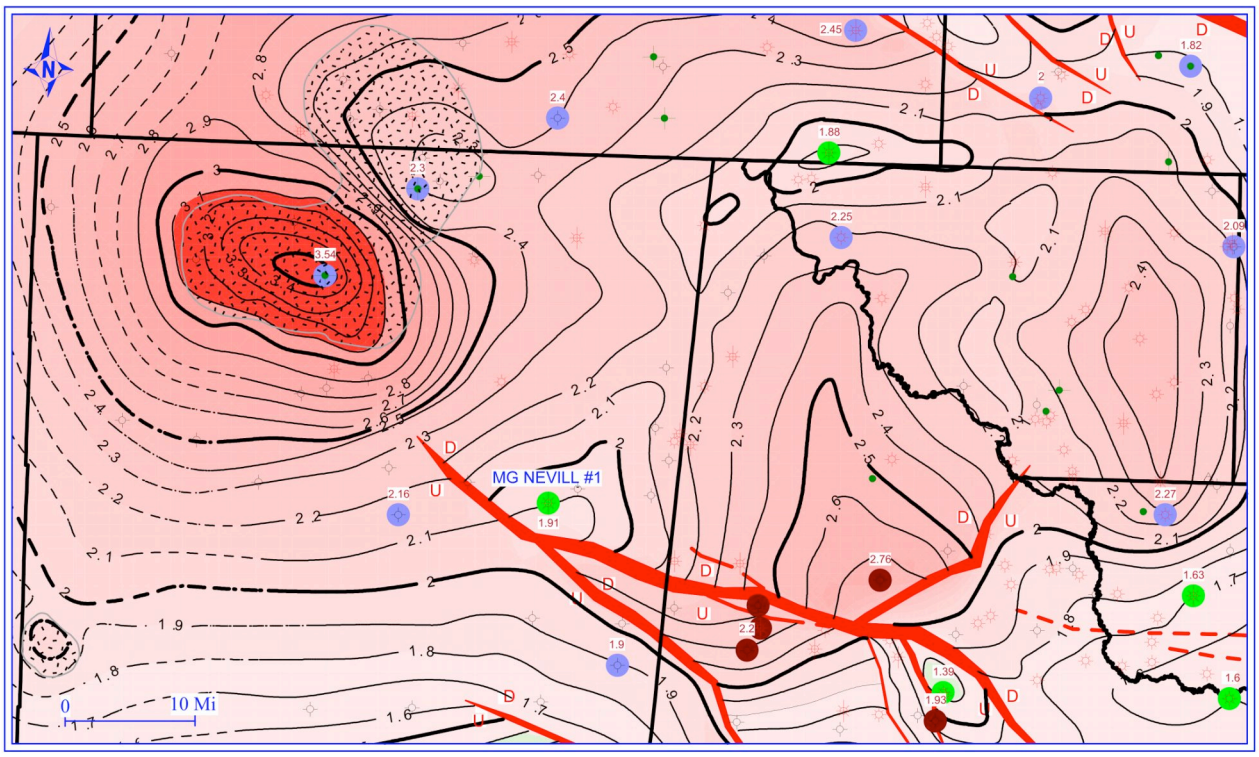

Figure 26. Isoreflectance map (%Ro) for lower Barnett interval A. Warmer colors indicate areas of higher thermal maturity. Stipples show location of subsurface igneous intrusions mapped by Barker and Pawlewicz (1987). Data from wells highlighted in violet taken from Pawlewicz *et al.* (2005). Data from wells highlighted in red were made available by D. Jarvie, Humble Geochemical Services. Wells highlighted in green yielded data gathered in this study. Contour interval, 0.1 %Ro. Position of faults taken from lower Barnett structure-contour map (Fig. 5).

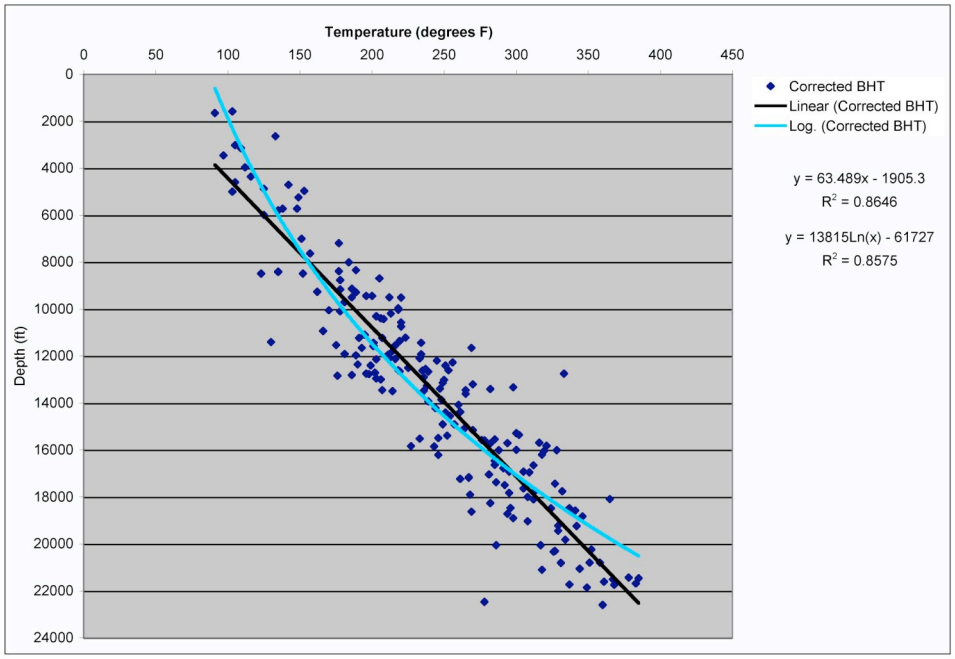

Figure 27. Measured bottom hole temperatures corrected for circulation time. Trend lines fit to data show the average geothermal gradient calculated by the equations given above.

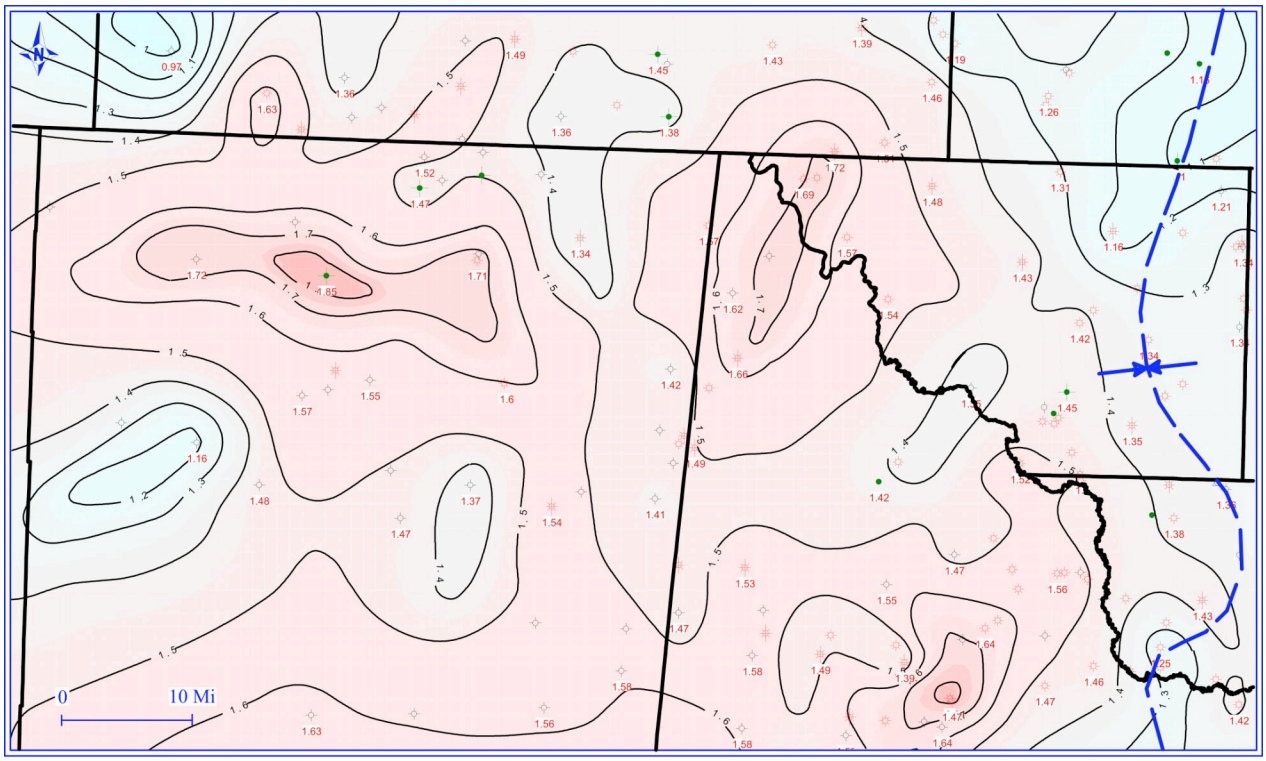

Figure 28. Isotherms of present-day geothermal gradient. Warm colors show areas of steep geothermal gradient relative to cool colors. Dashed blue line to the east shows the location of the basin axis. Contour interval, 0.1°F/100 ft.

Table 6. Stratigraphic data for burial history model constructed for the M. G. Nevill #1. Calculated and measured %Ro for lower Barnett shown in red.

			Present	Calculated	Measured	Eroded	Deposition Age		Erosion Age		
Name	Top	Bottom	Thickness	Ro	Ro	Thickness	from	to	from	to	Lithology
	[feet]	[feet]	[feet]	Value	Value	[feet]	[Ma]	[Ma]	[Ma]	[Ma]	
Quaternary	1.83	101.83	100				1.6	0			SANDsilty
Triasic-Tertiary	101.83	101.83	0			200	245	5	5	1.6	SANDcongl
Dewy Lake	101.83	357.83	256				246	245			SAND&SHALE
Rustler	357.83	1934.84	1577.01			400	255.4	248	248	246	EVAPshaly
Lamar	1934.84	1970.86	36.02				255.5	255.4			SAND&SHALE
Bell Canyon	1970.86	2951.85	980.99			100	256.5	255.5	247	246.3	SANDsilty
Cherry Canyon	2951.85	4099.83	1147.98				257.5	256.5			SAND&SHALE
Brushy Canyon	4099.83	5341.84	1242.01				258.1	257.5			SANDsilty
Bone Springs Ls	5341.84	6371.85	1030.01				258.8	258.1			LIMEsandy
FBSG	6371.85	7001.86	630.01				259.3	258.8			SANDSTONE
SBSG	7001.86	7933.87	932.01				259.8	259.3			SANDSTONE
TBSG	7933.87	8224.88	291.01				260	259.8			SAND&SHALE
Wolfcamp	8224.88	13878.85	5653.97				286	260			SHALEsand
Strawn	13878.85	13878.85	0			200	300	284	284	286	LIMEcarbo
Atoka	13878.85	14001.85	123			200	310	299	299	300	SANDshaly
Morrow	14001.85	14022.85	21				320	310			SAND&SHALE
Barnett Upper	14022.85	14467.86	445.01			100	340	319	319	320	SHALEsilt
Barnett Lower	14467.86	14810.87	343.01	1.77	1.91		350	340			SHALEcalc
Mssp Limestone	14810.87	14844.86	33.99				360	350			LIMEshaly
Woodford	14844.86	14957.85	112.99			200	390	365	365	360	SHALEcalc
Devonian	14957.85	15289.83	331.98			200	408	389	389	390	LIMESTONE
Fusselman	15289.83	15770.83	481				438	408			LIMESTONE
Montoya	15770.83	15770.83	0				475	438			LIMEdolom

conductivities of the lithologies used in the stratigraphic table. Tertiary igneous activity was not incorporated in the model because the M. G. Nevill #1 is some distance removed from the area of intrusive activity (Fig. 29). The %Ro values calculated by the model following Sweeney and Burnham (1990) closely match those measured on organic matter in cuttings from the lower Barnett (Table 6 and Figs. 26 and 29).

Three episodes of hydrocarbon generation have taken place in the Delaware basin--the last in the Early and Middle Permian (Hills 1984). The burial history model shows that the basin subsided rapidly throughout the Pennsylvanian and Early Permian (Figs. 29 and 30). The Barnett Shale was buried quickly, and reached the critical temperature for oil generation in the Middle to Late Permian, approximately 250 Ma ago. It then reached the critical point for gas generation about 240 Ma ago. The Mississippian section has remained in the oil and gas window from the Permian to the present day (Fig. 31). The onset of hydrocarbon generation in the Barnett in the Delaware basin closely coincided with the onset of hydrocarbon generation in the Barnett in the Fort Worth basin (see Montgomery *et al*. 2005). However, the Fort Worth basin has undergone greater amounts of uplift and erosion during the Tertiary, which has brought the Mississippian section to much shallower depths than those observed in the Delaware basin.

Recent Activity

The success of the Barnett Shale play in the Fort Worth basin has sparked exploration and development interests in the Barnett in the Delaware basin (Plate I, in pocket). Dallas Production completed two wells in the Barnett in southeastern Reeves County in 2003 and 2004, which produced high amounts of condensate, indicating that the shale is not in the gas window in that area. Since then, operators have been actively pursuing and more recently drilling Barnett prospects throughout the Delaware basin,

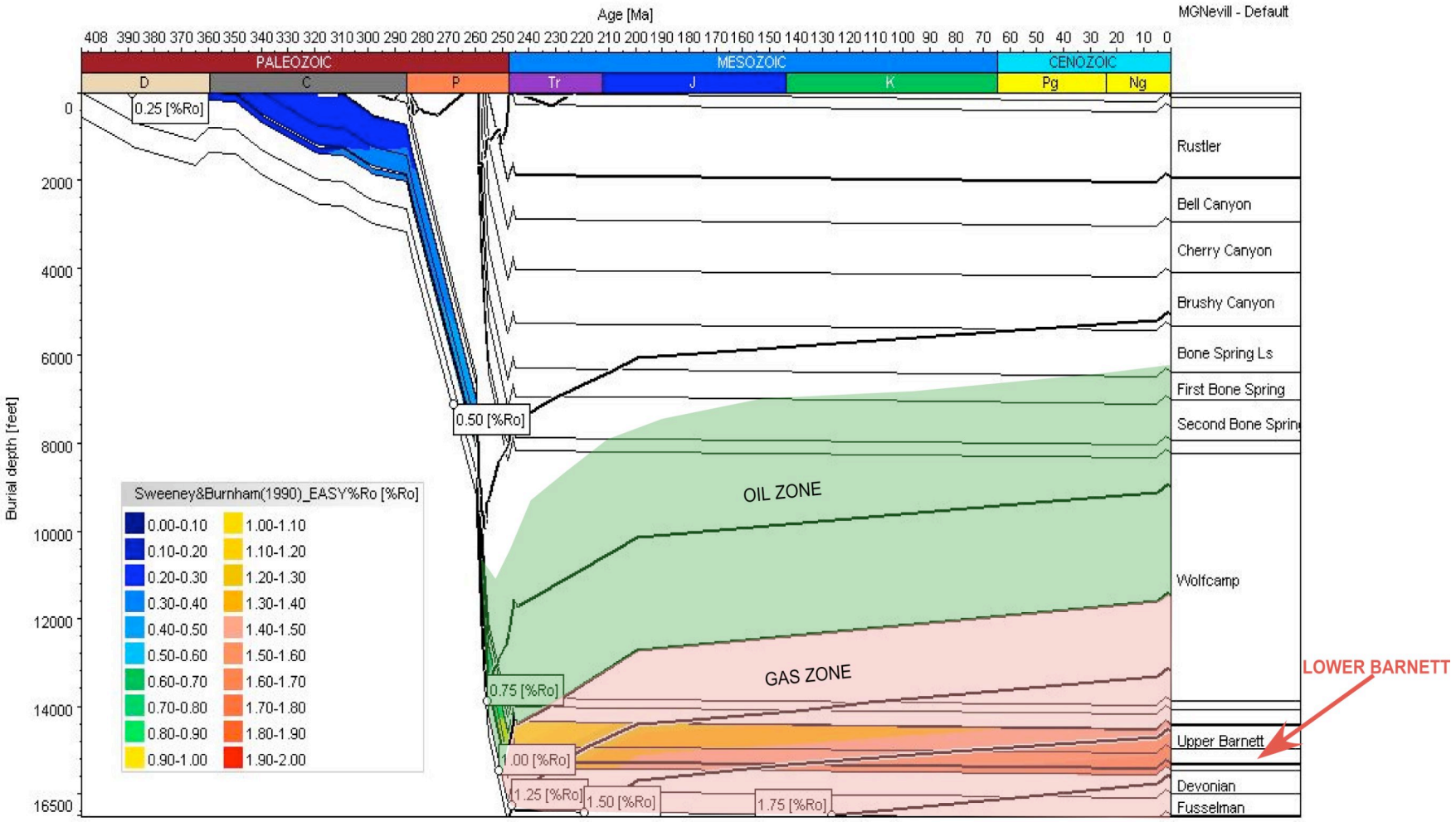

Figure 29. Burial history model for the M. G. Nevill #1 showing % Ro isoreflectance lines (%Ro) and modeled time-temperature index. Hydrocarbon generation zones based on the modeled %Ro values. Figure 25 shows the relation between hydrocarbon generation zones based on time-temperature index and %Ro.

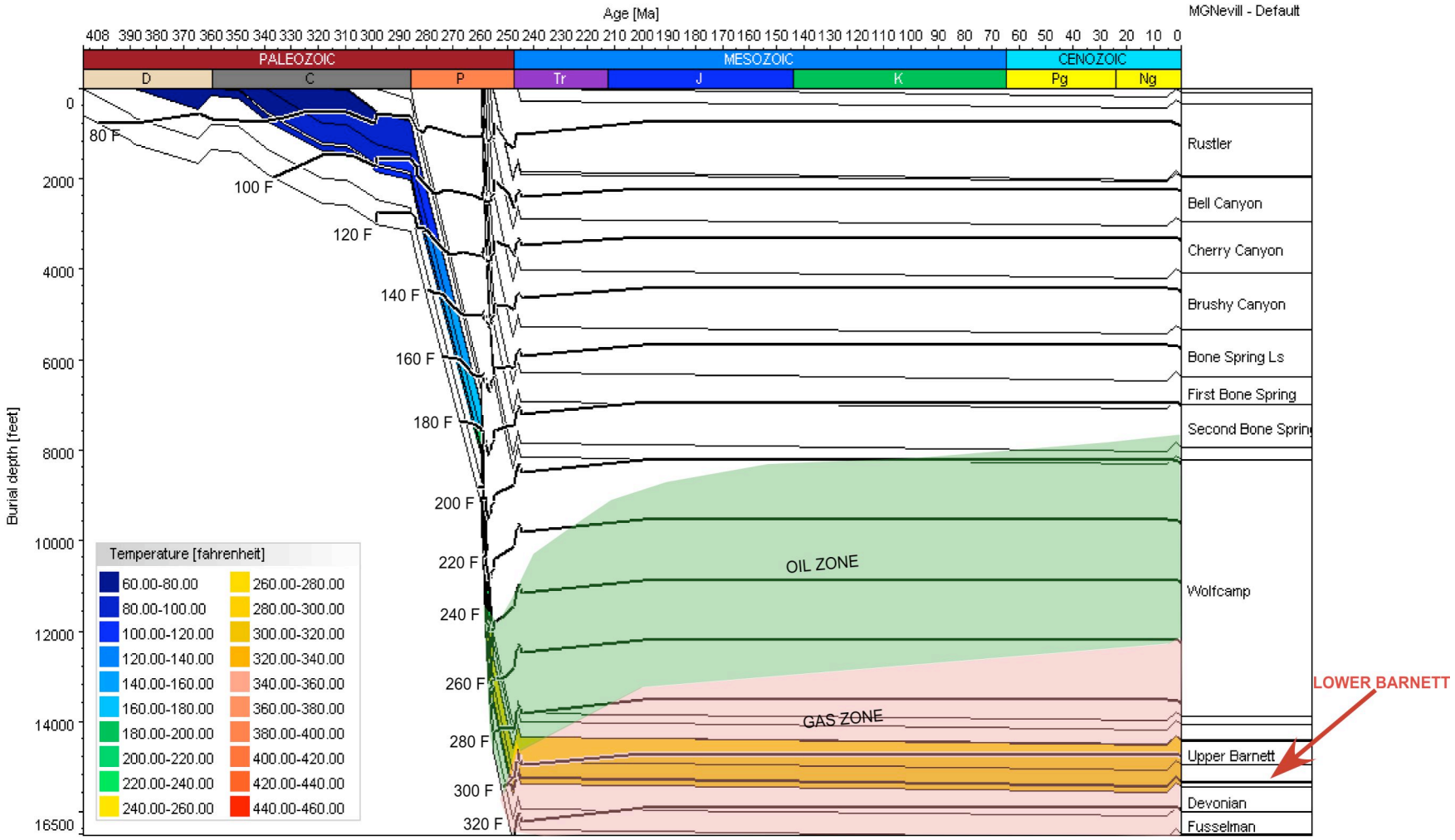

Figure 30. Burial history model for the M. G. Nevill #1 showing isotherms (°F) related to depth of burial and hydrocarbon generation zones. Hydrocarbon generation zones based on time-temperature index and %Ro.

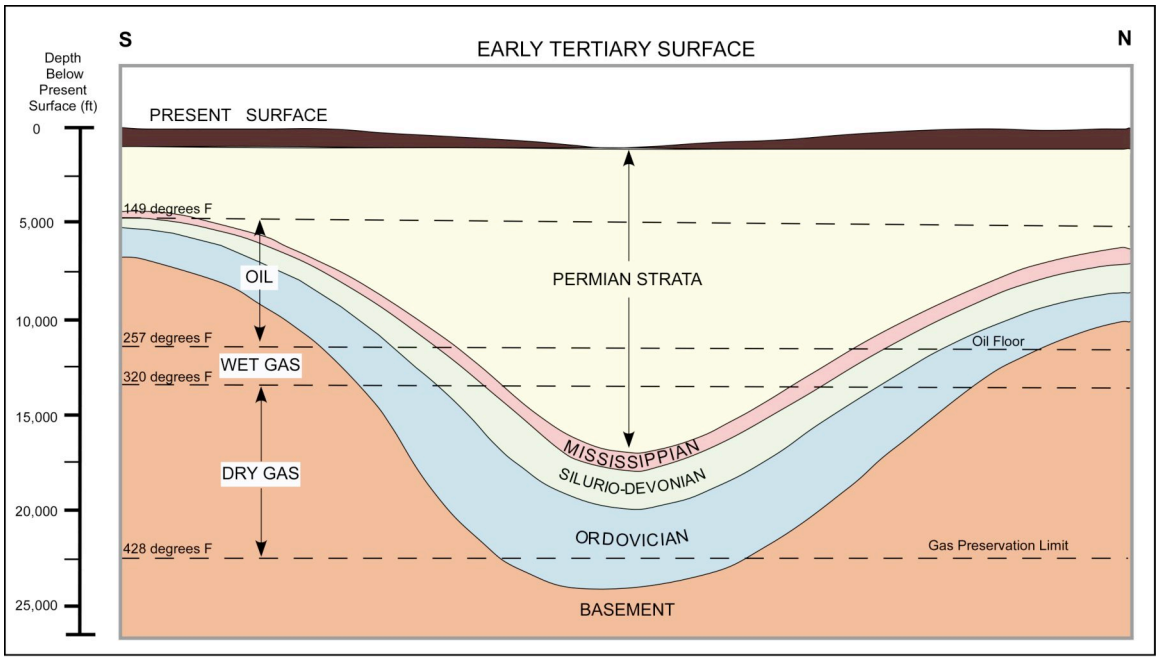

Figure 31. Oil and gas generation zones in the Delaware basin. Generalized north-south cross section with thickness of formations corrected for erosion and compaction. Modified from Hills (1984).

primarily along the western flank where the Barnett is at shallower depth. The primary operators and lease holders of the Barnett rights are EnCana USA, EOG Resources, Alpine (K2X Company and 777), Petro-Hunt and Burlington Resources.

Substantial amounts of drilling are taking place, but not much well completion, testing or production data are available in the public domain. Barnett production rates, mostly from initial production (IP) tests, range from 141 MCFD to 3 MMCFD in the Delaware basin. No production trends have been defined yet. Typical horizontal Barnett wells in the Fort Worth basin have had IP rates ranging from 1.0 MMCFD to 4.5 MMCFD, and up to 8.0 MMCFD (Scott Kelley, XTO Energy, personal communication). While initial production rates look promising in the Delaware basin, well costs are significantly higher than in the Fort Worth basin because the Barnett is at much greater depths. The greater depth not only increases drilling costs, but also increases fracture stimulation costs. The shale may not even respond to conventional fracture stimulation at the depths it is found in the Delaware basin.

Conclusions and Recommendations

The Barnett Shale in the Delaware basin has the potential to be a prolific gas producer. It is organic rich and thermally mature throughout large portions of the basin. The shale can be divided into an upper clastic unit and a lower limy unit by changes in resistivity. The lower unit can be subdivided into five subunits by distinctive well-log markers. The lower Barnett has a higher TOC content than the upper Barnett. Depth to the top of the Barnett ranges from 7,000 ft (2,333 meters) on the western side of the basin to more than 18,000 ft (6,000 meters) along the basin axis. The Barnett Shale began generating gas 250 Ma ago and remains in the gas window to this day over much of the area.

Initial production tests on a few wells have flow rates up to 3 MMCFD. Preliminary analyses suggest that intervals in the lower Barnett marked by high resistivity and high neutron porosity readings on well-logs have high gas contents. Although I cross-plotted all of the available data, I found no significant correlations among the petrological, geochemical and petrophysical variables. Areas in which to focus future exploration and production efforts can be delineated by mapping net resistivity greater than 50 ohmm in the lower Barnett.

The study of the Barnett in the Delaware basin has future potential in continuing with petrophysical, petrological, and geochemical analysis. This may be carried out by further investigations and the utilization of existing well-logs, and continued correlation efforts between the log characteristics, geochemistry, rock properties, and formation fluids. Also, the ability to map and predict natural fracturing within the shale reservoir may be of future benefit in defining more prolific production trends within organic rich and mature fairways. In addition to the Barnett, the Woodford Formation should be evaluated thoroughly in terms of its maturity and hydrocarbon potential.

References

Adams, J. E., 1965, Stratigraphic-tectonic development of Delaware basin: American Association of Petroleum Geologists Bulletin, v. 49, p. 2140-2148.

Barker, C. E., and Pawlewicz, M. J., 1987, The effects of igneous intrusions and higher heat flow on the thermal maturity of Leonardian and younger rocks, western Delaware basin, Texas, *in* Cromwell, D. M., and Mazzulo, J., eds., Glass Mountains: SEPM Guidebook, v. 87-27, p. 69-81.

Burst, J. F., 1969, Diagenesis of Gulf Coast clayey sediments and its possible relation to petroleum migration: American Association of Petroleum Geologists Bulletin, v. 53, p. 73-93.

Cys, J.M., and Gibson, W.R., 1988, Pennsylvanian and Permian geology of the Permian basin region, *in* Frenzel *et al.,* 1988, The Permian basin region, *in* Sloss, L. L., ed., Sedimentary Cover--North American Craton; U.S.: Boulder, Colorado, Geological Society of America, The Geology of North America, v. D-2, p. 277-289.

Flawn, P. T., 1956, Basement rocks of Texas and southeast New Mexico: University of Texas Publication 5605, 261 p.

Frenzel, H.N., and 13 others, 1988, The Permian basin region, *in* Sloss, L. L., ed., Sedimentary Cover--North American Craton; U.S.: Boulder, Colorado, Geological Society of America, The Geology of North America, v. D-2, p. 261-306.

Hayden, J., and Pursell, D., 2005, The Barnett Shale, Visitors Guide to the Hottest Gas Play in the US: Pickering Energy Partners Inc., 52 p. <http://www.pickeringenergy.com/pdfs/TheBarnettShaleReport.pdf>, Accessed October 2006.

Hills, J. M., 1984, Sedimentation, tectonism, and hydrocarbon generation in Delaware basin, West Texas and southeastern New Mexico: American Association of Petroleum Geologists Bulletin, v. 68, p. 250-267.

Hills, J. M., 1985, Structural evolution of the Permian basin of West Texas and New Mexico, *in* Dickerson, P. W., and Muehlberger, W. R., eds., Structure and Tectonics of Trans-Pecos Texas; West Texas Geological Society Guidebook, Midland, Texas, v. 85-81, p. 89-99.

Hills, J. M., and Galley, J. E., 1988, General introduction, the pre-Pennsylvanian Tobosa basin, *in* Frenzel *et al.,* 1988, The Permian basin region, *in* Sloss, L. L., ed., Sedimentary Cover--North American Craton; U.S.: Boulder, Colorado, Geological Society of America, The Geology of North America, v. D-2, p. 261-277.

Hunt, J. M., 1996, Petroleum Geochemistry and Geology, Freeman and Co., San Francisco, California, USA, 2nd ed., 615 p.

Jarvie, D. M., and Claxton, B. L., 2002, Barnett Shale oil and gas as an analog for other black shales, [abs.], American Association of Petroleum Geologists Southwest Section Meeting, Ruidoso, New Mexico, 2 p.

Kreis, L. K., and Costa, A., 2005, Hydrocarbon potential of the Bakken and Torquay Formations, southeastern Saskatchewan, *in* Summary of Investigations 2005, v. 1, Saskatchewan Geological Survey, Saskatchewan Industry Recources, Misc. Rep., 2005-4.1, 10 p.

Montgomery, S. L., Jarvie, D. M., Bowker, K. A., and Pollastro, R. M., 2005, Mississippian Barnett Shale, Fort Worth basin, north-central Texas: Gas-shale play with multi-trillion cubic foot potential: American Association of Petroleum Geologists Bulletin, v. 89, p. 155-175.

Passey, Q. R., Creaney, S., Kulla, J. B., and Stroud, J. D., 1990, A practical model for organic richness from porosity and resistivity logs: American Association of Petroleum Geologists Bulletin, v. 74, p. 1777-1794.

Pawlewicz, M., Barker, C. E., McDonald, S., 2005, Vitrinite reflectance data for the Permian basin, west Texas and southeast New Mexico, United States Geological Survey, Open-File Report, 2005-1171, 25 p.

Schad, S. T., 2004, Hydrocarbon potential of the Caney Shale in southeastern Oklahoma: Tulsa, Oklahoma, University of Tulsa, unpublished M.S. Thesis, 576 p.

Shepard, T. M., and Walper, J. L., 1982, Tectonic evolution of Trans-Pecos, Gulf Coast Association of Geological Societies Transactions, v. 32, p. 165-172.

Sweeney, J. J., and Burnham, A. K., 1990, Evaluation of a simple model of vitrinite reflectance based on chemical kinetics: American Association of Petroleum Geologists Bulletin, v. 74, p. 1559-1570.

Vertrees, C., Atchison, C.H., Evans, G.L., 1959, Paleozoic geology of the Delaware and Val Verde basins, *in* Geology of the Val Verde Basin and Field Trip Guidebook: West Texas Geological Society, Midland, TX, p. 64-73.

Wright, W. F., 1979, Petroleum Geology of the Permian Basin: West Texas Geological Society, Midland, TX, 98 p.

APENDIX I. Isopach Maps of the Lower Barnett Intervals

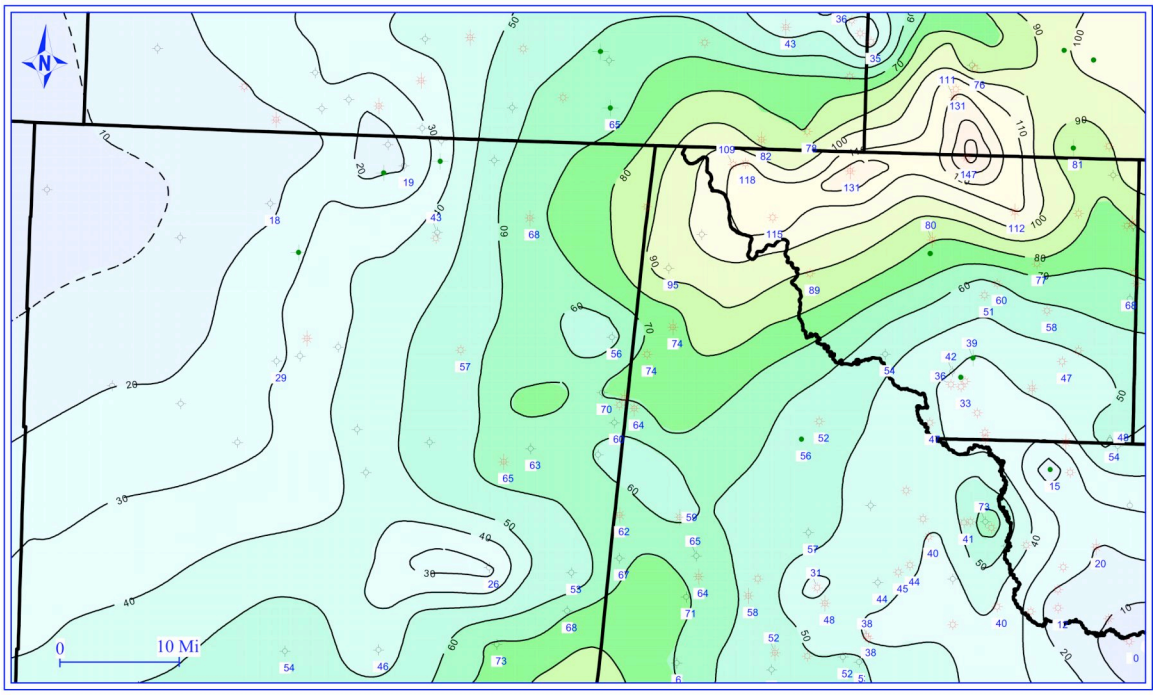

Figure I. 1. Isopach map of lower Barnett interval A. Contour interval, 10 feet.

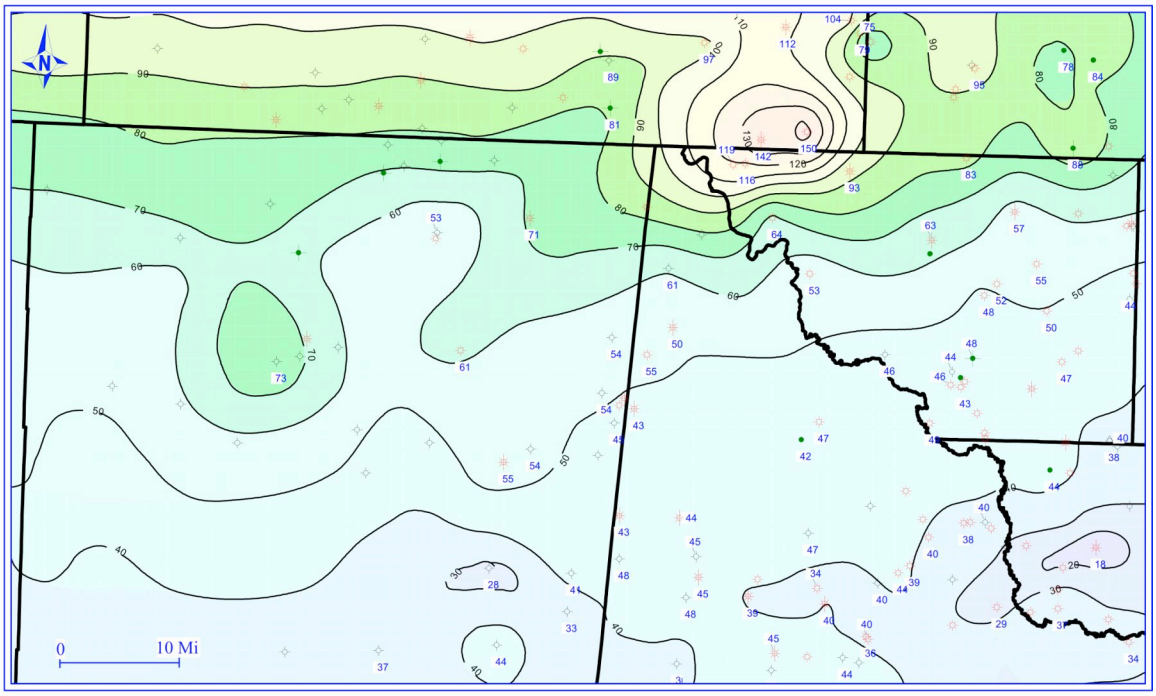

Figure I. 2. Isopach map of lower Barnett interval C. Contour interval, 10 feet.

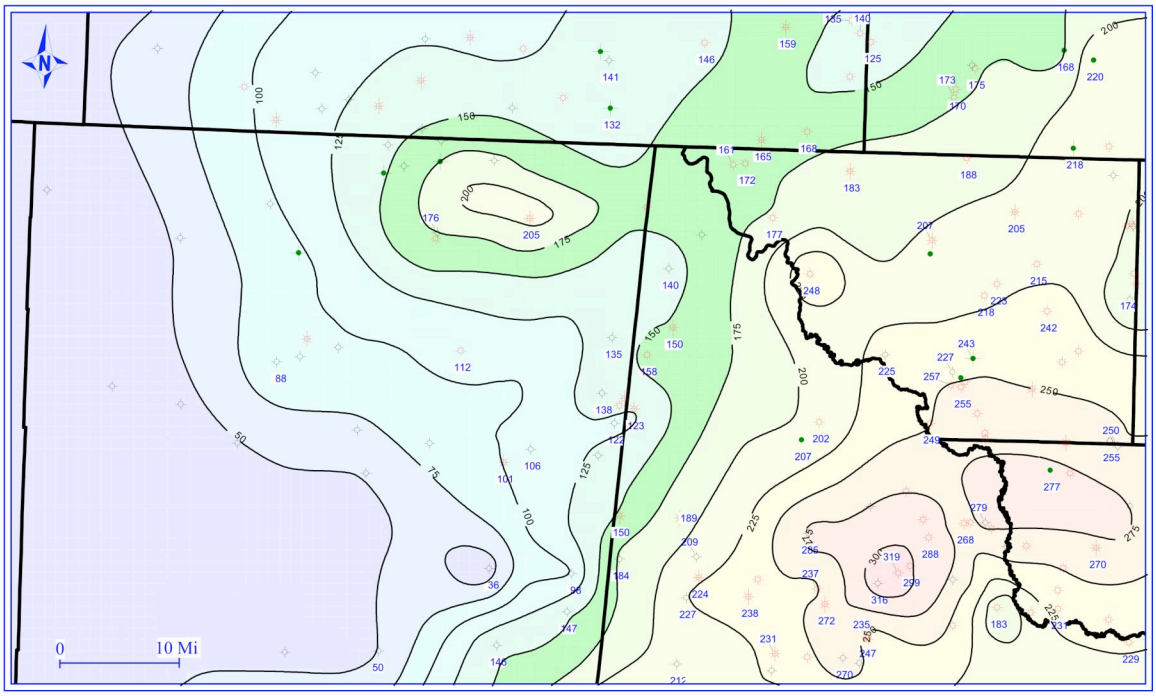

Figure I. 3. Isopach map of lower Barnett interval D. Contour interval, 25 feet.

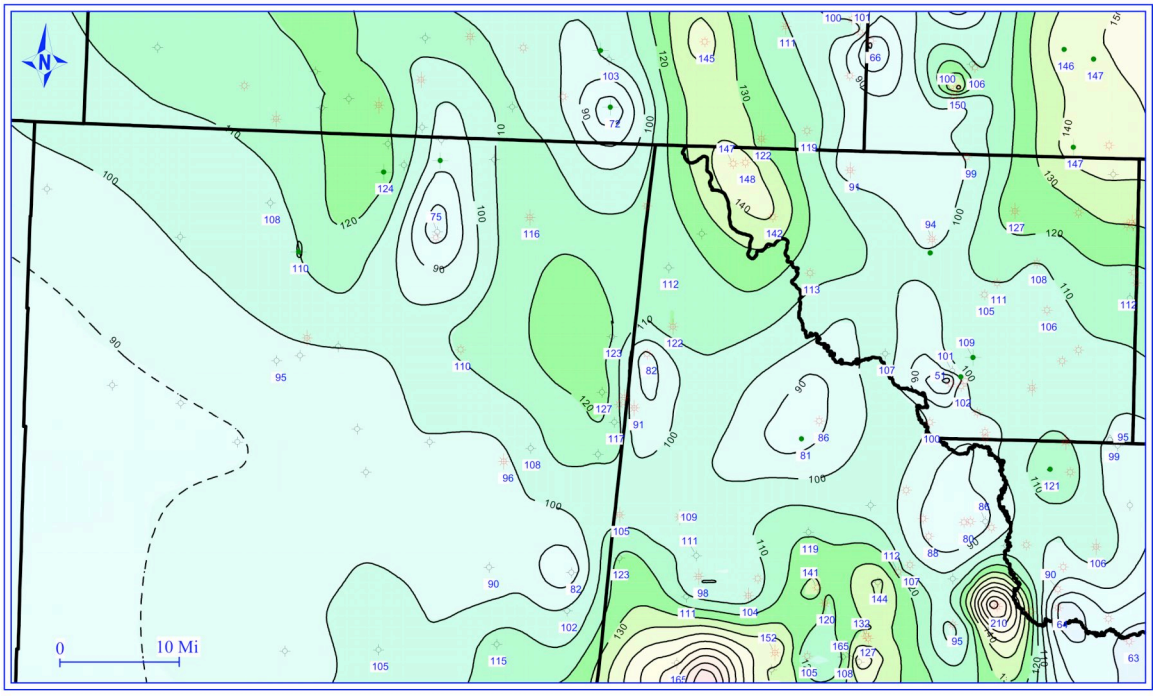

Figure I. 4. Isopach map of lower Barnett interval E. Contour interval, 20 feet.

APENDIX II. Well-logs and Descriptions of Well Cuttings

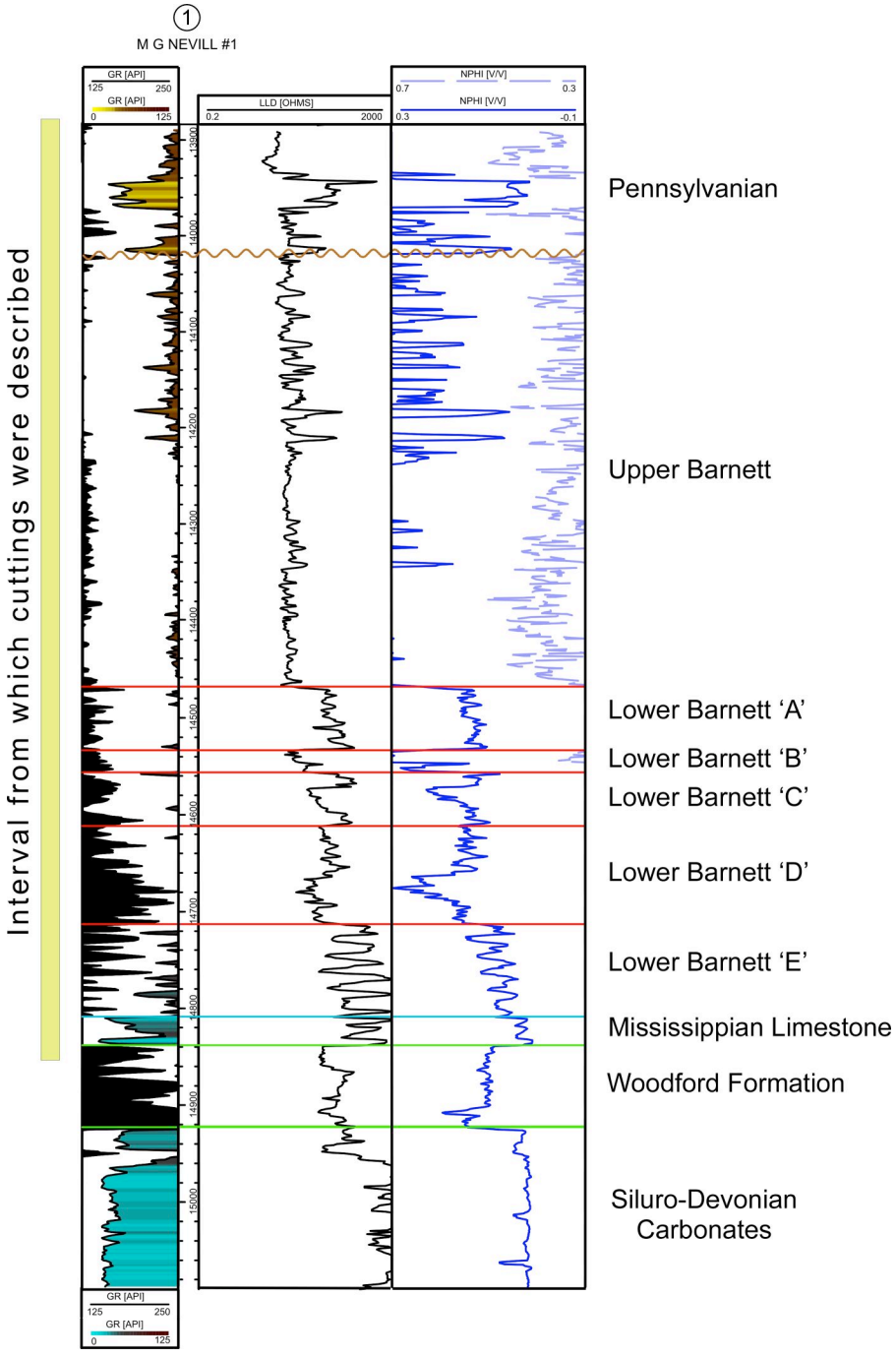

Figure II. 1. Well-log for the M.G. Nevill #1 showing the interval from which detailed cuttings were described. See the following pages for description of cuttings.

42-109-30824
MG NEVILL
Culberson Co, TX

Measured Depth (ft)	Sample Description
13,800	shale, dark grey, calcite
13,820	shale, grey, sandstone, fine grained
13,840	shale, dark grey to black, silty
13,860	same as above
13,880	same as above
13,900	shale, black, very silty
13,920	same as above
13,940	fossiliferous limestone, very silty
13,960	shale, same as above
13,980	shale sandy, calcite cement
14,000	shale, dark grey to black, pyrite
14,020	shaley limestone, grey
14,040	shale same as above, abundant pyrite
14,060	shale, dark grey, silty
14,080	shale, dark grey, pyrite
14,100	shale, dark grey, silty
14,120	same as above
14,140	shale, dark grey silty, pyrite
14,160	same as above
14,180	same as above
14,200	shale, sandy
14,220	shale, dark grey to brown, silty, pyrite
14,240	same as above
14,260	same as above
14,280	same as above
14,300	same as above
14,320	same as above
14,340	same as above
14,360	same as above
14,380	same as above
14,400	shale, dark grey, silty to sandy, friable, pyrite
14,420	same as above
14,440	same as above
14,460	same as above
14,480	same as above
14,500	shale, dark grey, hard, silty calcite
14,520	same as above
14,540	same as above
14,560	shale same as above, pyrite
14,580	same as above
14,600	same as above

14,620	same as above
14,640	shale, grey, silty
14,660	shale, dark grey, calcite
14,680	same as above
14,700	same as above
14,720	shale, black friable, dissolves in HCL, limey shale fragments, calcareous
14,740	same as above
14,760	shale, dark grey, limey
14,780	shale, grey to black, soft, very calcareous, dark grey limestone
14,800	same as above
14,820	shale, dark grey to black, pyrite, calcite
14,840	shale, dark grey to black
14,860	shale, dark grey to black, some limestone

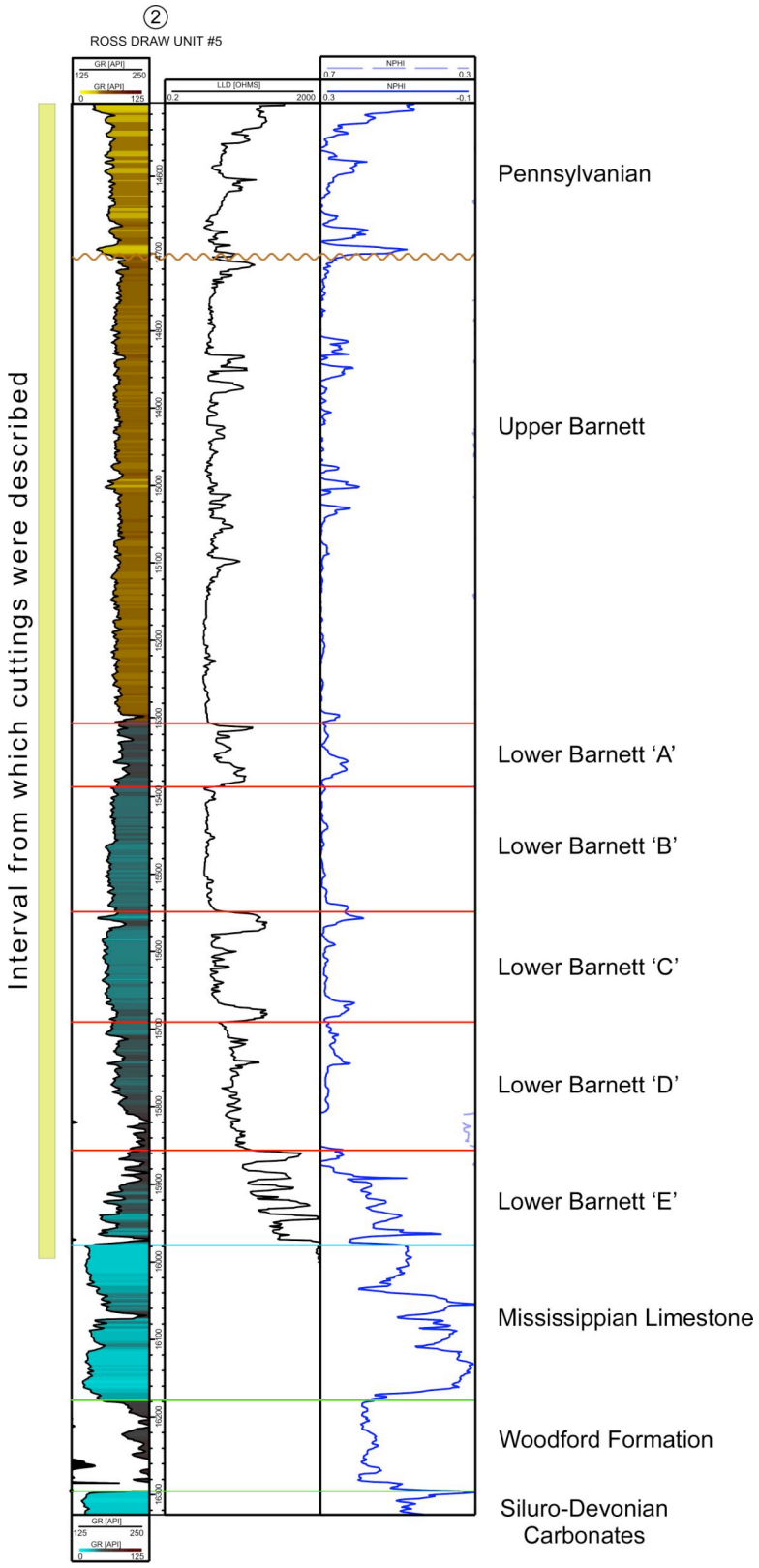

Figure II. 2. Well-log for the Ross Draw Unit #5 showing the interval from which detailed cuttings were described. See the following pages for description of cuttings.

Measured Depth (ft)	Sample Description
14,400	sandstone, grey, veryfine upper-very fine lower, calcite cement
14,410	same as above
14,420	same as above
14,430	same as above
14,440	shale, light grey, clay
14,450	shale, light grey, calcite, quartz, orthoclase fragments
14,460	sandstone same as above, increase shale
14,470	shale, same as above, friable shale-clay
14,480	same as above
14,490	same as above
14,500	same as above
14,510	same as above
14,520	same as above
14,530	same as above
14,540	same as above
14,550	same as above
14,560	same as above
14,570	same as above
14,580	same as above
14,590	same as above
14,600	shale grey shale, lithified
14,610	same as above
14,620	same as above
14,630	same as above
14,640	same as above
14,650	shale, darker grey
14,660	same as above
14,670	same as above
14,680	same as above
14,690	shale, grey, silty
14,700	same as above
14,710	same as above
14,720	same as above
14,730	same as above
14,740	same as above
14,750	shale, dark grey, orthoclase, calcite, quartz, iron stained
14,760	same as above
14,770	same as above
14,780	same as above
14,790	same as above
14,800	shale dark grey, increase silt, very fine upper
14,810	same as above
14,820	same as above

14,830	same as above
14,840	same as above
14,850	same as above
14,860	same as above
14,870	same as above
14,880	same as above
14,890	shale same as above, decrease silt
14,900	same as above
14,910	same as above
14,920	same as above
14,930	same as above
14,940	shale, dark grey, some silt, very fine upper
14,950	same as above
14,960	same as above
14,970	same as above
14,980	same as above
14,990	same as above
15,000	same as above
15,010	same as above
15,020	same as above
15,030	same as above
15,040	shale, same as above, pyrite
15,050	same as above
15,060	same as above
15,070	same as above
15,080	same as above
15,090	shale, grey to black, little silt
15,100	same as above
15,110	same as above
15,120	same as above
15,130	same as above
15,140	shale, dark grey to black
15,150	same as above
15,160	same as above
15,170	same as above
15,180	same as above
15,190	same as above
	missing 15,200-15,280
15,290	shale, black
15,300	shale, black, some silt, calcareous
15,310	same as above
15,320	same as above
15,330	same as above
15,340	same as above
15,350	same as above
15,360	same as above
15,370	same as above
15,380	shale, dark grey to black, silty, iron stained
15,390	same as above

15,400	shale, darker grey, decreased silt
15,410	shale, black, calcite
15,420	same as above
15,430	same as above
15,440	same as above
15,450	same as above
15,460	same as above
15,470	same as above
15,480	same, little silt
15,490	same as above
15,500	shale, black
15,510	same as above
15,520	same as above
15,530	same as above
15,540	same as above
15,550	same as above
15,560	same as above
15,570	same as above
15,580	shale, same as above, calcite
15,590	same as above
15,600	shale, grey friable, some silt, calcareous
15,610	same as above
15,620	same as above
15,630	same as above
15,640	shale, black, calcite
15,650	same as above
15,660	shale, same as above, some silt
15,670	same as above
15,680	same as above
15,690	same as above
15,700	shale, black, pyrite, calcite
15,710	shale, same as above, iron stained
15,720	same as above
15,730	same as above
15,740	same as above
15,750	shale, black, calcite
15,760	same as above
15,770	shale, same as above, pyrite
15,780	shale, same as above, no pyrite
15,790	shale, black, increased calcite, limey
15,800	same as above
15,810	same as above
15,820	same as above
15,830	same as above
15,840	same as above
15,850	same as above
15,860	shale, black, some calcite, pyrite
15,870	shale, dark limey, very calcareous
15,880	same as above

15,890	shale, dark grey to black, non-calcareous
15,900	same as above
15,910	shale, same as above, calcite crystals
15,920	shale, same as above, pyrite
15,930	shale, same as above, pyrite
15,940	same as above
15,950	same as above
15,960	same as above
15,970	limey shale, dark grey (gradational contact)
15,980	limestone, shaley, dark grey
15,990	same as above

42-475-30090
BASS WILLIAMS #1
Ward Co., TX

Measured Depth (ft)	Sample Description
15,700	shale, dark grey to black
15,710	same as above
15,720	same as above
15,730	siltstone, light grey, fine lower-very fine upper
15,740	same as above
15,750	same as above, orthoclase, quartz
15,760	increase shale
15,770	shale, grey silty
15,780	same as above
15,790	shale, grey
15,800	shale, dark grey to black
15,810	same as above, calcite
15,820	shale, dark grey, plagioclase, calcite
15,830	same as above
15,840	same as above
15,850	same as above
15,860	same as above
15,870	same as above
15,880	shale, dark grey, K-feldspar, calcite
15,890	shale, brown to dark grey, pyrite
15,900	same as above
15,910	same as above
15,920	shale, dark grey to black
15,930	same as above
15,940	same as above
15,950	same as above
15,960	same as above
15,970	same as above, calcite
15,980	same as above
15,990	shale, dark grey, silty

16,000	shale, black, little calcite & pyrite
16,010	shale, black friable, some calcite
16,020	same as above
16,030	same as above
16,040	same as above, dissolves in HCl leaves yellow-orange stain
16,050	shale, black lithified, calcite, pyrite
16,060	same as above
16,070	same as above
16,080	shale, black friable shale
16,090	shale, dark grey to black, calcite pyrite
16,100	shale, dark grey to black friable, dissolves in HCl
16,110	same as above
16,120	shale, grey to black lithified
16,130	same as above
16,140	same as above
16,150	same as above, calcite
16,160	same as above, pyrite
16,170	same as above
16,180	same as above
16,190	same as above
16,200	same as above
16,210	same as above
16,220	shale, friable black, dissolves in HCl
16,230	shale, lithified black
16,240	shale, friable black, calcite, pyrite (powdery)
16,250	same as above, dissolves in HCl
16,260	same as above
16,270	same as above
16,280	same as above
16,290	same as above
16,300	same as above
16,310	same as above
16,320	shale, lithified black, calcareous
16,330	same as above
16,340	same as above
16,350	same as above
16,360	same as above
16,370	same as above
16,380	shale, dark grey, decreased calcite
16,390	shale, grey, increased calcite
16,400	same as above
16,410	same as above
16,420	same as above, dissolves in HCl
16,430	limey shale, grey
16,440	limestone, dark grey
16,450	same as above
16,460	same as above
16,470	same as above
16,480	same as above

16,490	same as above
16,500	same as above
16,510	same as above
16,520	same as above
16,530	same as above
16,540	same as above
16,550	same as above
16,560	same as above
16,570	same as above
16,580	same as above
16,590	same as above
16,600	same as above
	missing 16,600-16,700
16,700	shale, black
16,710	same as above
16,720	same as above

42-389-00564
TOYAH UNIT #6
Reeves Co., TX

Measured Depth (ft)	Sample Description
11,180	silty shale, light grey, very fine lower
11,190	same as above, pyrite, calcite crystals
	missing 11,200-11,290
11,290	silty shale, grey, quartz, K-feldspar fragments
11,300	same as above
11,310	same as above
11,320	same as above
11,330	same as above, calcite, coarse lower-medium upper
11,340	same as above
11,350	same as above
11,360	same as above
11,370	same as above
11,380	same as above
11,390	same as above
11,400	same as above
11,410	silty shale, dark grey, very fine lower
11,420	same as above
11,430	same as above
11,440	same as above
11,450	same as above, pyrite
11,460	same as above
11,470	silty shale, dark grey
11,480	same as above
11,490	same as above
11,500	same as above

11,510	same as above
11,520	shale, dark grey to black
11,530	same as above
11,540	same as above
11,550	same as above
11,560	same as above
11,570	same as above
11,580	silty shale, dark grey to black, calcite
11,590	shale, dark grey, orthoclase fragments
11,600	shale, dark grey, calcite
11,610	same as above
11,620	same as above
11,630	same as above
11,640	shale, dark grey to black, K-feldspar, calcite
11,650	same as above
11,660	same as above
11,670	same as above
11,680	same as above
11,690	same as above
11,700	same as above
11,710	same as above
11,720	shale, dark grey to black, increase K-feldspar
11,730	same as above, calcite crystals
11,740	same as above
11,750	same as above
11,760	same as above
11,770	shale, dark grey
11,780	same as above
11,790	same as above
11,800	same as above
11,810	same as above
11,820	same as above. Pyrite
11,830	shale, black
11,840	same as above
11,850	same as above
11,860	same as above
11,870	same as above
11,880	shale, dark grey, dissolves in HCl, leaves orange residue
11,890	same as above, calcite crystals
11,900	same as above
11,910	shale, grey to black, soft, calcite fragments
11,920	same as above
11,930	limestone, hard, grey to black, very calcareous
11,940	same as above
11,950	same as above
11,960	same as above
11,970	limey shale, dark grey
11,980	same as above

Measured Depth (ft)	Sample Description
14,700	sandstone, dirty, fine lower-very fine upper
14,710	same as above
14,720	same as above
14,730	same as above
14,740	same as above
14,750	same as above
14,760	same as above
14,770	same as above
14,780	same as above
14,790	same as above
14,800	sandy shale, dark grey, calcite, orthoclase
14,810	shale, dark grey, calcite
14,820	same as above
14,830	shale, dark grey, increased orthoclase & quartz, calcite
14,840	same as above
14,850	shale, dark grey, decreased orthoclase & quartz
14,860	same as above
14,870	same as above, increased orthoclase & quartz
14,880	same as above
14,890	same as above, pyrite
14,900	silty shale, grey to black
14,910	same as above
14,920	siltstone, grey, fine upper-fine lower
14,930	shale, grey to black
14,940	same as above, pyrite
14,950	same as above
14,960	shale, black, calcite, pyrite
14,970	same as above
14,980	same as above
14,990	same as above
15,000	same as above
15,010	silty shale, black
15,020	same as above
15,030	same as above
15,040	same as above
15,050	shale, dark grey to black
15,060	same as above
15,070	same as above, pyrite
15,080	shale, grey to black, calcite
15,090	same as above
15,100	same as above
15,110	same as above

15,120	shale, grey to black, calcite, pyrite
15,130	same as above
15,140	same as above
15,150	same as above
15,160	same as above
15,170	shale, dark grey to black, calcite
15,180	same as above
15,190	same as above
15,200	same as above
15,210	same as above
15,220	same as above
15,230	same as above
15,240	same as above
15,250	same as above, pyrite
15,260	same as above
15,270	same as above
15,280	same as above
15,290	shale, black, calcite
15,300	same as above
15,310	same as above
15,320	same as above, pyrite
15,330	same as above
15,340	limey shale, dark grey
15,350	limey shale, grey friable, calcareous
15,360	shaley limestone
15,370	same as above
15,380	limestone, light grey
15,390	same as above

APENDIX III. Thin-section Images From Lower Barnett Intervals A, C and D

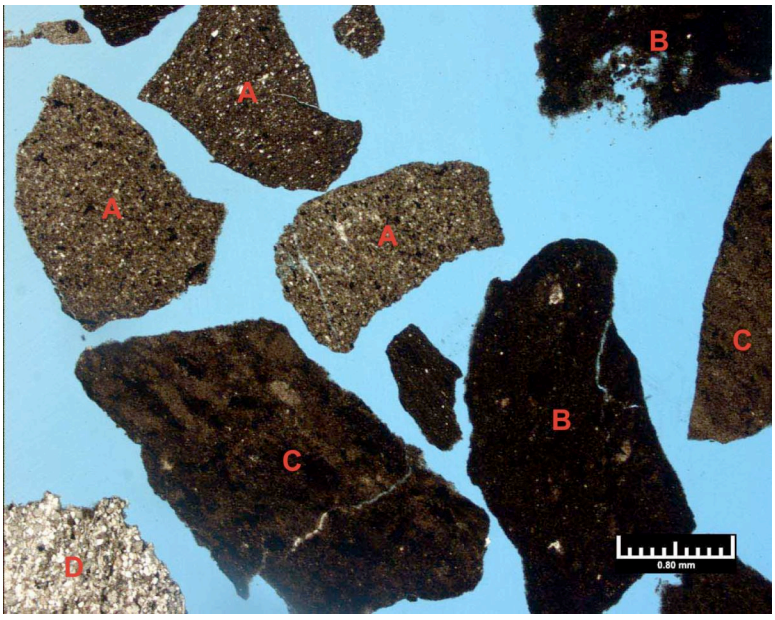

Figure III. 1. M.G. Nevill #1, lower Barnett interval A, 14,510 feet–14,520 feet (magnification 25x). A, brown shale; B, black shale; C, laminated silty shale; D, dolomitic sandstone.

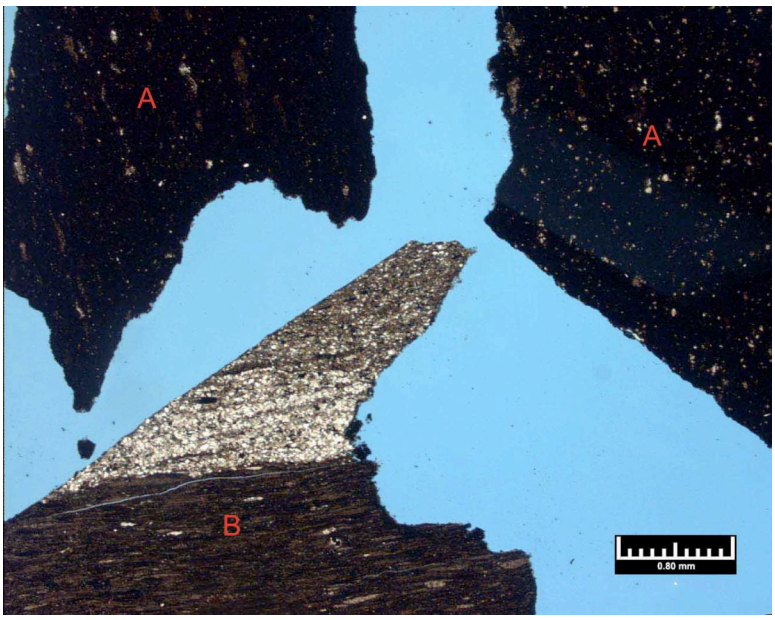

Figure III. 2. M.G. Nevill #1, lower Barnett interval C, 14,570 feet–14,580 feet (magnification 25x). A, shale; B, laminated silty shale.

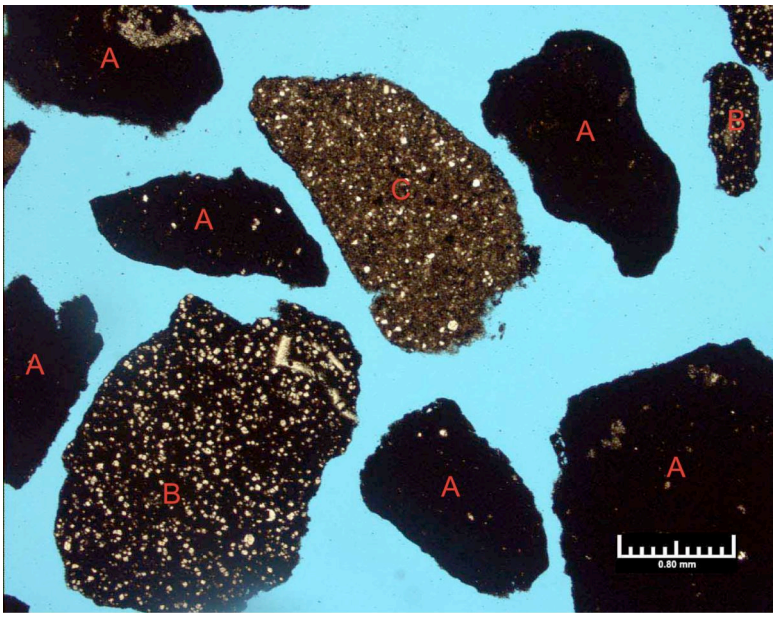

Figure III. 3. M.G. Nevill #1, lower Barnett interval D, 14,690 feet–14,700 feet (magnification 25x). A, black shale; B, black organic-rich shale with dolomite crystals; C, brown shale with dolomite crystals.

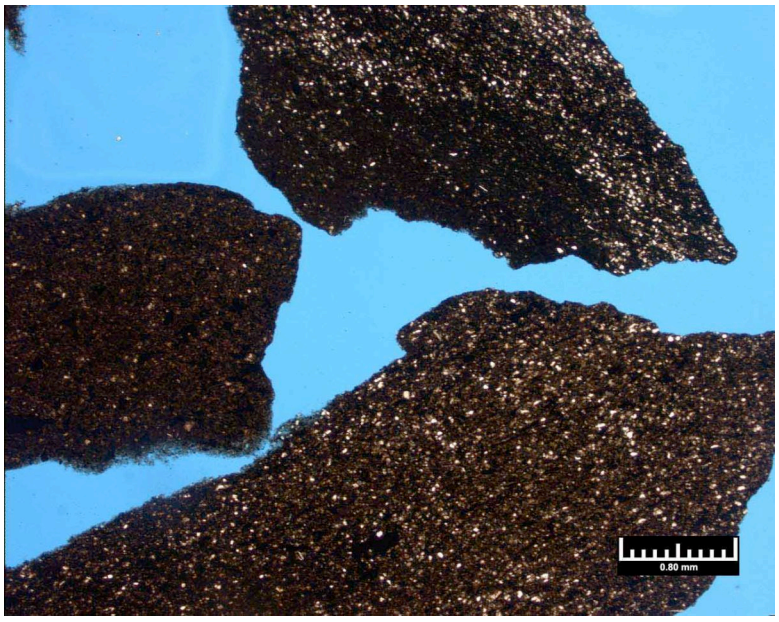

Figure III. 4. Ross Draw Unit #5, lower Barnett interval A, 15,340 feet–15,350 feet (magnification 25x). Shale with vague silty laminations and dolomite crystals.

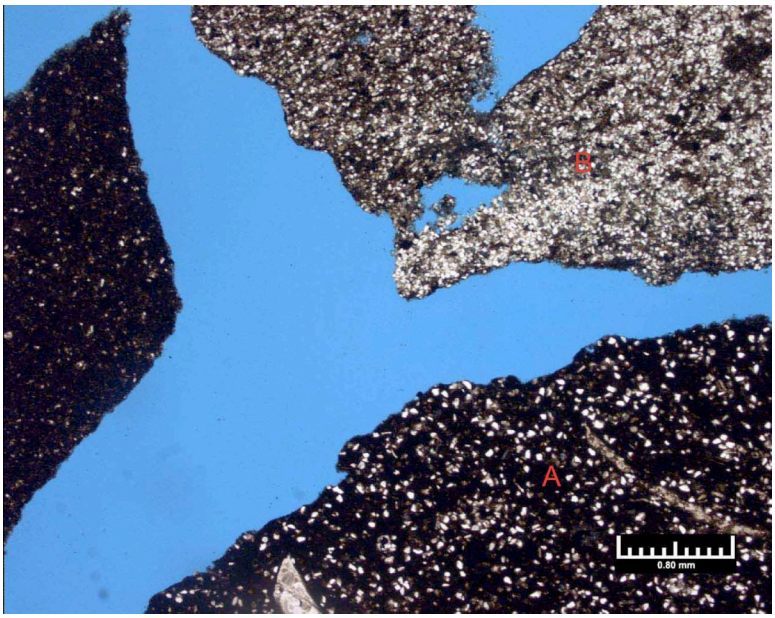

Figure III. 5. Ross Draw Unit #5, lower Barnett interval C, 15,560 feet–15,570 feet (magnification 25x). Shale with vague silty laminations. A and B show increased calcite and dolomite crystals.

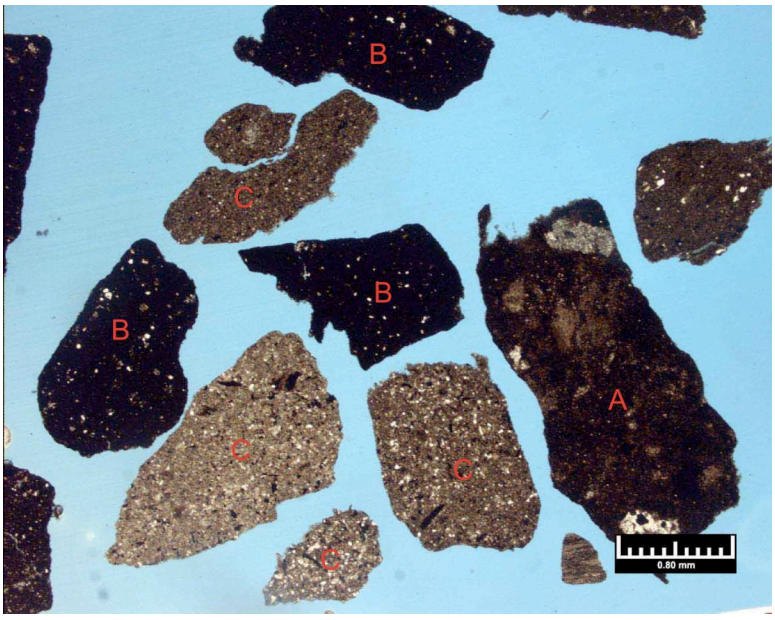

Figure III. 6. Ross Draw Unit #5, lower Barnett interval D, 15,820 feet–15,830 feet (magnification 25x). A, laminated silty shale; B, black shale with few dolomite crystals; C, brown shale with dolomite crystals.

APENDIX IV. SEM Images From Lower Barnett Intervals A, C and D

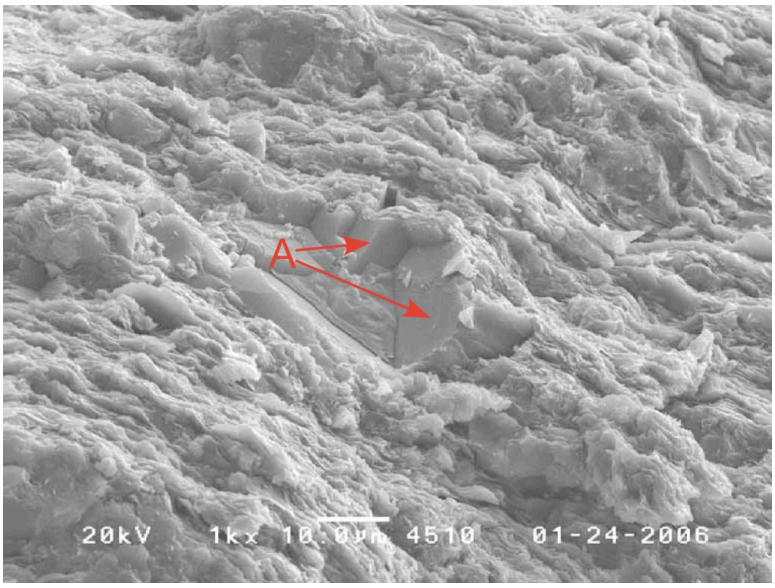

Figure IV. 1. M. G. Nevill #1, lower Barnett interval A, 14,510 feet–14,520 feet (magnification 1000x). Illite clay with dolomite rhombs (A).

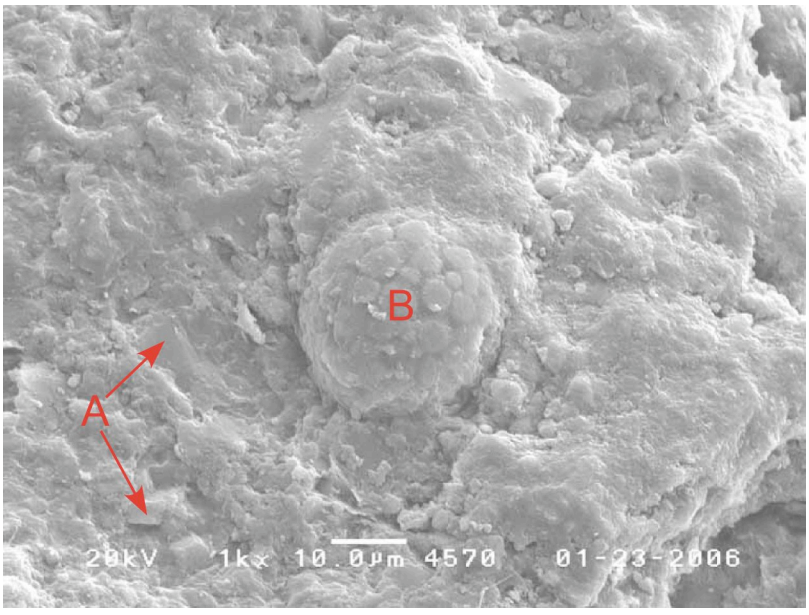

Figure IV. 2. M. G. Nevill #1, lower Barnett interval C, 14,570 feet–14,580 feet (magnification 1000x). Illite clay with dolomite rhombs (A) and a pyrite framboid (B).

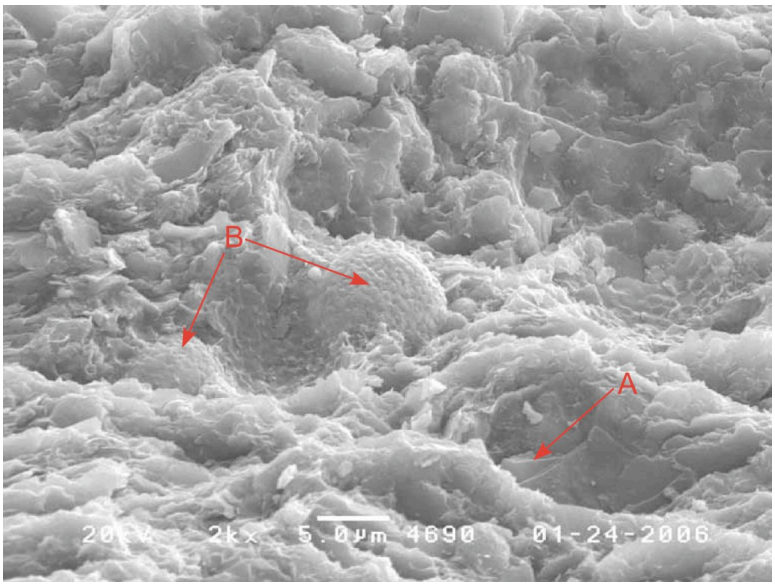

Figure IV. 3. M. G. Nevill #1, lower Barnett interval D, 14,690 feet–14,700 feet (magnification 2000x). Illite clay with dolomite rhombs (A) and pyrite framboids (B).

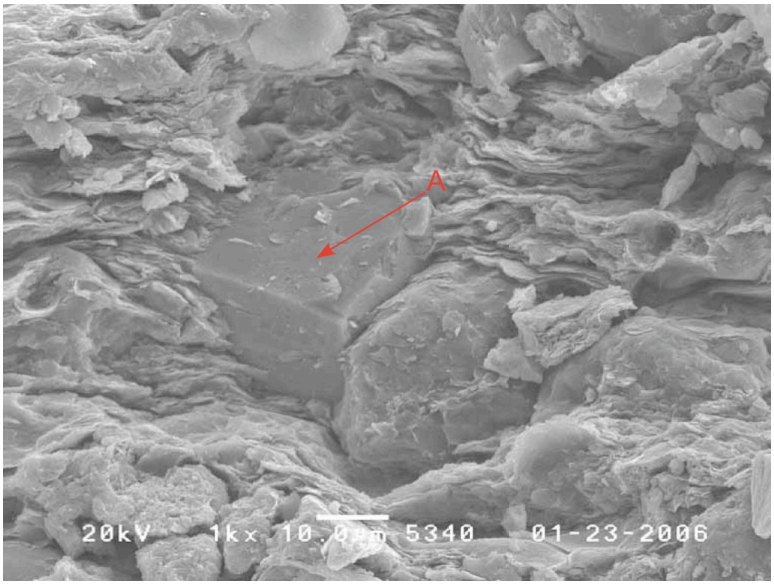

Figure IV. 4. Ross Draw Unit #5, lower Barnett interval A, 15,340 feet–15,350 feet (magnification 1000x). Kaolinite clay with dolomite rhomb (A).

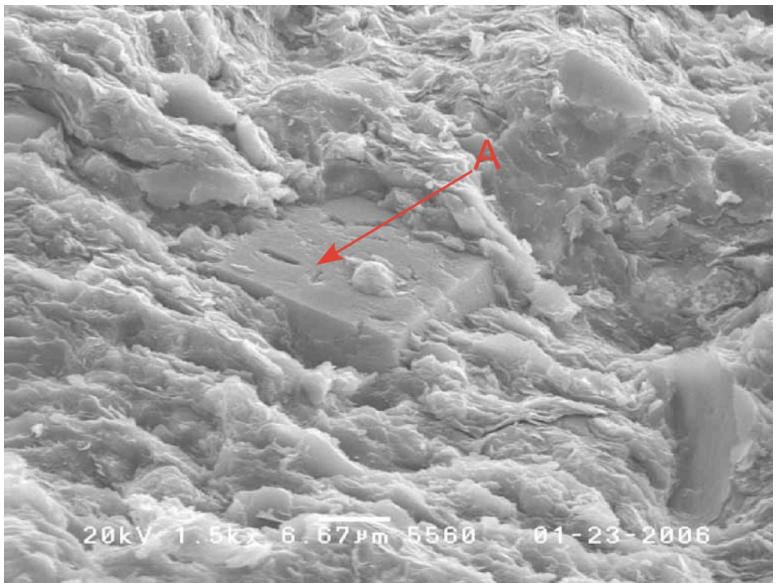

Figure IV. 5. Ross Draw Unit #5, lower Barnett interval C, 15,560 feet–15,570 feet (magnification 1500x). Kaolinite clay matrix with dolomite rhomb (A).

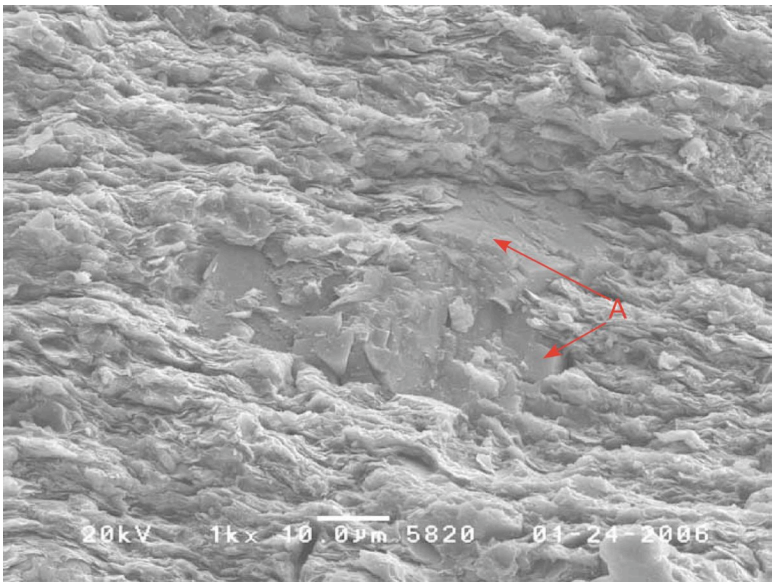

Figure IV. 6. Ross Draw Unit #5, lower Barnett interval D, 15,820feet–15,830 feet (magnification 1000x). Kaolinite clay with scattered dolomite rhombs (A).

APENDIX V. Geochemical Report

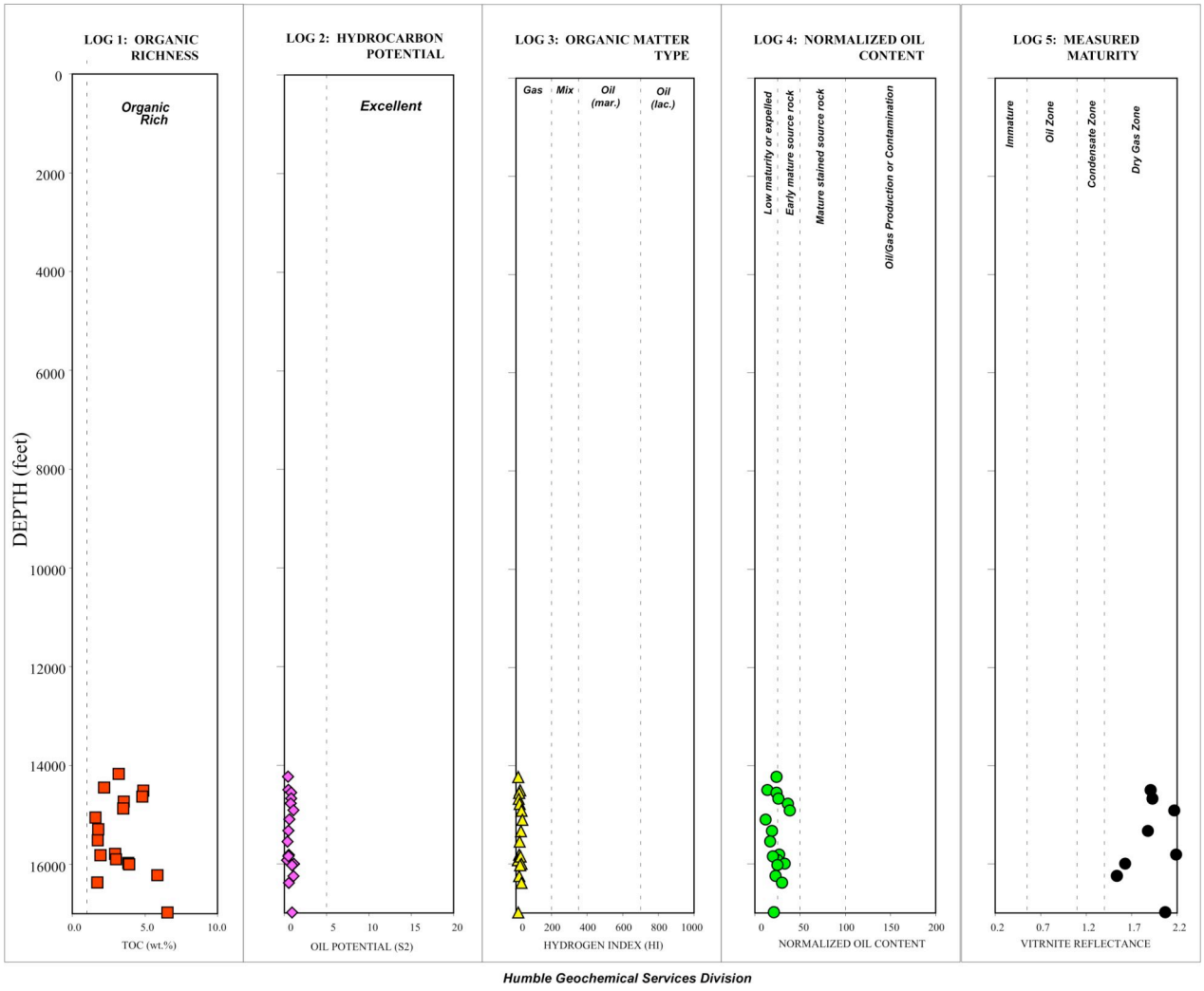

Figure V. 1. Geochemical logs for wells shown in Table 5.

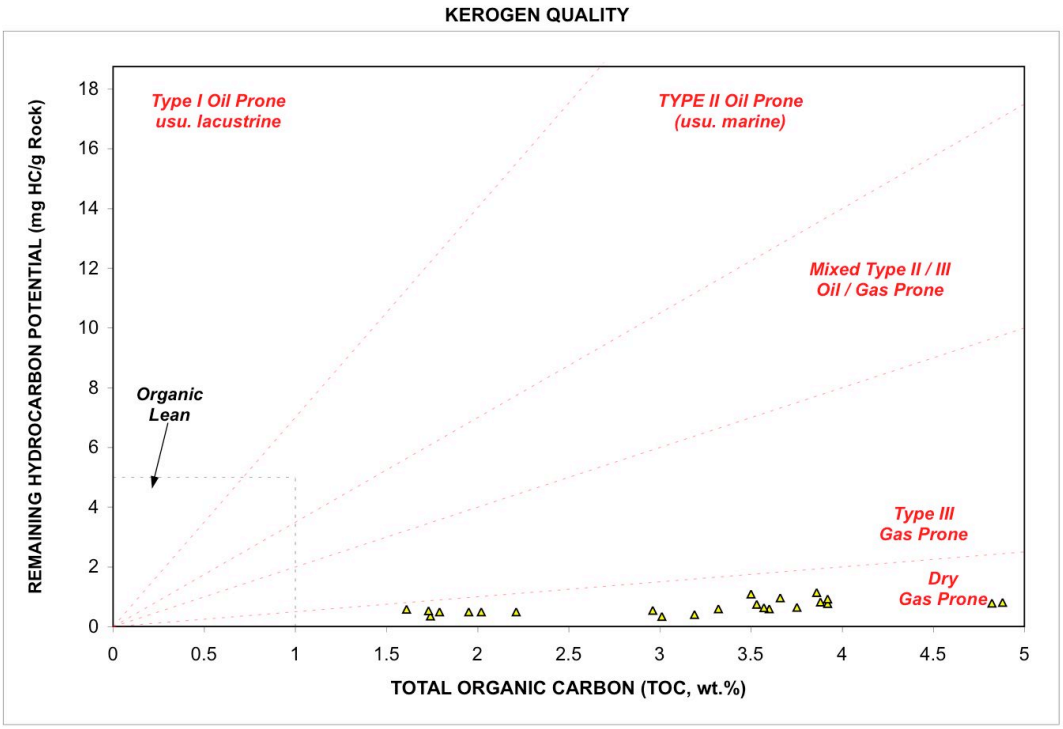

Figure V. 2. Kerogen quality relative to TOC and the hydrocarbon potential for wells shown in Table 5.

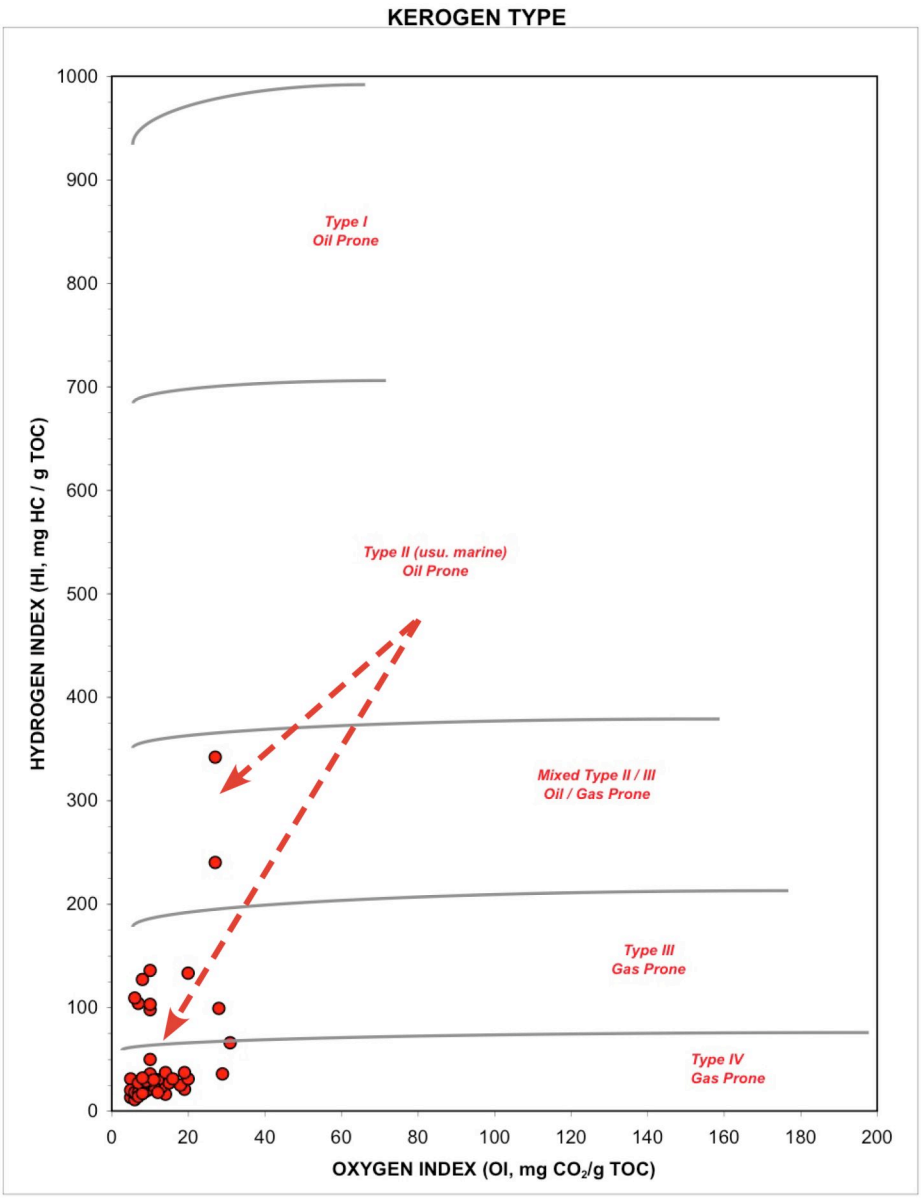

Figure V. 3. Kerogen type based on calculated Oxygen and Hydrogen indices for wells shown in Table 5. Arrows show approximate maturation paths of the samples through time.

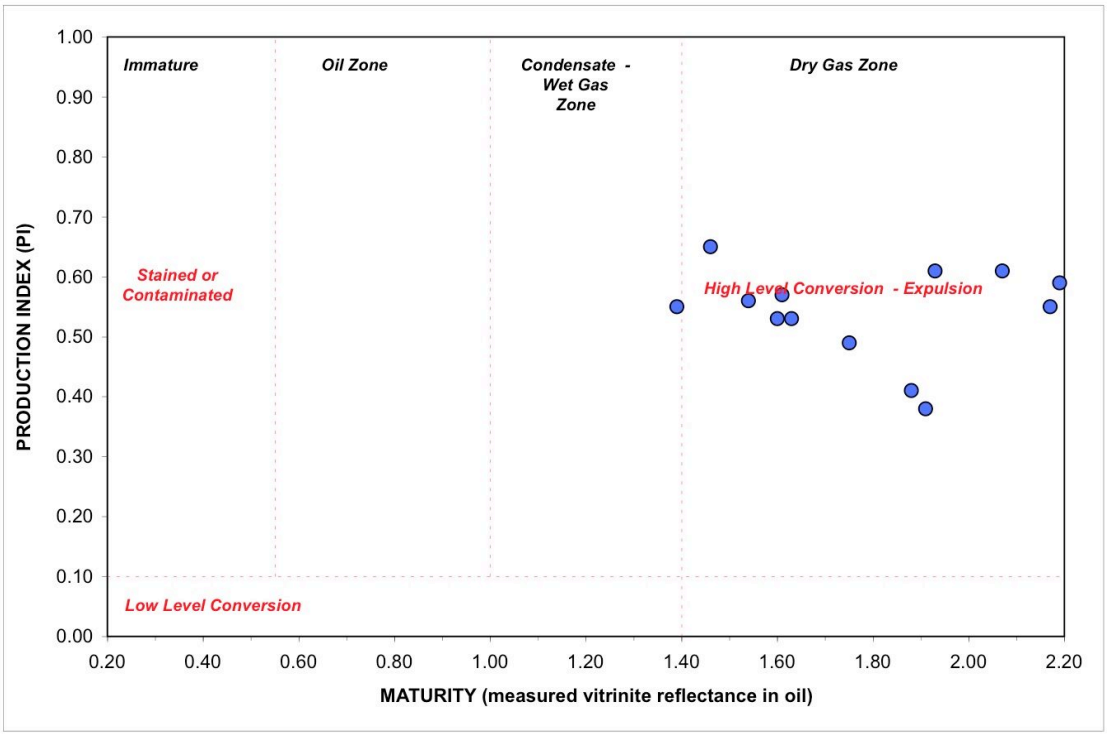

Figure V. 4. Kerogen conversion-maturity relative to maturity based on the measured vitrinite reflectance and the calculated production index for the wells in Table 5.

Vita

Personal Background	Travis James Kinley Fort Worth, Texas Born September 15, 1978, Sheridan, WY Son of Mike and Sandy Neubauer Married to Crissy Kinley, July, 10, 1999
Education	Associate of Science in Geology, 2002 Casper College, Casper, WY Bachelor of Science in Geology, 2004 University of Wyoming, Laramie, WY Master of Science in Geology, 2006 Texas Christian University, Fort Worth, TX
Experience	Intern Geologist, 2003 and 2004 Double Eagle Petroleum, Casper, WY Teaching Assistant, 2004-2006 Texas Christian University, Fort Worth, TX Intern Geologist, 2004-2006 XTO Energy, Fort Worth, TX
Professional Memberships	Fort Worth Geological Society (FWGS) American Association of Petroleum Geologists (AAPG)

Abstract

GEOLOGY AND HYDROCARBON POTENTIAL OF THE BARNETT SHALE (MISSISSIPPIAN) IN THE NORTHERN DELAWARE BASIN, WEST TEXAS AND SOUTHEASTERN NEW MEXICO

By Travis J. Kinley, M.S., 2006
Department of Geology
Texas Christian University

Dr. John Breyer – Professor of Geology
Dr. Richard Hanson – Professor of Geology and Department Chair
Lance Cook – Manager, Rocky Mountains, Geology, XTO Energy

The Barnett Shale (Mississippian) in the Delaware basin has the potential to be a prolific gas producer. It is organic-rich and thermally mature over large portions of the basin. Depths to the Barnett range from 7,000 feet (2,333 meters) along the western edge of the basin to more than 18,000 feet (6,000 meters) along the basin axis. The Barnett Shale began generating gas 250 Ma ago and remains in the gas window to this day. The shale can be divided into an upper clastic unit and a lower limy unit by changes in resistivity. The lower unit can be subdivided into five subunits by distinctive well-log markers. Preliminary analyses suggest that intervals in the lower Barnett marked by high resistivity and high neutron porosity readings on well-logs have high gas contents. Areas in which to focus future exploration can be delineated by mapping net-resistivity greater than 50 ohmm in the lower Barnett.